Journal of Medicinal Chemistry

Article

Potent and Highly Selective Aldo–Keto Reductase 1C3 (AKR1C3) Inhibitors Act as Chemotherapeutic Potentiators in Acute Myeloid Leukemia and T-Cell Acute Lymphoblastic Leukemia

Kshitij Verma, Tianzhu Zang, Trevor M. Penning, and Paul C. Trippier

J. Med. Chem., **Just Accepted Manuscript** • DOI: 10.1021/acs.jmedchem.9b00090 • Publication Date (Web): 05 Mar 2019

Potent and Highly Selective Aldo–Keto Reductase 1C3 (AKR1C3) Inhibitors Act as Chemotherapeutic Potentiators in Acute Myeloid Leukemia and T-Cell Acute Lymphoblastic Leukemia

Kshitij Verma,[a] Tianzhu Zang,[b] Trevor M. Penning[b] and Paul C. Trippier[a,c*]

[a] Department of Pharmaceutical Sciences, Texas Tech University Health Sciences Center, School of Pharmacy, Amarillo, TX 79106, USA.

[b] Center of Excellence in Environmental Toxicology, Department of Systems Pharmacology & Translational Therapeutics, Perelman School of Medicine, University of Pennsylvania, Philadelphia, PA 19104, USA.

[c] Center for Chemical Biology, Department of Chemistry and Biochemistry, Texas Tech University, Lubbock, TX 79409, USA.

ABSTRACT

Aldo–keto reductase 1C3 (AKR1C3) catalyzes the synthesis of 9α,11β-prostaglandin (PG) $F_{2\alpha}$ and $PGF_{2\alpha}$ prostanoids that sustain the growth of myeloid precursors in the bone marrow. The enzyme is overexpressed in acute myeloid leukemia (AML) and T-cell acute lymphoblastic leukemia (T-ALL). Moreover, AKR1C3 confers chemotherapeutic resistance to the anthracyclines; first-line agents for the treatment of leukemias. The highly homologous isoforms AKR1C1 and AKR1C2 inactive 5α-dihydroprogesterone and their inhibition would be undesirable. We report herein, the identification of AKR1C3 inhibitors that demonstrate exquisite isoform selectivity for AKR1C3 over the other closely related isoforms to the order of >2800-fold. Biological evaluation of our isoform selective inhibitors revealed a high degree of synergistic drug action in combination with the clinical leukemia therapeutics daunorubicin and cytarabine in *in vitro* cellular models of AML and primary patient-derived T-ALL cells. Our developed compounds exhibited >100-fold dose reduction index that results in complete resensitization of a daunorubicin-resistant AML cell line to the chemotherapeutic and >100-fold dose reduction of cytarabine in both AML cell lines and primary T-ALL cells.

INTRODUCTION:

Acute myeloid leukemia (AML) is a debilitating condition that affects both pediatric and elderly populations. With an estimated incidence rate of more than 19,520 it is the second most common type of hematologic malignancy.[1] The underlying pathophysiology for AML is marked by a differentiation block and clonal expansion of immature blast cells in the bone marrow that can be ascribed to various chromosomal translocations offering a proliferative advantage.[2, 3] Clinically, AML is classified into seven distinct subtypes (M0-M7) depending on the type of cells affected within the myelocytic lineage during hematopoiesis. The M3 subtype or Acute Promyelocytic Leukemia (APL) stems from a reciprocal chromosomal translocation of promyelocytic leukemia / retinoic acid receptor alpha (PML / RARα) oncogene that prevents cellular differentiation.[4] Treatment with retinoic acid is a primary therapeutic intervention that is employed along with arsenic trioxide or chemotherapy to induce remission.[5] However, the use of retinoic acid is limited to only the M3 subtype, due to adverse effects.[6] Standard treatment of care for the other types of AML relies heavily on the use of anthracyclines and the antimetabolite cytarabine as first line chemotherapeutics for remission induction as well as for maintenance therapy. Continuous infusion of cytarabine for 7 days in combination with daunorubicin for 3 days is employed as induction chemotherapy (7+3 regimen) followed by cytarabine administration for maintenance.[2] Since AML predominantly affects the elderly with higher incidence rates among patients >65 years of age, the tolerability of intensive chemotherapy remains a grave concern.[7] Moreover, the disease prognosis among older patients is poor due to higher relapse rates and unfavorable cytogenetics.[8]

Acute lymphocytic leukemia (ALL) stems from a malignant transformation of the lymphoid precursors in the bone marrow and is estimated to affect 5960 individuals per year in the US, predominantly children and adolescents.[1] Approximately 25% of all ALL cases are classified as T-cell ALL (T-ALL) that affects the T lymphocytes of the white blood cell lineage.[9] Owing to chromosomal translocation of transcription factors that are then placed under the control of strong T-cell receptor gene promoters, immature precursor T-cells gain a proliferative advantage. The clinical outcome for patients suffering from primary refractory or relapsed T-ALL remains bleak.[10, 11] Chemotherapeutics used to treat AML are commonly used to treat T-ALL and encounter

similar resistance profiles in relapse.[11] Development of non-toxic chemical agents that can increase the efficacy of currently employed chemotherapeutics and prevent the development of resistance represent an attractive therapeutic strategy to manage leukemic disease progression.

Aldo–keto reductase 1C3 (AKR1C3) is overexpressed in a range of leukemic cell lines spanning various AML subtypes and in high risk T-ALL.[12, 13] By virtue of the enzyme's prostaglandin F synthase (PGFS) activity, AKR1C3 converts the precursor prostanoid PGD_2 to 11β-$PGF_{2\alpha}$, that induces proliferation of leukemic blasts. The proliferative activity of 11β-$PGF_{2\alpha}$ is attributed to the activation of prostaglandin $F_{2\alpha}$ receptor (FP) and the downstream mitogen-activated protein kinase (MAPK) cascade.[14] In the absence of AKR1C3, PGD_2 non-enzymatically converts to PGJ_2 and eventually to 15-deoxy-$\Delta^{12,14}$-prostaglandin J_2 (15Δ-PGJ_2). The 15Δ-PGJ_2 serves as a ligand for the peroxisome proliferator-activated receptor-γ (PPARγ) and promotes cellular differentiation.[15] Prior reports have validated the role AKR1C3 plays in inducing myeloid cell proliferation and demonstrate that upon AKR1C3 upregulation the cells become resistant to differentiation by all-trans retinoic acid (ATRA), whereas the loss of AKR1C3 trans-gene expression confers sensitivity to ATRA.[12] Studies have shown that PGD_2 synergizes with ATRA in HL-60 promyelocytic cells to induce differentiation and apoptosis, while in contrast, incubation with 11β-$PGF_{2\alpha}$ significantly increased cell proliferation.[12] Since direct administration of pro-differentiation prostaniods PGJ_2 and 5Δ-PGJ_2 is severely limited by high toxicity and low bioavailability, a superior therapeutic strategy will be to inhibit the activity of AKR1C3 in order to divert the prostanoid metabolism towards the production of PGJ_2 series prostanoids in order to gain a beneficial therapeutic outcome.[16] The related AKR1C3 isoforms AKR1C1 and 1C2 share >84% sequence homology to 1C3 and are responsible for the inactivation of potent androgens (e.g. 5α-DHT) thus the inhibition of these isoforms is undesirable as it cannot cause androgen insufficency.[17, 18] Importantly, AKR1C3 acts as a phase I biotransformation enzyme, transforming anthracyclines (doxorubicin, daunorubicin and idarubicin) into their less potent C-13 hydroxy metabolites that results in chemotherapeutic resistance.[19, 20] Apart from AML and T-ALL, AKR1C3 is overexpressed in a variety of neoplasms of the breast,[21] colon,[22] prostate,[23, 24] endometrium[25, 26] and lungs.[27]

Significant efforts have been made to discover and develop different classes of AKR1C3 inhibitors from diverse structural classes (steroids,[26] flavones,[28] jasmonates[29] and non-steroidal anti-inflammatory drugs (NSAID's))[21, 24, 26, 30] (Figure 1). Among steroids, medroxyprogesterone acetate (MPA) and an estrogen lactone (EM1404) are potent inhibitors of AKR1C3 but are limited in application due to the lack of isoform-selectivity. Jasmonic acids suffer from the same fate and lack inhibition potency and selectivity towards AKR1C3. Among flavonoids, 2-hydroxyflavone exhibits moderate potency while inhibiting AKR1C3 with 157-fold isoform selectivity. Repurposed NSAIDs possess high inhibitory potency for AKR1C3 and selectivity but have not made it into the clinic. For example derivatization of the indomethacin scaffold to the *des*-methyl indomethacin analogue, modification of naproxen to *R*-ethyl naproxen and the structural optimization of flufenamic acid to a *meta* isomer abrogated cyclooxygenase (COX) inhibition activities while retaining inhibitory potency for AKR1C3. The *N*-naphthylamino benzoate analogue was found to be a bifunctional AKR1C3 inhibitor that also antagonizes androgen receptor (AR) functions.[21, 26, 31-35] Inhibitor SN33638 demonstrated only a moderate inhibition of testosterone production and a modest reduction in cell viabilities evaluated in AKR1C3 dependent castration-resistant prostate cancer (CRPC) cell lines whereas ASP9521, taken through a phase I/II clinical trial in metastatic CRPC patients established no observable clinical activity.[36-38] Another bifunctional inhibitor GTX-560 has been shown to inhibit the AR coactivator functions of AKR1C3 in addition to being an AKR1C3 inhibitor.[39] Recently reported, a benzoisoxazole derivative designed by applying a scaffold hopping approach to flufenamic acid displayed a greater isoform selectivity for AKR1C3 inhibition as compared to AKR1C1. However, the inhibition potency still remained in mid-nanomolar range (Figure 1).[40] There may be multiple reasons for AKR1C3 inhibitor failure which has prevented their clinical use.

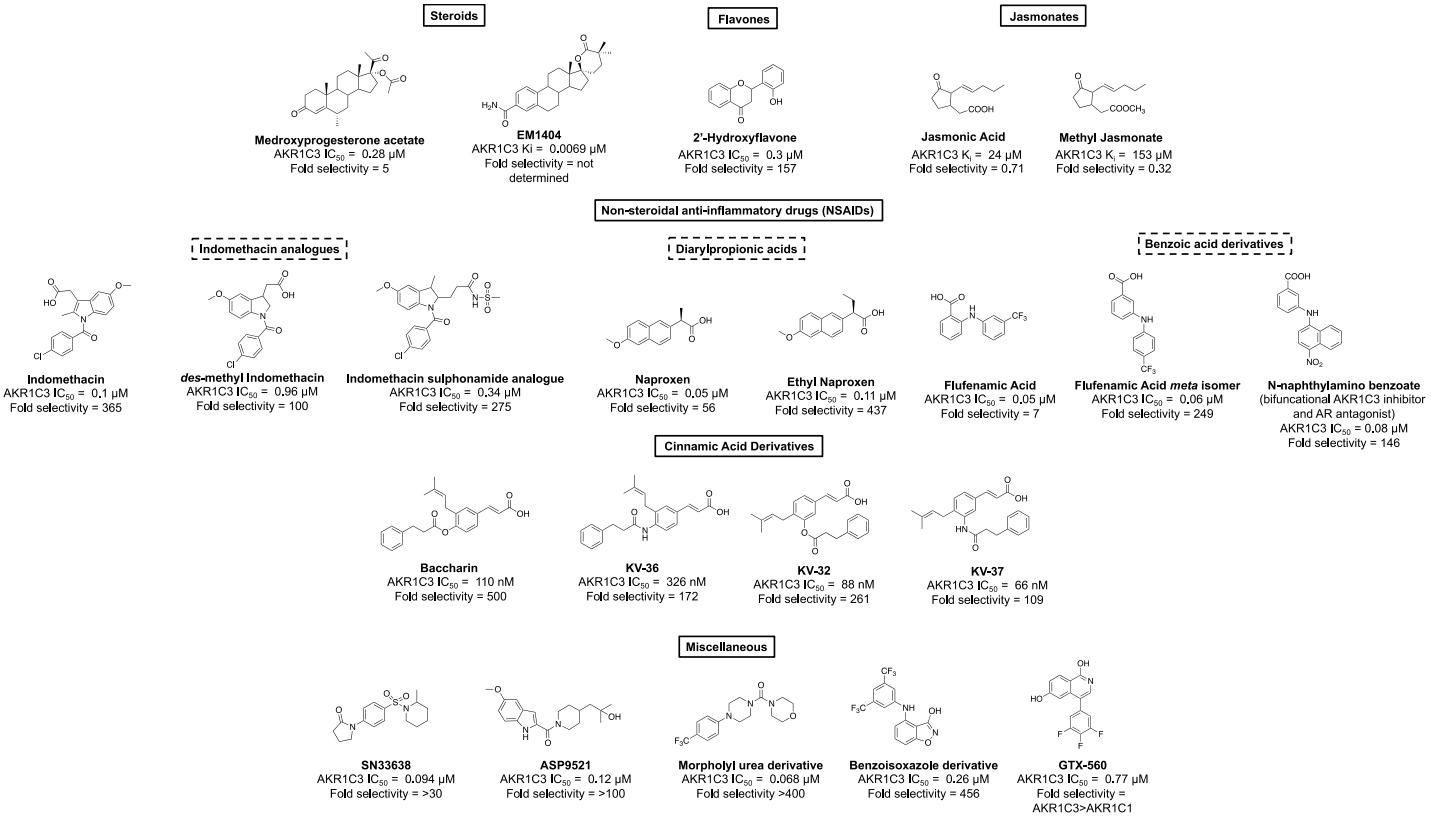

Figure 1. Structures of known AKR1C3 inhibitors.

Even though indomethacin yielded an IC_{50} value = 0.1 μM and exhibited a 356-fold selectivity for AKR1C3 it displayed a weak antiproliferative effect in AML cells.[12, 41] A study combining the pan-AKR1C inhibitor medroxyprogesterone acetate (MPA) (AKR1C3 IC_{50} = 2.7 μM, 0.66-fold selectivity for AKR1C3) and bezafibrate (a PPAR α/γ agonist) provided an approximate two-fold potentiation of bezafibrate activity; demonstrating a reduction in cell proliferation with an increased differentiation and apoptosis in AML cells.[16] However, further studies on the mechanism of action of MPA attributed this activity to targets other than the AKR1C family. A recent study reported that the specific AKR1C3 inhibitor 4-methyl(de-dimethylamine)-tetracycline (4-MDDT) (IC_{50} = 0.51 μM) does not give the adjuvant effect at concentrations up to 50 μM that a pan-AKR1C inhibitor does, thus requiring greater credentialing of the AKR1C3 target in leukemia.[42] Although inhibitors with nanomolar potency and relatively high selectivity to AKR1C3 (up to 500-fold) over the other

isoforms have been identified from prior studies, the discovery of new compounds for preclinical development is still required.

Derivatives of cinnamic acids have been shown to exhibit inhibition activities for AKR isozymes bearing selectivity towards AKR1C3. Among these compounds, baccharin (Figure 1), a natural product extracted from honeybee propolis has been shown to potently and selectively inhibit AKR1C3 with an IC_{50} of 0.11 μM and a fold selectivity of 500 over AKR1C2.[43] This discovery has made baccharin a promising hit to develop a new series of potent and specific inhibitors against AKR1C3. We adopted this natural product scaffold and have previously reported the synthesis and a preliminary structure-activity relationship (SAR) for AKR1C3 inhibition.[44] The dihydrocinnamoyloxy moiety of baccharin is reported as a structural prerequisite for AKR1C3 inhibition, and other groups have synthesized potent AKR1C3 inhibitors based on this scaffold.[45] However, the presence of an ester linkage introduces a hydrolytic lability into baccharin making these analogues unsuitable for drug discovery. Hydrolysis of the ester results in formation of the known phenol drupanin, with complete abrogation of AKR1C3 inhibitory potency.[46] Our prior studies have reported the design, synthesis and evaluation of potent AKR1C3 inhibitors bearing a more stable amide bioisostere (Figure 1). These AKR1C3 inhibitors exhibit a six-fold potentiation of etoposide and a ten-fold potentiation of daunorubicin in AML cell lines.[47] However, the selectivity over AKR1C1 and AKR1C2, while significantly improved above that of MPA (0.66-fold), remained relatively low (109-fold). Continuing our efforts to identify highly isoform-selective AKR1C3 inhibitors we herein report the discovery of a library of optimized compounds possessing >2800-fold selectivity for AKR1C3 inhibition, with retention of inhibitory potency in the nanomolar range. Further, we demonstrate that our highly isoform-selective AKR1C3 inhibitors provide up to 100-fold potentiation of the clinical chemotherapeutics daunorubicin and cytarabine across a panel of AML cell lines and in primary patient-derived T-ALL cells.

RESULTS AND DISCUSSION:

Chemistry. Based on the baccharin structural scaffold, three different classes of analogues were synthesized and evaluated for AKR1C3 inhibitory potency and selectivity towards the other highly homologous AKR isoforms (Figure 2). To explore modifications of the dihydrocinnamoyloxy moiety, Class I compounds possess an ester or amide link to the terminal phenyl B ring. The spacer is of varied length and features a diversity of substituents on the phenyl ring. Class II compounds have the acrylate side chain moved to the meta-position and substitution on the terminal phenyl ring is varied. In addition, class II compounds also explore 1,3,5 substituents on the central A-ring. Class III compounds constitute varying substitution patterns on the central A ring and also explore boronic acid bioisosteres of the cinnamic acid.

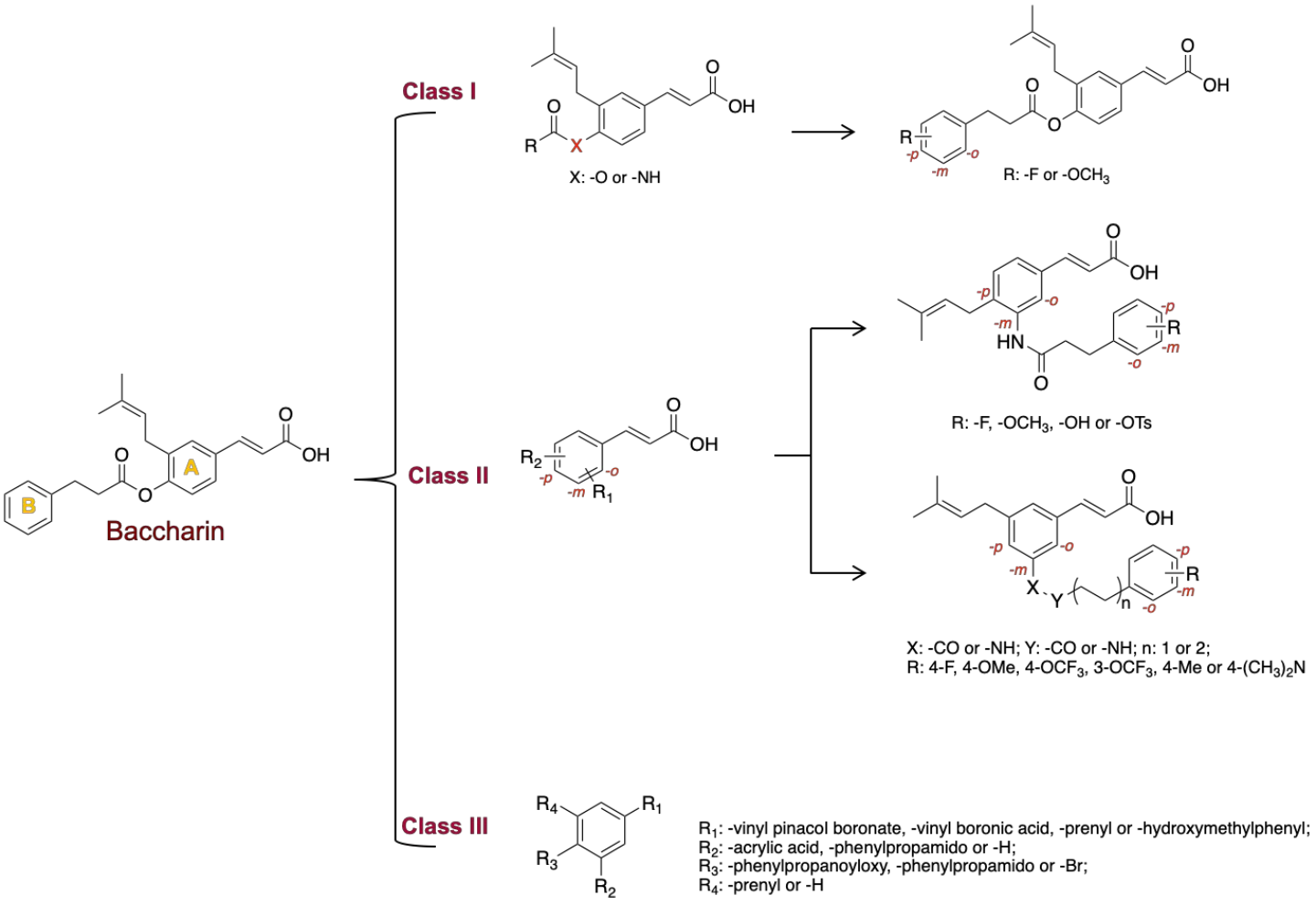

Figure 2. SAR strategy for the design of Baccharin derivatives.

Baccharin (**1**), compounds **7**-**7a** (class III) and **8b**-**n** (class I) were synthesized using a modified literature procedure.[48] Nucleophilic substitution of commercially available 4-iodophenol (**2**) with prenyl bromide yielded

the alkylated intermediate **3**,[49] which was subsequently esterified with an appropriately substituted acid chloride (**4a-n**) to yield ester intermediates (**5a-n**). Mizoroki-Heck[50, 51] coupling of the aryl iodide intermediates (**5a-n**) with *tert*-butyl acrylate or vinyl boronic acid pinacol ester using $Pd(OAc)_2$ and PPh_3 as a catalyst-ligand complex produced α,β-unsaturated olefins **6a-n** and **7** respectively. Chemoselective hydrolysis of the *tert*-butyl ester[52] of **6a-n** afforded baccharin (**1**) and derivatives **8b-n**, whereas hydrolysis of the pinacol ester[53, 54] afforded boronic acid **7a** (Scheme 1).

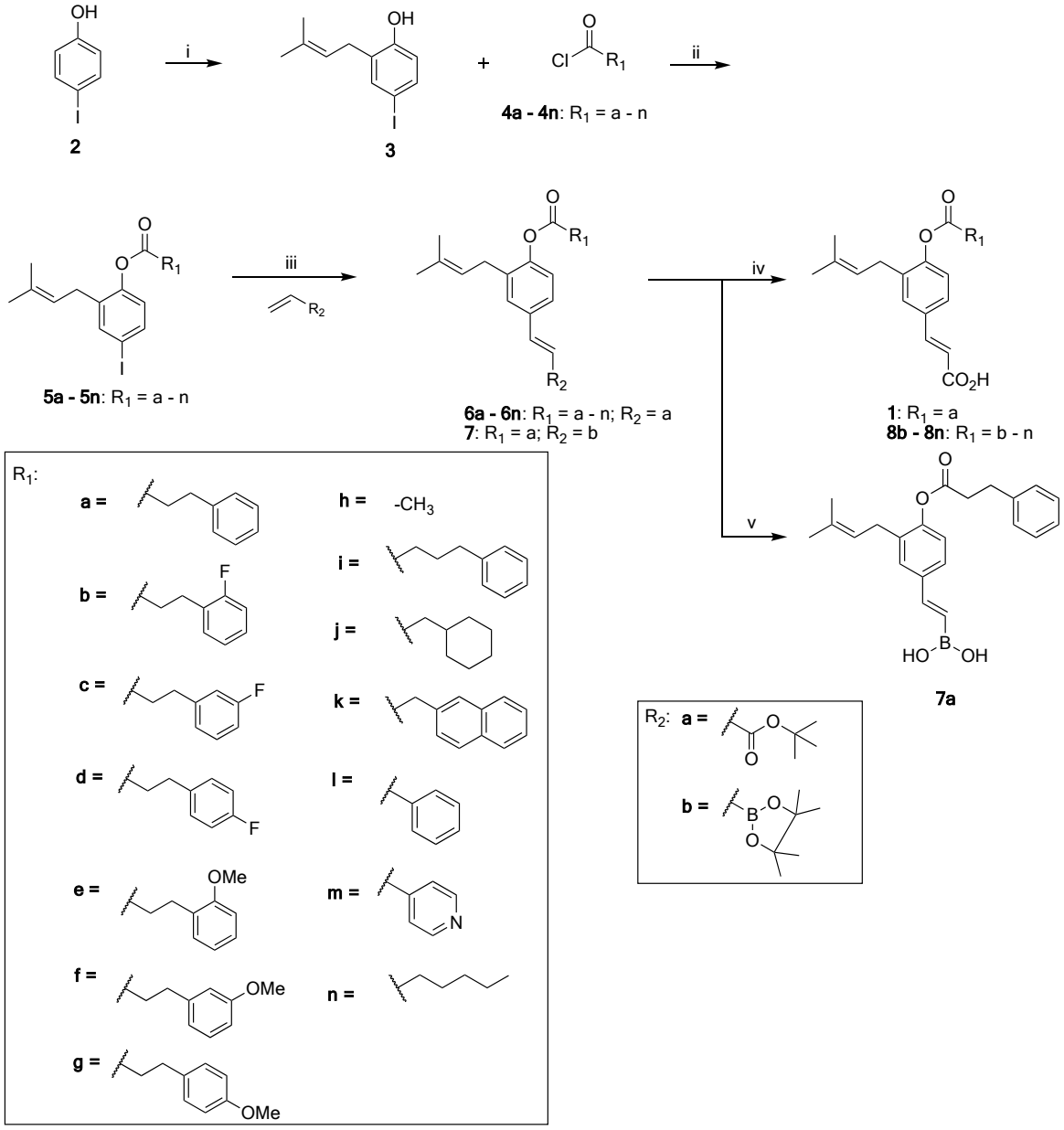

Reagents and conditions: (i) Prenyl Bromide, NaH, PhMe, 55%; (ii) DMAP, NEt_3, DCM; (iii) NEt_3, $P(Ph)_3$, $Pd(OAc)_2$, PhMe, reflux; (iv) SiO_2, PhMe, reflux; (v) $MeOH/H_2O$, 80 ^oC.

Scheme 1: Synthesis of baccharin (**1**),[44] substituted ester derivatives (**8b-g**, **8h**,[44] **8i-n**) of class I and boronic acid analogues (**7** and **7a**) of class III.

The reaction sequence was then modified where *p*-iodoaniline (**9**) was regioselectively brominated using a modified literature procedure that afforded dihalide **10**.[55] Exploiting the greater reactivity of iodide over bromide[56] in Mizoroki-Heck[51] couplings, **10** was selectively coupled with *tert*-butylacrylate yielding the intermediate aniline **11**. Coupling with the corresponding acid chloride gave amide intermediates (**12a-e**). A palladium-catalyzed Suzuki-Miyaura[57, 58] cross-coupling reaction installed the prenyl side chain that yielded intermediates (**13a-e**) which underwent chemoselective hydrolysis of the *tert*-butyl ester to afford the final compounds (**14a**[47] and **14b-e**) of class I (Scheme 2).

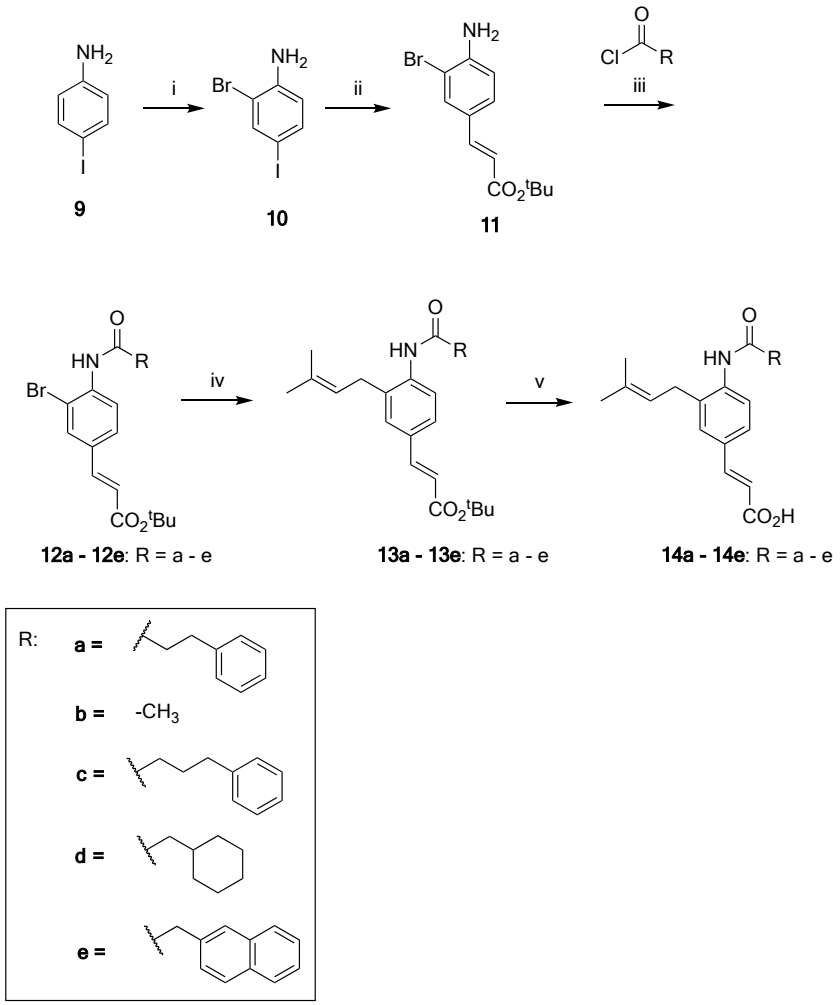

Reagents and conditions: (i) Br_2, AcOH, RT, 44%; (ii) *tert*-butylacrylate, NEt_3, $P(Ph)_3$, $Pd(OAc)_2$, PhMe, reflux, 64%; (iii) NEt_3, DMAP, DCM, 40 ^oC; (iv) prenylboronic acid pinacol ester, $Pd(dppf)Cl_2$, Cs_2CO_3, DMF, 90 ^oC; (v) SiO_2, PhMe, reflux.

Scheme 2: Synthesis of amide bioisosteres (**14a**,[47] **14b-e**) of class I derivatives.

Class II compounds in which the substitution pattern on the A-ring of baccharin is altered, in which the ester chain was moved to the *meta*-position relative to the acrylate side chain. Commercially available *m*-coumaric acid (**15**) was protected as the methyl ester and subsequently brominated, with column chromatography providing access to the desired regioisomer in 35% yield. The brominated intermediate (**17**) was deprotected under basic conditions to yield compound **17a** which was followed by esterification of the phenol using phenylpropionyl acid chloride to yield ester derivative **18**. Suzuki-Miyaura[57] reaction with the appropriately substituted boronic acid pinacol ester afforded prenyl and allyl derivatives (**19a**[47] and **19b**) of class II analogues (Scheme 3).

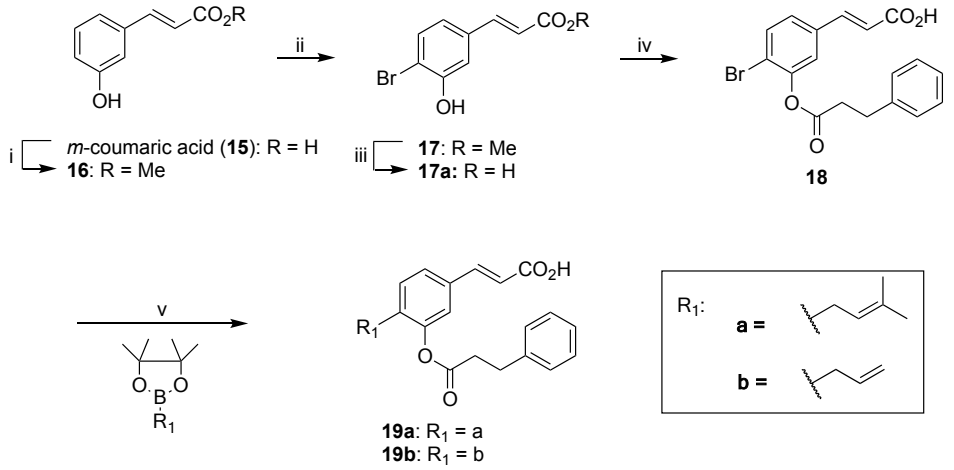

Reagents and conditions: (i) MeOH, H_2SO_4, reflux, 93%; (ii) Br_2, AcOH, RT, 35%; (iii) NaOH, H_2O, reflux, 90%; (iv) 3-phenylpropanoyl chloride, DMAP, NEt_3, DCM, RT, 36%; (v) Pd(dppf)Cl_2, Cs_2CO_3, DMF, 90 ^oC.

Scheme 3: Synthesis of *meta*-substituted ester derivatives (**19a**[47] and **19b**) of class II.

The amide bioisosteres **26a-l**, **28** (class II) and **24** (class III) were accessed through Mizoroki-Heck[51] reaction of commercially available 4-bromo-2-iodoaniline (**20**) with *tert*-butyl acrylate or vinyl boronic acid pinacol ester to afford **21a** and **21b** respectively. Amide formation with the appropriate acid chloride as previously described yielded amides **23a**-**23j** and **24**. Subsequent Suzuki-Miyaura[57] cross-coupling afforded intermediates **25a**-**25j** and **27** which were chemoselectively hydrolyzed to yield final compounds **26a**[47] and **26b**-**26j** and **28**. Further, hydrolysis of the tosyl moieties in **26i** and **26j**, afforded phenols **26k** and **26l** respectively (Scheme 4).

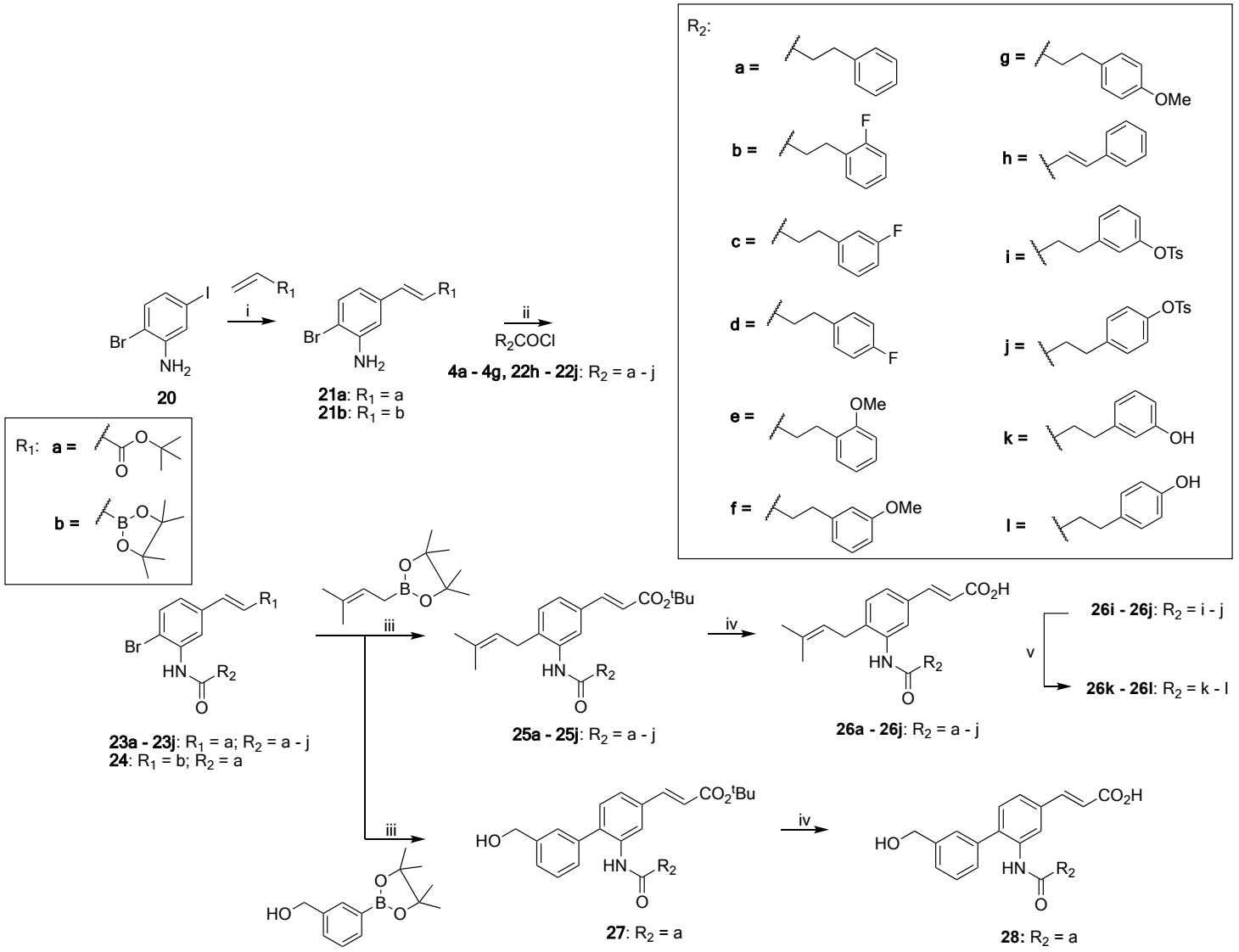

Reagents and conditions: (i) $Pd(OAc)_2$, $P(Ph)_3$, NEt_3, PhMe, 110 °C; (ii) DMAP, NEt_3, DCM, 40 °C; (iii) $Pd(dppf)Cl_2$, Cs_2CO_3, DMF, 90 °C; (iv) SiO_2, PhMe, reflux; (v) MeOH, 1M NaOH, H_2O, reflux.

Scheme 4: Synthesis of *meta*-substituted amide derivatives (**26a**,[47] **26b-l** and **28**) of class II and boronic ester derivative **24** of class III.

Class III analogues (**33a** and **33b**) were prepared from the commercially available 4-bromo-2-iodoaniline (**29**) as a starting material. After installation of the amide chain by reaction with acid chloride as previously described, Mizoroki-Heck cross-coupling chemoselectively afforded intermediate **31** due to the increased reactivity of iodide over bromide for the reaction.[51] Suzuki-Miyaura[57] cross coupling with substituted pinacol boronate followed by *tert*-butyl ester deprotection yielded compounds **33a** and **33b** (Scheme 5).

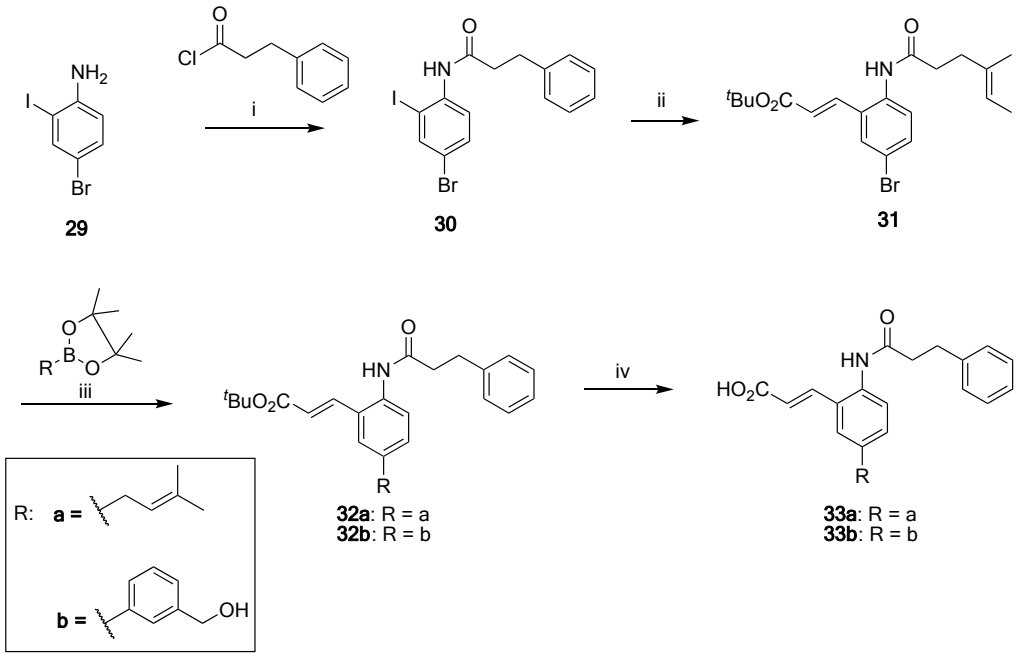

Reagents and conditions: (i) NEt_3, DMAP, DCM, 40 °C, 69%; (ii) *tert*-butylacrylate, NEt_3, $P(Ph)_3$, $Pd(OAc)_2$, PhMe, reflux, 70%; (iii) $Pd(dppf)Cl_2$, Cs_2CO_3, DMF, 90 °C; (iv) SiO_2, PhMe, reflux.

Scheme 5: Synthesis of **33a** and **33b** as amide derivatives of class III.

Further, to modify the side chain substitution pattern of the parent scaffold A ring to the 1,3,5 all *meta*-substituted pattern, 3-bromo-5-iodobenzoic acid (**34**) was used as the common starting material for the synthesis of amide, ester or retroinverse amide analogues. Conversion of **34** to 3-bromo-5-iodoaniline (**35**) was achieved by a modified Curtius rearrangement,[59] followed by *tert*-butyloxycarbonyl (Boc) deprotection. A reaction sequence of amide synthesis using acid chloride, followed by Pd-catalyzed cross-couplings in the order of Mizoroki-Heck reaction followed by Suzuki-Miyaura reaction afforded *tert*-butyl protected intermediates that were subsequently hydrolyzed to afford compounds **39a** and **39b**. Conversion of **34** to its acid chloride followed by esterification or amide formation using phenylethyl alcohol, or substituted primary amine, yielded the ester and amide intermediates (**42, 41a-h**) respectively. The reaction sequence of Mizoroki-Heck, Suzuki-Miyaura and *tert*-butyl ester hydrolysis was used to obtain compounds **49a-h** and **50-52** of class III (Scheme 6).

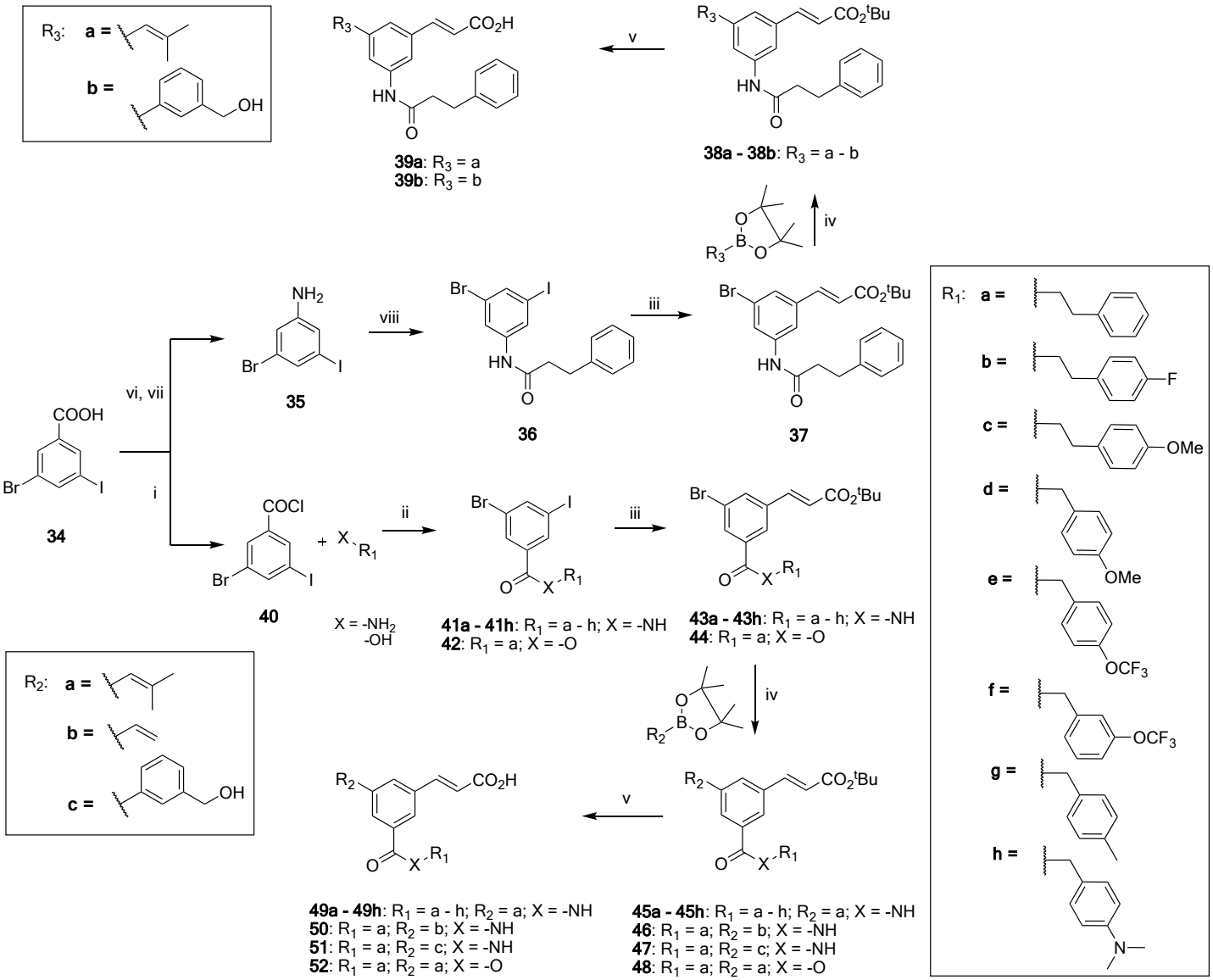

Reagents and Conditions: (i) $SOCl_2$, PhMe, reflux; (ii) DMAP, NEt_3, DCM, 40 ^oC; (iii) *tert*-butylacrylate, $Pd(OAc)_2$, $P(Ph)_3$, NEt_3, PhMe, 110 ^oC; (iv) $Pd(dppf)Cl_2$, Cs_2CO_3, DMF, 90 ^oC; (v) SiO_2, PhMe, reflux; (vi) DPPA, NEt_3, tBuOH; (vii) 4M HCl, dioxane, 40%; (viii) 3-phenylpropanoyl chloride, DMAP, NEt_3, DCM, 40 ^oC, 33%.

Scheme 6: Synthesis of 1,3,5-*meta*-substituted derivatives (**39a** and **39b, 49a-h** and **50-52**) of class II.

Ether analogues **59a-b** were synthesized using 3-bromo-4-hydroxybenzoic acid (**53**) as the starting material which was reacted with benzyl bromide or 3-methoxy benzyl bromide to install the ether side chain. After activating the carboxylic acid to an acid chloride, a reaction sequence of amide formation followed by Mizoroki-Heck reaction and *tert*-butyl ester hydrolysis afforded final compounds (**59a** and **59b**) of class II (Scheme 7).

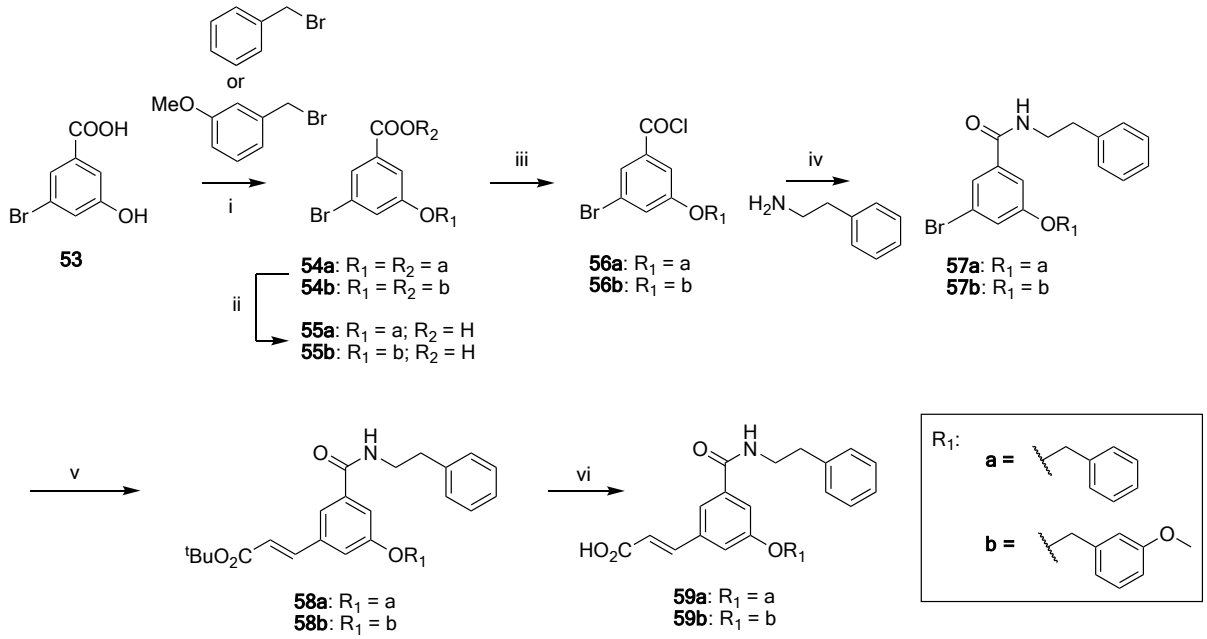

Reagents and conditions: (i) DIPEA, 150 ^{o}C; (ii) 1M KOH, MeOH, reflux; (iii) $SOCl_2$, PhMe, reflux; (iv) DMAP, NEt_3, DCM, 40 ^{o}C; (v) *tert*-butylacrylate, $Pd(OAc)_2$, DABCO, K_2CO_3, DMF, 110 ^{o}C; (vi) SiO_2, PhMe, reflux.

Scheme 7: Synthesis of 1,3,5-*meta*-substituted ether derivatives (**59a** and **59b**) of class II

Structure-activity relationship.

Class I analogues: Consistent with previous findings,[43, 44, 47] baccharin exhibited an IC_{50} of 105 nM for AKR1C3 inhibition with 510-fold selectivity over AKR1C2. Removal of the dihydrocinnamoyloxy group to afford **1a** (drupanin), resulted in complete abrogation of AKR1C3 inhibitory potency and selectivity. Replacement of the dihydrocinnamoyloxy group (compounds **8h-n**) resulted in low or sub-micromolar inhibition potency for AKR1C3, with significant reduction of selectivity. Introduction of an acetoxy group (**8h**) and a cyclohexylacetoxy group (**8j**), decreased both AKR1C3 inhibitory potency and selectivity by four-fold. As compared to **1** an increase in the carbon spacer in **8i** decreased AKR1C3 inhibitory potency and selectivity by two-fold and four-fold respectively. Excision of the ethyl linker to afford the benzoyloxy moiety (**8l**) reduced inhibitory potency by three-fold and isoform selectivity to AKR1C3 by eight-fold. Replacement of the terminal phenyl moiety of **1** with a bulky napthyl (**8k**) or simple hexane chain (**8n**) resulted in decrease of the inhibitory potency by three-fold with loss of selectivity being twelve-fold (**8k**) and six-fold (**8n**) as compared to **1**. Replacement of the phenethyl moiety

in **1** with a pyridine ring (**8m)** significantly reduced potency and selectivity. Comparison with the phenyl derivative (**8l**) indicates the pyridine ring is largely responsible for this drop in potency, potentially due to its ability to ionize under the assay conditions. Replacement of the ester linkage with an amide linkage (**14a-e**) led to less potent inhibitors than their bioisosteric counterparts (**1**, **8h-n**). Differences in potency varied from three-fold reduction (compare **1** to **14a** and **8i** to **14c**) to an eight-fold reduction in AKR1C3 inhibitory potency (compare **8h** to **14b**). Likewise, the amide derivatives, with the exception of **14a** were also significantly more promiscuous between AKR1C isoforms with only moderate to minimal selectivity for the AKR1C3 isoform over AKR1C2. Fortuitously the amide derivative of baccharin (**14a)** retained potency and high selectivity, IC_{50} = 0.420 μM with 93-fold selectivity for AKR1C3 over the closely related AKR1C2 isozyme. Additionally, ligand-lipophilicity efficiency (LLE) which is a measure of 'drug-likeliness' and takes into account the potency and lipophilicity of compounds was also calculated. Even though the amide bioisosteres (**14a-e**) are less potent inhibitors of AKR1C3 they exhibit a more favorable LLE profile (except **14b**) as compared to the ester derivatives (**1**, **8i-k**) due to their greater lipophilicity (Table 1).

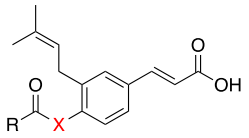

Compound	R	X	IC_{50} AKR1C3 (μM)	IC_{50} AKR1C2 (μM)	Selectivity 1C2:1C3	LLE*
1[44]	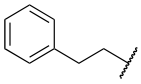	O	0.105	51	510	1.29
1a[44] **(Drupanin)**	-	OH	15	107	7	1.30
8h[44]	$-CH_3$	O	0.440	45	102	2.76
8i	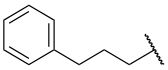	O	0.233	29	124	0.56
8j	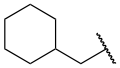	O	0.453	44	97	0.10
8k	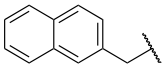	O	0.370	16	43	-0.17
8l		O	0.348	21	60	0.74
8m	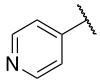	O	1.8	14	7.8	1.52
8n	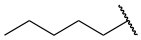	O	0.300	25	83	0.81
14a	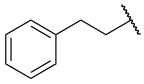	NH	0.420	39	93	1.89
14b	$-CH_3$	NH	3.6	30	8	2.15
14c	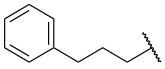	NH	0.866	30	35	1.19
14d	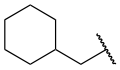	NH	2.8	38	14	0.51
14e	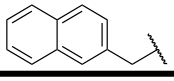	NH	1.8	42	23	0.64

IC_{50} values were performed in quadruplicate and technical replicates gave mean + SE. The SE is less than 10% and the mean value is reported.
*LLE. Ligand-lipophilicity efficiency (calculated as pIC_{50}-clogP).

Table 1. Inhibitory properties of class I analogues on AKR1C3 and AKR1C2.

Introduction of electron withdrawing groups onto the phenyl B ring (**8b-d**) resulted in compounds with similar inhibitory profiles to **1** with only marginally decreased selectivity. Introduction of an electron-donating methoxy

group on the B-ring, gave compounds equipotent with the parent baccharin scaffold at all substitution positions. However, a clear correlation between selectivity and substitution position was observed. When substitution occurs at the *para* (**8g**) or *ortho* (**8e**) positions a two-fold loss of selectivity is apparent. When substitution occurs at the *meta* position (**8f**) selectivity is retained. The derivatives **8e-g** display a similar LLE profile as **1**. (Table 2).

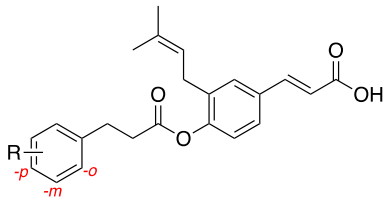

Compound	R	IC_{50} AKR1C3 (μM)	IC_{50} AKR1C2 (μM)	Selectivity 1C2:1C3	LLE*
8b	2-F	0.125	45	360	1.07
8c	3-F	0.156	62	397	0.97
8d	4-F	0.135	67	496	1.04
8e	2-OMe	0.135	37	274	1.26
8f	3-OMe	0.126	57	452	1.29
8g	4-OMe	0.132	34	258	1.27

IC_{50} values were performed in quadruplicate and technical replicates gave mean + SE. The SE is less than 10% and the mean value is reported.
*LLE. Ligand-lipophilicity efficiency (calculated as pIC_{50}-clogP).

Table 2. Inhibitory properties of class I analogues on AKR1C3 and AKR1C2.

Class II analogues: The central A-ring *meta*-substituted derivatives **19a**, **26a** and **26h** showed enhanced AKR1C3 inhibitory potency. The *meta*-ester derivative (**19a**) provided the best combination of potent inhibition (IC_{50} = 0.088 μM) and selectivity in all of the derivatives discussed thus far, with 261-fold selectivity for AKR1C3 (Table 3). The *meta*-amide derivative (**26a**) is the most potent AKR1C3 inhibitor identified among all the baccharin derivatives synthesized to date (IC_{50} = 0.066 μM), equipotent with the most active reported AKR1C3 enzyme inhibitors.[26] Selectivity is diminished over the parent scaffold, but the compound still retains a 109-fold selectivity for AKR1C3. Compounds that have mid-nanomolar potency for AKR1C3 and > 100 fold selectivity are leads for further development. Moreover, **26a** displayed an increase in LLE by two-fold as compared to **1** and by 1.3-fold in comparison to its isomer **14a**. Introduction of rigidity in the side chain amide chain via formation

of a *trans* alkene (**26h**) decreased the inhibitory potency for AKR1C3 (IC_{50} = 0.098 μM) as compared to **26a** but resulted in 50% increased selectivity. In comparison with the parent scaffold (**1**), **26h** retained equipotency but suffered a three-fold loss of selectivity. This data suggests that free rotation on this side chain is essential for high selectivity. Replacement of the prenyl side chain with a 3-hydroymethylphenyl group (**28**) decreased inhibitory potency (five-fold reduction over **1**) and selectivity (34-fold loss over **1**). Removal of the terminal methyl groups on the prenyl chain, to form a terminal alkene **19b**, also diminished potency and selectivity suggesting that the methyl groups extend into an open sub-pocket in the active site of AKR1C3 to confer potency and selectivity. Removal of the prenyl and ester side chains (**17a**) completely abrogated activity. Consistent with class I analogues, the amide derivatives (**26a, 26h** and **28**) exhibit more promising physicochemical traits as evidenced by their LLE values when compared to the ester derivatives (**17a** and **19a-b**) (Table 3).

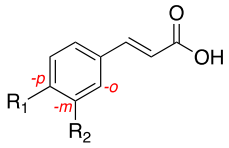

Compound	R_1	R_2	IC_{50} AKR1C3 (μM)	IC_{50} AKR1C2 (μM)	Selectivity 1C2:1C3	LLE*
17a	-Br	-OH	38	85.3	2	2.26
19a[47]	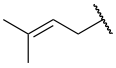	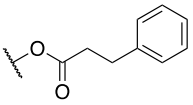	0.088	23	261	1.36
19b		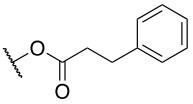	0.273	44	161	1.80
26a[47]	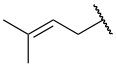	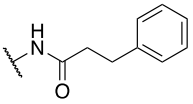	0.066	7.2	109	2.69
26h	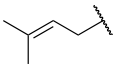	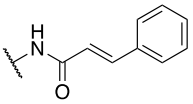	0.098	14	143	2.11
28	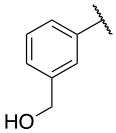	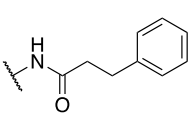	0.540	8.2	15	3.09

IC_{50} values were performed in quadruplicate and technical replicates gave mean + SE. The SE is less than 10% and the mean value is reported.
*LLE. Ligand-lipophilicity efficiency (calculated as pIC_{50}-clogP).

Table 3. Inhibitory properties of class II analogues on AKR1C3 and AKR1C2.

Based on the enhanced potency of **26a** we next sought to investigate the effect of substituents on the terminal B-ring of the parent scaffold. Such derivatives exhibited a range of activities from compounds that were slightly more potent than **1** (**26b-g**) to a reduction of approximately 1.5-fold in AKR1C3 inhibition potency (**26i-k**). Introduction of fluorine displayed fairly similar potencies, comparable to **26a**, with *meta* substitution (**26c**) showing a slight advantage over the *ortho* and *para* positions. However, the selectivity decreased by approximately 1.5-fold (**26b-d**). Interestingly, methoxy substitution at the *para* position (**26g**) increased isoform selectivity as compared to **26a** and all substitution patterns conserved inhibitory potency (**26e-g**). The inhibition profiles of tosyl (**26i** and **26j**) and hydroxy (**26k** and **26l**) substituted analogues were comparable to **1** with only a marginal decrease in potency, however selectivity decreased by 5-10 fold. The LLE value remained similar to **26a** among all the derivatives except hydroxy substituted compounds (**26k** and **26l**) that displayed an increased LLE to more than three (a 2.4-fold increase over **1**) (Table 4).

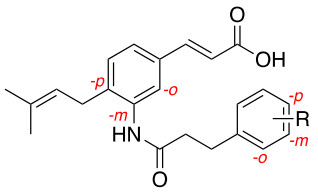

Compound	R	IC_{50} AKR1C3 (μM)	IC_{50} AKR1C2 (μM)	Selectivity 1C2:1C3	LLE*
26b	2-F	0.098	5.8	59	2.37
26c	3-F	0.076	6	79	2.49
26d	4-F	0.091	7.8	86	2.41
26e	2-OMe	0.081	7	86	2.68
26f	3-OMe	0.089	10	112	2.64
26g	4-OMe	0.094	16	170	2.62
26i	3-OTs	0.180	7.6	42	0.81
26j	4-OTs	0.190	16	84	0.78
26k	3-OH	0.140	23	164	3.03

26l	4-OH	0.110	14	127	3.13

IC_{50} values were performed in quadruplicate and technical replicates gave mean + SE. The SE is less than 10% and the mean value is reported.

*LLE. Ligand lipophilicity efficiency (calculated as pIC_{50}-clogP).

Table 4. Inhibitory properties of class II analogues on AKR1C3 and AKR1C2.

Rearrangement of the substituents on the central A ring to adopt a 1,3,5 substitution pattern greatly enhanced the selectivity for AKR1C3 inhibition over the highly related AKR1C1, 1C2 and 1C4 isoforms, as compared to **1**. With the exception of **39b** (Table 5) all compounds possessing this substitution pattern showed inhibitory potency in the low sub-micromolar range, with the majority exhibiting comparable or greater potency than **1** (**39a**, **49a-h**) (Tables 5 and 6). The *meta*-amide **39a** displayed inhibitory potency similar to **1** with a 1.5-fold increase in selectivity over AKR1C2, while the selectivity over other AKR isoforms also increased. Replacement of the prenyl side chain with a 3-hydroymethylphenyl group (**39b**) diminished potency and selectivity over 1C2 by 100-fold and 21-fold, respectively. When the amide was reteroinverted (**49a**), we observed isoform selectivity >2857-fold over AKR1C2, an increase of 5.6-fold as compared to **1**. Selectivity over the other isozymes, AKR1C1 and AKR1C4, increased by 1.5 and seven-fold respectively when compared to **1**. Moreover, **49a** demonstrated an IC_{50} of 0.07 μM for AKR1C3, which is a 1.5-fold increase from **1**. Additionally, **49a** also exhibited a 1.6-fold increase in LLE as compared to the *meta*-amide **39a**. Replacement of the prenyl side chain with an allyl group (**50**) resulted in a seven-fold reduction in isoform selectivity and four-fold reduction in potency in agreement with prior data (**19b**). Although compound **50** did exhibit similar selectivity over AKR1C2 with a two-fold reduction in potency as compared to our hit scaffold (**1**), replacement of the prenyl chain with a 3-hydroymethylphenyl moiety (**51**) reduced AKR1C3 inhibitory potency (three-fold from **1**) as well as selectivity (1.7-fold from **1**), although to a lesser extent than **39b** and showed an improvement in LLE value (two-fold from **1**). The *meta*-ester analogue (**52**) decreased AKR1C3 inhibitory potency by 1.7-fold and selectivity over 1C2 by five-fold from its amide counterpart (**49a**), while maintaining comparable selectivity (1C2) to **1** and equipotent inhibition for 1C3,

although LLE reduction was dramatic (3.4-fold as compared to **49a**). The ether analogues (**59a-59b**) suffered significant loss (18-46 fold) in inhibition selectivity over 1C2, a decrease in inhibition potency (two – four-fold) and a slight reduction of LLE (1.01-1.1 fold) when compared to **49a** (Table 5).

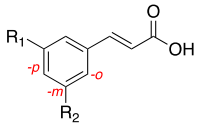

Compound	R_1	R_2	IC_{50} AKR isoform (μM)				Fold Selectivity			LLE*
			1C1	1C2	1C3	1C4	1C1: 1C3	1C2: 1C3	1C4: 1C3	
1	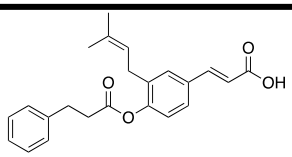 Baccharin		187	51	0.10	21	1870	510	210	1.29
39a	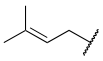	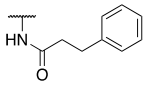	35.5% inhibition at 200 μM	94	0.13	206	>1538	723	1584	1.53
39b	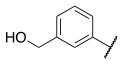	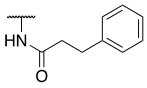	N.D.	41	1.20	N.D.	N.D.	34	N.D.	1.71
49a	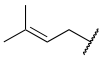	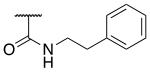	No inhibition at 200 μM	39% inhibition at 200 μM	0.07	99	>2857	>2857	1414	2.09
50		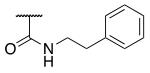	N.D.	88	0.26	N.D.	N.D.	400	N.D.	2.45
51	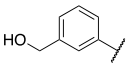	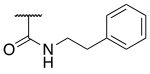	N.D.	40% inhibition at 100 μM	0.33	N.D.	N.D.	>300	N.D.	2.57
52	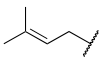	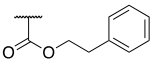	47.0% inhibition at 200 μM	62	0.12	15	>1666	517	125	0.61
59a	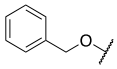	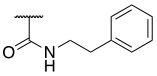	N.D.	26	0.16	N.D.	N.D.	163	N.D.	2.05
59b	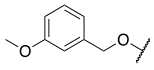	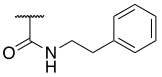	N.D.	18	0.29	N.D.	N.D.	62	N.D.	1.87

N.D.; Not Determined
AKR1C3 IC_{50} and fold selectivity over AKR1C2 highlighted in red.

IC_{50} values were performed in quadruplicate and technical replicates gave mean + SE. The SE is less than 10% and the mean value is reported.

*LLE. Ligand lipophilicity efficiency (calculated as pIC_{50}-clogP).

Table 5. Inhibitory properties of class II analogues on AKR1C1–AKR1C4.

When substitutions on the B-ring were coupled with homologation of the amide-containing chain, all the substitutions were generally well tolerated, increasing the selectivity for AKR1C3 inhibition by three – seven-fold in comparison to **1** and maintaining the inhibition potency equivalent to or greater than **1** (**49b-f**) (Table 6). The 4-fluoro (**49b**) and 4-methoxy (**49c**) substitutions on the phenethyl side chain exhibited similar inhibitory potency to **1**, increasing the selectivity over 1C2 by three-fold and 2.4-fold respectively, without any significant change in LLE over **1**. Reduction of the carbon spacer length, along with substitution with *N*,*N*-dimethyl (**49h**), methoxy (**49d**) or methyl (**49g**) groups at the 4-position on the benzyl side chain further increased the inhibitory potency as compared to **1**. Compounds **49h** and **49d** were three-fold more selective than **1**, whereas **49g** exhibited the best combination of potency (IC_{50} = 0.07 μM) and selectivity (>2800, a seven-fold increase from **1**). The 4-trifuoromethoxy benzyl containing analogue (**49e**) exhibited a similar inhibition and selectivity profile as **49b**. However, movement of the -OCF_3 group to the *meta* position (**49f**) diminished inhibitory potency by 1.2-fold and selectivity over AKR1C2 by 1.5-fold compared to **49e**. With the exception of **49d** none of the derivatives displayed an increase in the LLE value as compared to **49a** (Table 6).

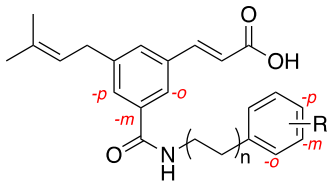

Compound	n	R	IC_{50} AKR isoform (μM)				Selectivity			LLE*
			1C1	1C2	1C3	1C4	1C1:1C3	1C2:1C3	1C4:1C3	
49b	2	4-F	No inhibition at 200 μM	148	0.10	140	>2000	1480	1400	1.80
49c	2	4-OMe	No inhibition at 200 μM	136	0.11	72	>1802	1236	649	0.98
49d	1	4-OMe	No inhibition at 100 μM	87	0.07	60	>1315	1144	789	2.27
49e	1	4-OCF_3	No inhibition at 200 μM	165	0.11	151	>1802	1500	1360	0.99

49f	1	3-OCF_3	10.6% inhibition at 200 μM	129	0.13	133	>1538	992	1023	0.93
49g	1	4-Me	No inhibition at 200 μM	66.5% inhibition at 200 μM	0.07	145	>2817	>2817	2042	1.72
49h	1	4-NMe_2	No inhibition at 100 μM	80	0.06	59	>1493	1194	880	1.27

IC_{50} values were performed in quadruplicate and technical replicates gave mean + SE. The SE is less than 10% and the mean value is reported.
*LLE. Ligand lipophilicity efficiency (calculated as pIC_{50}-clogP).

Table 6. Inhibitory properties of class II analogues on AKR1C1–AKR1C4.

Class III analogues: Boronic acid bioisosteres of carboxylic acids are expected to demonstrate increased binding affinity to their molecular targets since they would provide a strong counterion in the oxyanion hole as compared to ionic interactions with their carboxylic acid counterparts, as well as their ability to form covalent bonds with amino acid residues.[60, 61] Bioisosteric replacement of the carboxylic acid of our parent scaffold with a pinacol boronate (**7**) or a boronic acid (**7a**) decreased AKR1C3 inhibitory potency by 66- and 23-fold respectively compared to **1**, with a concurrent 500-fold decrease in selectivity, in addition to exhibiting a poor LLE profile. Removal of the prenyl moiety (**24**) abrogated bioactivity in agreement with our previous findings.[44] Surprisingly, when the amide chain was placed *ortho* relative to the carboxylic acid group (**33a**) a 1.4-fold increase in potency was observed compared to **14a** with comparable selectivity and a similar LLE as **1**. Replacement of the prenyl moiety in **33a** with a 3-hydroymethylphenyl moiety (**33b**) diminished potency and selectivity by five-fold and 12-fold respectively in comparison to **33a** without any appreciable impact in LLE (Table 7).

Compound	R_1	R_2	R_3	R_4	IC_{50} AKR1C3 (μM)	IC_{50} AKR1C2 (μM)	Selectivity 1C2:1C3	LLE*
7	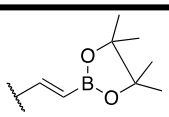	H	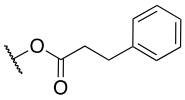	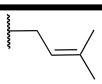	6.6	4.7	0.71	-2.89
7a	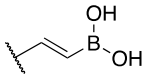	H	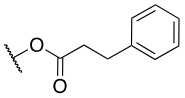		2.3	3.8	1.7	0.26
24	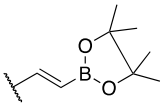	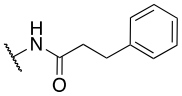	-Br	H	16.0	109	6.8	-0.93
33a	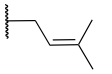	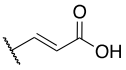	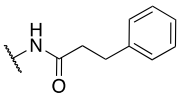	H	0.2	39	163	1.26
33b	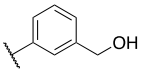	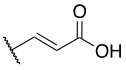	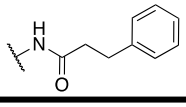	H	1.0	14	14	1.79

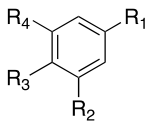

*LLE. Ligand lipophilicity efficiency (calculated as pIC_{50}-clogP).

Table 7. Inhibitory properties of class III analogues on AKR1C3 and AKR1C2.

In this study, the inhibitory potency and selectivity of several analogues of **1** against AKR1C3 were investigated. Compound **26a** showed the most potent inhibition (IC_{50}: 66 nM) whereas compound **49a** displayed the highest selectivity for AKR1C3 over AKR1C2 (IC_{50} ratio: >2857). Analysis of crystal structures of AKR1C3.$NADP^+$- inhibitor complexes have revealed that the ligand binding site can be dissected into five subsites: the oxyanion site (consisting of catalytic residues Tyr55, His117 and cofactor $NADP^+$), the steroid channel for the binding of steroid ligands, and three sub-pockets (SPs): SP1, SP2 and SP3 to accommodate other ligands.[23, 26] In the AKR1C3.$NADP^+$.**1** complex model (Figure 3A),[43] the carboxylate group on the cinnamic acid was predicted to occupy the SP1 pocket and could form hydrogen bonds with the side chain of Ser118, which contributes to strong binding affinity. In addition, several polar amino acids (e.g. Ser308 and Tyr319) also reside in the SP1 pocket of AKR1C3 which provide the possibility for ligand-protein interactions. These polar interactions would be expected to increase the selectivity of **1** for AKR1C3 over the other AKR1C isoforms where the amino acids in the corresponding positions of the SP1 pocket are Phe118, Leu308 and Phe319.[23, 26]The docking model predicted that the benzyl moiety of the 4-dihydrocinnamoyloxy group was located in the SP3 pocket and could form hydrophobic interactions with the side chain of Gln222 or Phe306 to provide high binding affinity.[43] In addition, recent studies have shown that polar substitutions (e.g. hydroxyl and carboxylate group) on the phenyl ring of the cinnamic acid, or the phenyl ring of the 4-dihydroxycinnamoyloxy group decreased inhibition for AKR1C3[43, 45, 62]. For example, the displacement of the 4-dihydrocinnamoyloxy group by a hydroxyl group to form drupanin (**1a**) resulted in a loss of inhibitory potency (IC_{50}: 15 μM) and only a seven-fold selectivity for AKR1C3 versus AKR1C2. Increase or decrease of carbon spacer along with replacement of the B-ring in class I analogues exhibited low or sub-micromolar inhibition activities (**8h**-**8n**) but still exhibited >50-fold isoform selectivity. In order to impart hydrolytic stability to our derivatives, replacement of the ester functional group with an amide was performed. The corresponding amide bioisosteres displayed diminished potency and selectivity (**14a**-**14e**) suggesting that the increased rigidity of the side chain amide is not tolerated at the *para*-position of the A ring. The B-ring substitutions on the dihydrocinnamoyloxy moiety were very well tolerated and only a marginal reduction of potency and selectivity was observed (**8b**-**8g**).

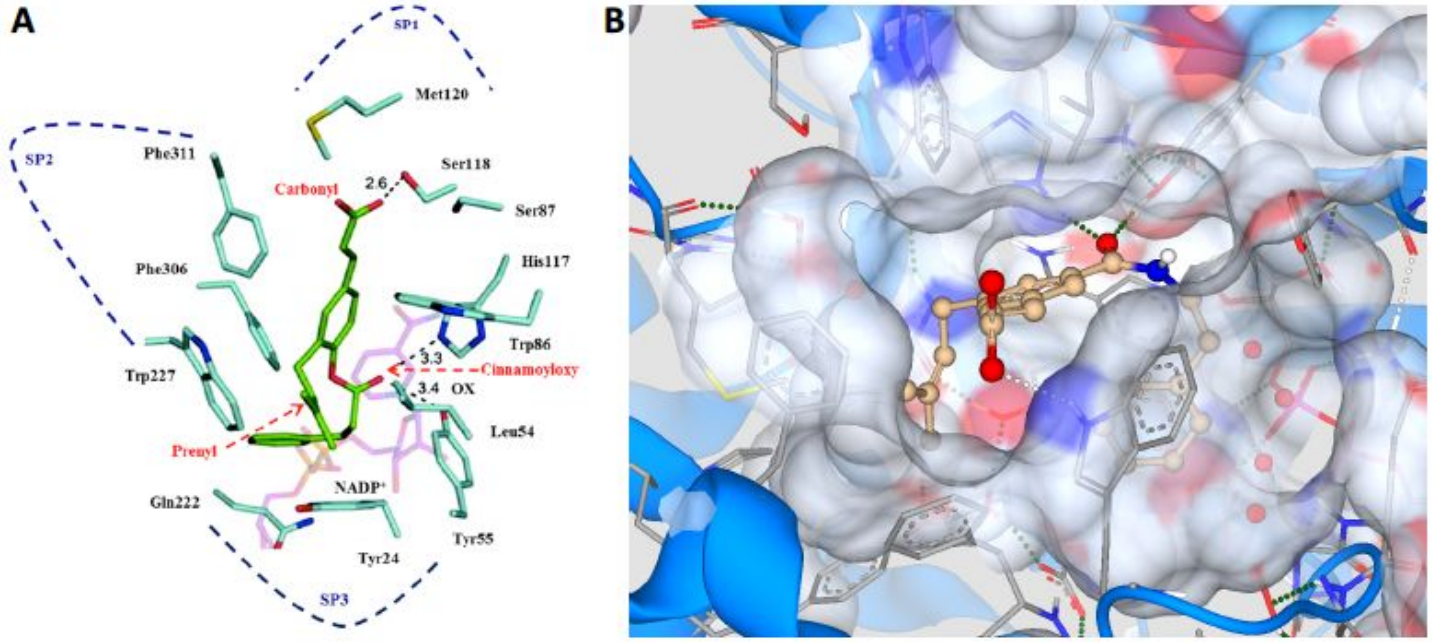

Figure 3. Modeling of parent compound (**1**) and the most selective analogue **49a**. A) Model of the AKR1C3.NADP$^+$.**1** complex. AKR1C3 residues (light blue); NADP$^+$ (pink); and baccharin (green). Dotted line: possible hydrogen bond; OX: oxyanion site; SP: subpocket. The docking model of AKR1C3. NADP$^+$.**1** complex was constructed by calculation using the program Glide 5.0. The generated docking structure showing the highest score was selected for further structural analysis. The crystal structure of AKR1C3.NADP$^+$ complex was chosen from RCSB protein data bank (PDB code: 1S2C). Reproduced with permision from reference.[43] B) Quantitative structure activity-relationship prediction of analogue **49a** (gold) with amino acid residues of the AKR1C3 binding site (grey). Green dotted line: strong predicted hydrogen bond; white dotted line: weak predicted hydrogen bond. Model constructed with SeeSAR 8.1 (BioSolveIT GmbH) using AKR1C3 protein from RCSB protein data bank (PDB code: 3UG8).

When the substitution pattern of the dihydrocinnamoyloxy side chain was changed to the *meta*-position (analogues **19a** and **26a**) the inhibitory potency increased in comparison to **1**. The presence of either a carbonyl or carboxylate group is required to anchor many ligands to the oxyanion site because it can form a strong hydrogen-bond with Tyr55 and His117 and bring the ligands into close proximity of the nicotinamide head group of the cofactor.[26] Based on the model of baccharin-docked into the AKR1C3-NADP$^+$ complex structure (Figure 3A),[43] the carbonyl of the 4-dihydrocinnamoyloxy group of **1** was found to be close to the oxyanion site and could form a hydrogen bond interaction with Tyr55 and His117, which could contribute to the high inhibitory potency. Thus, it seems plausible that in the meta substituted analogues, the change in the position of the carbonyl group

results in close proximity to the oxyanion site; imparting enhanced potency due to a shorter hydrogen bond distance. The presence of a side chain amide (**26a**) increased potency even further, along with exhibiting good tolerability of B-ring substituents (**26b-l**). Further modification of the side chain substitution pattern did not increase potency or selectivity (**33a**-**33b**). Contrary to expectation, the boronic acid analogue (**7a**) lost inhibition potency by more than ten-fold and abrogated isoform-selectivity.

Modelling experiments performed on compound **49a** (Figure 3B), predict that the designed derivatives with a retroinverted amide group (**49a**-**h**, **51** and **52)** form a stronger hydrogen bond interaction in comparison to their non-inverted counterparts (**39a** and **39b**) within the oxyanion site, due to the switch in position of the carbonyl group, resulting in formation of a shorter hydrogen bond to amino acid residues Tyr55 and His117, leading in turn to superior inhibitory potency and selectivity. Substituting the side chains in a 1,3,5 arrangement at the central A-ring places the prenyl chain in close proximity to the hydrophobic amino acid residues of the SP2 subpocket that imparts strong hydrophobic interactions and increases selectivity over the closely related isoforms AKR1C1 and AKR1C2 that do not possess this open pocket. This is further supported by the observation that removal of the terminal methyl groups to form the allyl derivative (**50**) results in reduced potency and selectivity as this would be expected to result in retraction of the chain from the open pocket, weakening the hydrophobic interactions. This model also predicts the formation of a hydrogen bond between the carboxylic acid of compound **49a** and the Trp227 residue, rather than Ser118 residue as in the parent compound **1**. Homologation of the carbon linker between the two phenyl rings to reduce the length results in little observable effect (compare **49a** and **49g**) as the area occupied by the terminal phenyl ring in analogues with either one or two methylene groups is rich in pi systems that can maintain the predicted pi-pi stacking interactions.

Evaluation of AKR1C3 inhibitors in leukemic cell models.

The hit compound **1**, *m*-amide analogue (**26a**) and 1,3,5 trisubstituted analogues **49a** and **49g** were selected for further studies in AML cell models as they represent a range of the most active (AKR1C3 IC_{50} = 0.105, 0.066,

0.07 and 0.07 μM respectively) and selective (AKR1C3 fold selectivity of 420, 109, 2857 and 2817 respectively) AKR1C3 inhibitors. Consistent with our previous findings,[47] the inhibitors did not induce cytotoxicity in a panel of AML cell lines up to concentrations as high as 100 μM with the exception of **26a** that did not reduce AML cell viability up to 50 μM (SI Figures S1-S3). Low inhibitor concentrations of 0.1, 1 and 10 μM were chosen to evaluate the adjuvant effect of AKR1C3 inhibitor in combination with clinically approved chemotherapeutic agents. The AML cell lines HL-60 (M3 sub-type),[47] KG1a (M0 subtype) and THP-1 (M5 subtype), expressing varying levels of AKR1C3 along with AKR1C3 overexpressing (SI Figure S4) primary patient-derived T-ALL cells (COG-LL-317h and COG-LL-329h) were chosen to evaluate the effects of AKR1C3 inhibitors.

Synergistic effect of combination AKR1C3 inhibitor and daunorubicin in AML cell lines

Daunorubicin, an anthracycline used as front-line treatment for AML[63, 64] and as induction chemotherapy for T-ALL,[11] is most susceptible to AKR1C3-mediated metabolism among all the anthracycline chemotherapeutic agents, rendering the agent inactive.[65] In order to evaluate if a combination of an AKR1C3 inhibitor with daunorubicin provides a synergistic effect, a dose response curve of daunorubicin in AML cells was first obtained (SI Figure S5) and AKR1C3 inhibitors were then dosed with daunorubicin in a fixed ratio of 100:1 (inhibitor : daunorubicin). Combination co-treatments of AKR1C3 inhibitors **1**, **26a**, **49a** or **49g** with daunorubicin did not reduce cell viability beyond what was observed with daunorubicin treatment alone. The combination, when analyzed by the Chou-Talalay method,[66] showed a slight antagonistic to additive effect, in HL-60 cells (M3) with all the inhibitors tested (CI = 1.2 – 2.3), with the exception of **49a** which was weakly synergistic (CI = 0.8). In KG1a cells (M0) which are daunorubicin-resistant,[67, 68] none of the co-treatments of AKR1C3 inhibitors with daunorubicin reduced cell viability by more than 50%. Only concentrations of 0.1–10 μM AKR1C3 inhibitors with 0.01 μM daunorubicin were able to reduce cell viability to >50% in THP-1 cells (M5) (SI Figure S6).

Pre-treatment of AKR1C3 inhibitors for 24 h followed by daunorubicin exposure for a further 72 h enhanced the cytotoxicity of the anthracycline in HL-60 cells. A near complete reduction in cell viability reduction was observed following pre-treatment with an AKR1C3 inhibitor followed by 0.1 μM daunorubicin. When the effect

was quantified, a strong to moderate drug synergism was noted (CI = 0.2 - 0.7) (Figure 4A and Table insert). The daunorubicin-resistant KG1a cells with high AKR1C3 expression displayed a complete abrogation of cell viability when pre-treated with AKR1C3 inhibitors at 0.1 μM concentration followed by 0.001 μM daunorubicin. A very strong synergistic drug effect with all inhibitors was seen (CI = >0.01), providing a chemotherapeutic dose reduction of >100-fold (DRI >100) and reducing the combination IC_{50} to <0.01 μM, indicating complete reversal of daunorubicin-resistance (Figure 4B and Table insert). A complete reduction in cell viability reduction was also observed in THP-1 cells following pre-treatment with all AKR1C3 inhibitors followed by 0.1 and 1 μM daunorubicin treatment and a 50% reduction in cell viability was seen with 0.01 μM daunorubicin when this concentration of daunorubicn alone had no effect on cell viability. A strong synergism was established in THP-1 cells (CI = 0.06 – 0.1) where the reduction in IC_{50} value of daunorubicin was greater than seven-fold. The more selective compounds **49a** and **49g** provided a greater reduction (DRI = 16) in chemotherapeutic dosing as compared to **1** and **26a** (DRI = 6.6 - 8.3) (Figure 4C and Table insert). Further, a direct correlation is observed between AKR1C3 expression in AML cell lines (KG1a>>THP-1>HL-60) (SI Figure S4) with the synergistic effect and dose reduction index. Overall, such high degree of drug synergism can be attributed to the inhibitory potency of compounds **1**, **26a**, **49a** and **49g** for AKR1C3 24 h prior to daunorubicin exposure in pre-treatment experiments as compared to the co-treatments where only an additive to moderate synergism was observed.

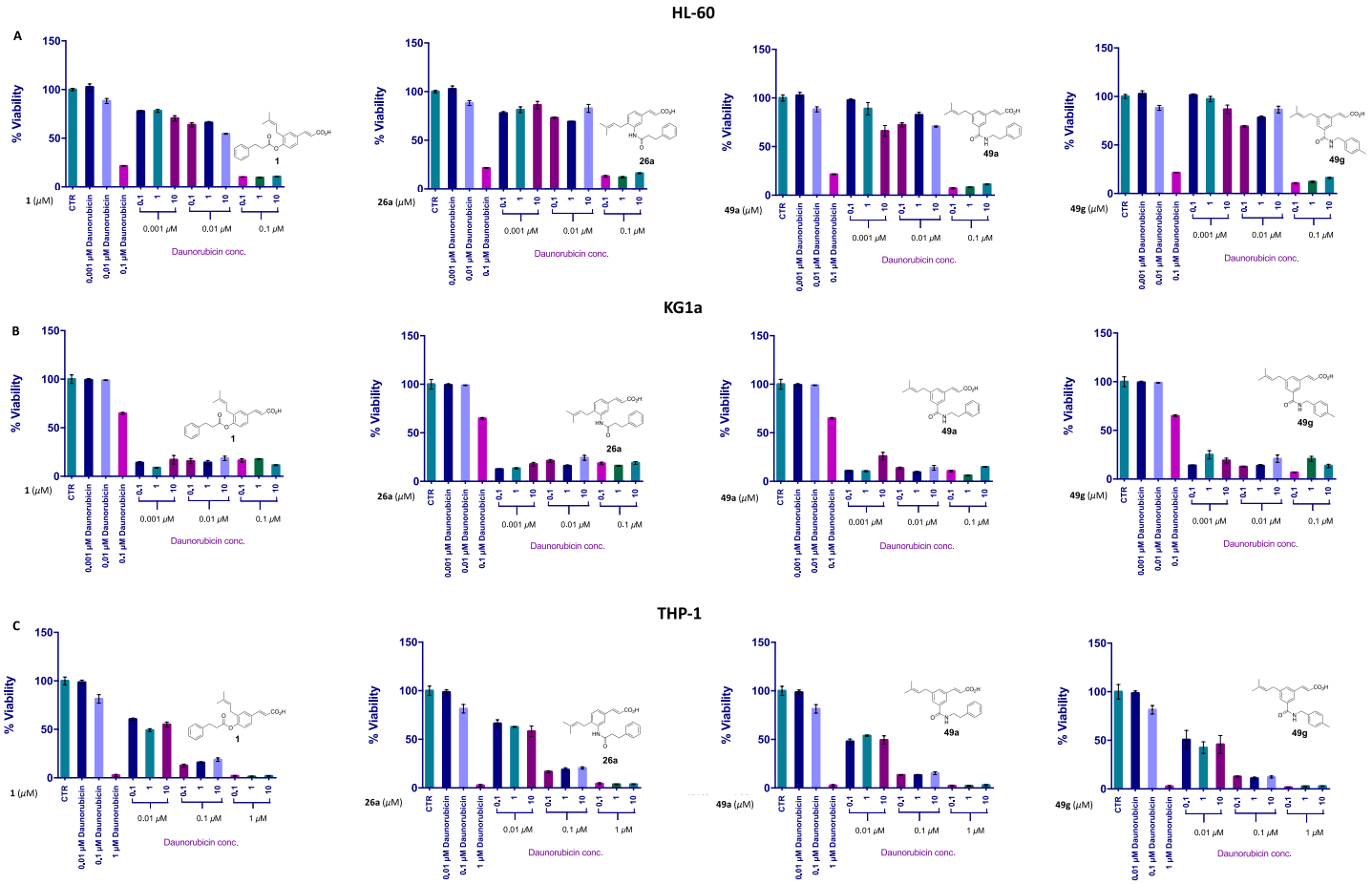

Compound	Selectivity 1C2:1C3	HL-60			KG1a			THP-1		
		CI[a]	DRI[b]	IC_{50}* (μM)	CI[a]	DRI[b]	IC_{50}* (μM)	CI[a]	DRI[b]	IC_{50}* (μM)
1	420	0.2	4.2	<0.01	<0.01	>100	<0.01	0.1	8.3	0.02
26a	109	0.3	3.0	0.01	<0.01	>100	<0.01	0.1	6.6	0.03
49a	>2857	0.5	1.7	0.02	<0.01	>100	<0.01	0.06	15.8	<0.01
49g	>2817	0.7	1.3	0.03	<0.01	>100	<0.01	0.06	15.9	<0.01
Daunorubicin	N/A	N/A	N/A	0.05	N/A	N/A	0.2	N/A	N/A	0.2

*Calculated for Daunorubicin + AKR1C3 inhibitor (μM)
[a]Combination index
[b]Dose reduction index
N/A; not applicable

Figure 4. Combination treatment of AKR1C3 inhibitors with daunorubicin in AML cells. Percentage cell viability after 24 h pre-treatment with **1**, **26a**, **49a** and **49g** followed by a 72 h exposure of daunorubicin in (A) HL-60 (B) KG1a and (C) THP-1 cells at indicated concentrations. Table insert showing the quantification of drug interactions.

Synergistic effect of combination AKR1C3 inhibitor and cytarabine in AML cell lines

The first line AML chemotherapeutic cytarabine (AraC) was combined with AKR1C3 inhibitors under a similar dosing regimen as described above. To the best of our knowledge, no relationship has been established between the enzymatic activity of AKR1C3 and sensitivity of leukemic cells to AraC. Upon co-treatment of

AKR1C3 inhibitors with AraC in HL-60 cells the change in cell viability reduction closely matched that of AraC alone (SI Figure S5). Effects ranged from moderate synergism (compounds **1** and **7**) (CI = 0.5) to slight antagonism (**4**) (CI = 3.4) to addition (**6**) (CI = 1). Similarly, KG1a and THP-1 cell lines displayed nearly identical dose response curves for AraC in the presence and absence of all AKR1C3 inhibitors. Only an additive drug effect was observed for the combination that was consistent among all tested inhibitors (CI = 0.9 – 1.4) (SI Figure S7 and Table insert).

The 24 h pre-treatment experiments with AKR1C3 inhibitors followed by AraC exposure provided strong synergistic effects in HL-60 cells. Combination index values ranged from 0.02–0.09 that provided a dose reduction in AraC ranging from 10–33-fold (Figure 5A and Table insert). Similar to the observations made with pre-treatment with AKR1C3 inhibitors followed by daunorubicin in the high AKR1C3 expressing KG1a cells, AKR1C3 inhibitor pre-treatments followed by AraC exposure also abrogated the cell viability at all compound concentrations; displaying a very strong degree of synergistic drug effect with all inhibitors (CI = <0.01). A chemotherapeutic DRI of >100-fold was achieved that reduced the combination IC_{50} to <0.01 μM (Figure 5B and Table insert). Similarly, a strong synergism was observed in THP-1 cells (CI = 0.05–0.07) where the reduction in IC_{50} value of AraC was greater than 13-fold (Figure 5C and Table insert).

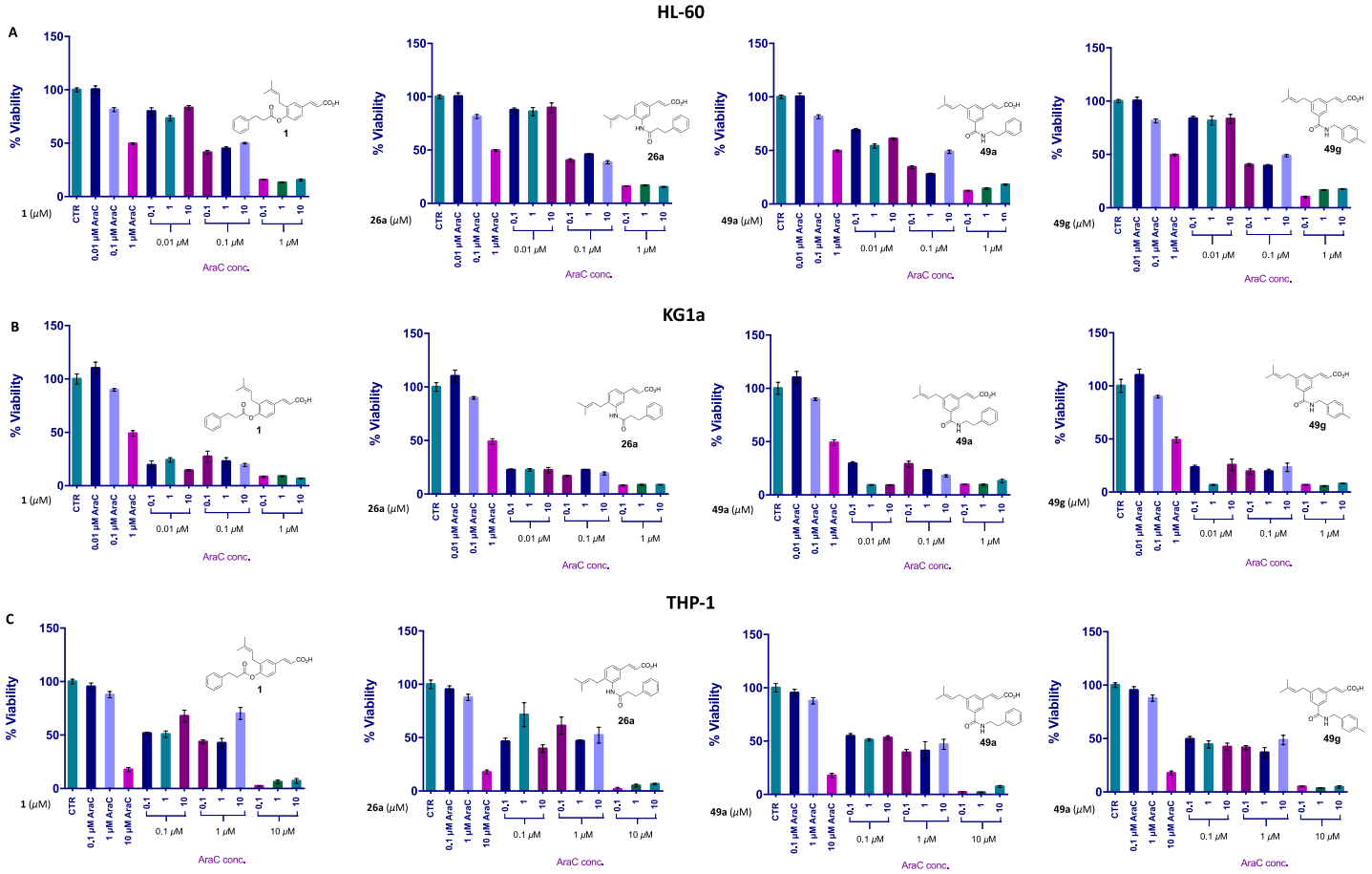

Compound	Selectivity 1C2:1C3	HL-60			KG1a			THP-1		
		CI[a]	DRI[b]	IC_{50}* (μM)	CI[a]	DRI[b]	IC_{50}* (μM)	CI[a]	DRI[b]	IC_{50}* (μM)
1	420	0.07	13.3	0.07	<0.01	>100	<0.01	0.06	15	0.2
26a	109	0.09	10.3	0.09	<0.01	>100	<0.01	0.05	18	0.1
49a	>2857	0.02	33	0.03	<0.01	>100	<0.01	0.07	13	0.2
49g	>2817	0.08	12	0.08	<0.01	>100	<0.01	0.05	18	0.1
AraC	N/A	N/A	N/A	1.0	N/A	N/A	0.2	N/A	N/A	2.8

*Calculated for AraC + AKR1C3 inhibitor (μM)
[a]Combination index
[b]Dose reduction index
N/A; not applicable

Figure 5. Combination treatment of AKR1C3 inhibitors with AraC in AML cells. Percentage cell viability after 24 h pre-treatment with **1**, **26a**, **49a** and **49g** followed by a 72 h exposure of AraC in (A) HL-60 (B) KG1a and (C) THP-1 cells at indicated concentrations. Table insert showing the quantification of drug interactions.

Synergistic effect of AKR1C3 inhibition in primary patient-derived T-ALL cells

For further evaluation of the adjuvant effects of AKR1C3 inhibitors, primary patient-derived T-ALL cells were employed as an in vitro model. The Children's Oncology Group COG-317h cell line represents a cell line derived

from samples of pediatric patients who relapsed after chemotherapy, whereas COG-329h cells were derived from samples of pediatric patients prior to chemotherapy treatment. After individual dose response curves of **49a**, daunorubicin and AraC were obtained (SI Figure S8), compound **49a**, possessing the best combination of AKR1C3 inhibitory potency (IC_{50} = 0.07 μM) and isoform selectivity (>2857), demonstrated a very strong synergistic drug effect in both COG-317h and COG-329h cells, when co-treated with daunorubicin (DRI = 19.8 and 13.0 respectively) (Figure 6A and Table insert).

The degree of drug synergism increased even further among pre-treatment experiments (DRI >100) and a near complete abrogation of cell viability was noted in COG-317h cells (Figure 6B and Table insert). Both co-treatment and pre-treatments of **49a** with AraC showed a very strong synergism in COG-317h cells (DRI >100). In COG-329h cells, the effect increased from a DRI of 15.7, among co-treatments, to >100 in pre-treatment experiments (Figure 6C, D and Table insert). Thus, the combination of our developed AKR1C3 inhibitors with either daunorubicin or AraC in patient-derived T-ALL cells reduces the IC_{50} of both clinically approved chemotherapeutics to less than one nanomolar.

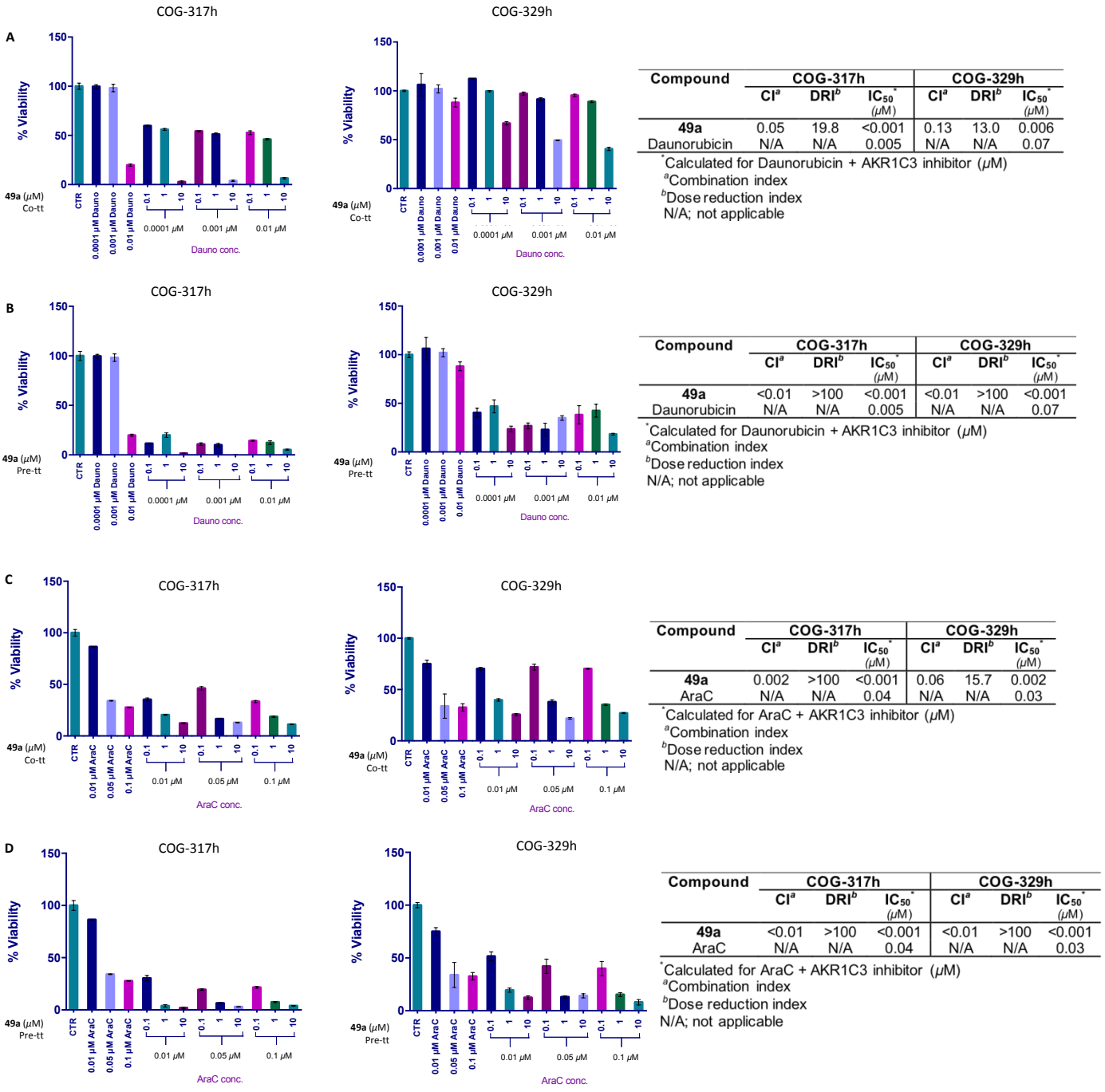

Compound	COG-317h			COG-329h		
	CI[a]	DRI[b]	IC50* (μM)	CI[a]	DRI[b]	IC50* (μM)
49a	0.05	19.8	<0.001	0.13	13.0	0.006
Daunorubicin	N/A	N/A	0.005	N/A	N/A	0.07

*Calculated for Daunorubicin + AKR1C3 inhibitor (μM)
[a]Combination index
[b]Dose reduction index
N/A; not applicable

Compound	COG-317h			COG-329h		
	CI[a]	DRI[b]	IC50* (μM)	CI[a]	DRI[b]	IC50* (μM)
49a	<0.01	>100	<0.001	<0.01	>100	<0.001
Daunorubicin	N/A	N/A	0.005	N/A	N/A	0.07

*Calculated for Daunorubicin + AKR1C3 inhibitor (μM)
[a]Combination index
[b]Dose reduction index
N/A; not applicable

Compound	COG-317h			COG-329h		
	CI[a]	DRI[b]	IC50* (μM)	CI[a]	DRI[b]	IC50* (μM)
49a	0.002	>100	<0.001	0.06	15.7	0.002
AraC	N/A	N/A	0.04	N/A	N/A	0.03

*Calculated for AraC + AKR1C3 inhibitor (μM)
[a]Combination index
[b]Dose reduction index
N/A; not applicable

Compound	COG-317h			COG-329h		
	CI[a]	DRI[b]	IC50* (μM)	CI[a]	DRI[b]	IC50* (μM)
49a	<0.01	>100	<0.001	<0.01	>100	<0.001
AraC	N/A	N/A	0.04	N/A	N/A	0.03

*Calculated for AraC + AKR1C3 inhibitor (μM)
[a]Combination index
[b]Dose reduction index
N/A; not applicable

Figure 6. Combination treatment of AKR1C3 inhibitors with daunorubicin and AraC in patient-derived primary T-ALL cells. Percentage cell viability of indicated cell lines after treatment with the indicated concentrations of daunorubicin and AKR1C3 inhibitor **49a** as (A) co-treatments and (B) 24-h pre-treatments. Percentage cell viability of indicated cell lines after treatment with the indicated concentrations of AraC and **49a** a as (C) co-treatments and (D) 24-h pre-treatments. Table insert showing the quantification of drug interactions.

Effect of AKR1C3 inhibition in primary bone marrow mononuclear cells (BMMNC):

In order to evaluate the selective chemotherapeutic potentiation of AKR1C3 inhibitor **49a** towards leukemic cells, 24 h pre-treatment experiments with **49a** followed by incubation with AraC or daunorubicin were performed in primary bone marrow mononuclear cells. No chemotherapeutic potentiation was noted with either AraC or daunorubicin combination treatments (SI Figure S9).

CONCLUSIONS:

The current study revealed a detailed SAR map for inhibition of AKR1C3 around the chemotype of **1**. The 1,3,5 *meta*-substituted retroinverted amides are disclosed as the most selective inhibitors of AKR1C3 across all known inhibitor classes reported thus far; a first of their kind to exhibit exquisite selectivity (>2857-fold) for AKR1C3 inhibition with inhibitory potency in the nanomolar range. These agents carry a potential to be further developed into advanced lead compounds and span applicability across a diverse variety of malignancies that are AKR1C3-dependent.

Inhibitors of AKR1C3 derived from modification of a natural product possess enhanced biological stability and exhibit extremely high selectivity and potency. Proof-of-concept that AKR1C3 inhibitors derived from **1** have a synergistic effect to sensitize AML and primary T-ALL cells to the chemotherapeutic effects of daunorubicin and AraC is demonstrated. These findings are in agreement to prior reports by us, and others, that establish an adjuvant effect of AKR1C3 inhibitors in combination with various chemotherapeutic agents.[46, 69] Treatment of the non-toxic AKR1C3 inhibitors in *in vitro* models of AML representing various French–American–British (FAB) sub-types of AML (M0, M3 and M5), along with co-administration of a range of clinical chemotherapeutics results in a synergistic drug action; potentiating cytotoxicity and reducing the IC_{50} value. This is contrary to recent reports detailing selective AKR1C3 inhibitors do not perform an adjuvant role as compared to pan-AKR1C isoform inhibitors. This observation is further extended to the primary patient-derived T-ALL cells where a very strong potentiation of the effects of daunorubicin and AraC was established.

Further development of the inhibitors described herein represents a significant drug discovery opportunity for the identification of potent adjuvants to enhance the therapeutic index of chemotherapeutics in the hope of availing this treatment regime to pediatric and geriatric leukemia patients.

EXPERIMENTAL SECTION

Chemistry: All reactions were carried out in oven- or flame-dried glassware under positive nitrogen pressure unless otherwise noted. Reaction progress was monitored by thin-layer chromatography (TLC) carried out on silica gel plates (2.5 cm x 7.5 cm, 200 μm thick, 60 F254) and visualized by using UV (254 nm) or by potassium permanganate and/or phosphomolybdic acid solution as indictor. Flash column chromatography was performed with silica gel (40-63 μm, 60 Å) using the mobile phase indicated or on a Teledyne Isco (CombiFlash R_f 200 UV/Vis). Commercial grade solvents and reagents were purchased from Fisher Scientific (Houston, TX), Sigma Aldrich (Milwaukee, WI) or for Prenyl boronic acid pinacol ester, Santa Cruz Biotechnology (Dallas, TX) and were used without further purification except as indicated. Anhydrous solvents were purchased from Across Organics and stored under an atmosphere of dry nitrogen over molecular sieves.

^{1}H, ^{13}C, COSY, HMQC and DEPT NMR spectra were recorded in the indicated solvent on a Bruker 400 MHz Advance III HD spectrometer at 400 and 100 MHz for ^{1}H and ^{13}C respectively with TMS as an internal standard. Multiplicities are indicated by s (single), d (doublet), dd (doublet of doublets), t (triplet), q (quartet), m (multiplet), br (broad). Chemical shifts (δ) are reported in parts per million (ppm), and coupling constants (*J*), in hertz. High resolution mass spectroscopy was performed on a LC/MS IT- TOF (Shimadzu) using an ESI source conducted at the University of Texas at Arlington, Shimadzu Center for Advanced Analytical Chemistry. High-pressure liquid chromatography was performed on a Gilson HPLC system with 321 pumps and a 155 UV/vis detector using Trilution software v2.1 with a Phenomenex® Luna (C18 100A, 250x4.6 mm) column. All final compounds were assessed to be of >96% purity and were consistent with their HRMS data.

General procedure A: Synthesis of ester intermediates: To a solution of 4-iodo-2-(3-methylbut-2-en-1-yl)phenol (**3**) (1 equiv) in DCM (5 mL) was added DMAP (0.1 equiv) followed by addition of substituted acid

chloride (1.5 equiv) and NEt_3 (1.5 equiv). The mixture was stirred overnight at RT. Saturated $NaHCO_3$ was added and the layers seperated. The organic layer was washed with H_2O, dried (Na_2SO_4), filtered and concentrated. The crude product was purified by column chromatography using Hexane/EtOAc gradient (10:1, 4:1, 2:1) and solvent evaporated *in vacuo* to provide pure esterified compounds.

General procedure B: *tert*-Butyl ester hydrolysis: To a solution of substituted *tert*-butyl intermediates in toluene was added chromatography grade silica gel and the mixture was refluxed with vigorous agitation overnight.[52] Upon cooling the reaction mixture was diluted with 10% methanol in DCM and filtered over celite® pad using 10% methanol in DCM as the solvent. The crude product was purified by column chromatography using DCM/MeOH gradient (20:1, 10:1) and solvent evaporated *in vacuo* to provide the final compounds.

(*E*)-3-(3-(3-methylbut-2-en-1-yl)-4-((3-phenylpropanoyl)oxy)phenyl)acrylic acid (**1**)[47]: Compound **6a** (280 mg, 0.6 mmol) was hydrolyzed following the general procedure B. The solvent was evaporated *in vacuo* and purified by column chromatography (Hexane:EtOAc = 9:1, 4:1, 2:1, 1:1) to provide the title compound as a white solid (140 mg, 0.4 mmol, 66%). **R_f:** 0.1 (Hexane:EtOAc, 4:1) **^{1}H NMR (400 MHz, $CDCl_3$):** δ 1.69 (3H, s, CH_3), 1.77 (3H, s, CH_3), 2.94 (2H, t, *J* = 7.7 Hz, CH_2), 3.11 (2H, t, *J* = 7.6 Hz, CH_2), 3.17 (2H, d, *J* = 7.4 Hz, CH_2), 5.20 (1H, t, *J* = 7.3 Hz, CH), 6.40 (1H, d, *J* = 16 Hz, CH), 7.00 (1H, d, *J* = 8.3 Hz, ArCH) 7.24-7.42 (7H, m, ArCH), 7.75 (1H, d, *J* = 16 Hz, CH). **^{13}C NMR (100 MHz, $CDCl_3$):** δ 17.8, 25.7, 28.4, 30.8, 35.8, 116.7, 120.8, 122.8, 126.5, 126.8, 128.6, 130.1, 131.9, 133.9, 134.3, 139.9, 146.3, 150.6, 170.6, 171.0. **ESI-HRMS** (*m/z*): [M - H]$^-$ calcd for $C_{23}H_{24}O_4$, 363.1602; found, 363.1620.

(*E*)-2-(3-methylbut-2-en-1-yl)-4-(2-(4,4,5,5-tetramethyl-1,3,2-dioxaborolan-2-yl)vinyl)phenyl 3-phenylpropanoate (**7**): To a solution of **5a** (350 mg, 0.8 mmol) in dry toluene (8 mL) was added PPh_3 (27 mg, 0.1 mmol), $Pd(OAc)_2$ (12 mg, 0.05 mmol) and NEt_3 (0.3 mL, 2 mmol) the mixture was sitirred for 10 min and 4,4,5,5-tetramethyl-2-vinyl-1,3,2-dioxaborolane (0.2 mL, 1 mmol) was added and the reaction refluxed overnight. The reaction was allowed to cool and was washed with a saturated aqueous NH_4Cl, water and extracted in DCM,

dried (Na_2SO_4), filtered and concentrated. Purification by column chromatography (Hexane:EtOAc = 10:1, 4:1) provided the title compound as a yellow oil (70 mg, 0.15 mmol, 20%). **R_f:** 0.74 (Hexane:EtOAc, 4:1) **^{1}H NMR (400 MHz; $CDCl_3$):** δ 1.34 (12H, s, CH_3), 1.68 (3H, s, CH_3), 1.76 (3H, s, CH_3), 2.92 (2H, t, *J* = 7.1 Hz, CH_2), 3.11 (2H, t, *J* = 7.8 Hz, CH_2), 3.14 (2H, d, *J* = 7.8 Hz, CH_2), 5.20 (1H, t, *J* = 7.8 Hz, CH), 6.12 (1H, d, *J* = 18.4 Hz, CH), 6.93 (1H, d, *J* = 8.6 Hz, ArCH), 7.23 – 7.39 (8H, m, ArCH and CH). **^{13}C NMR (100 MHz; $CDCl_3$):** δ 17.8, 24.8, 25.7, 28.4, 30.9, 35.8, 83.3, 121.1, 122.2, 125.5, 128.3, 128.3, 128.5, 128.6, 128.7, 133.5, 133.5, 135.4, 140.0, 148.7, 149.2, 171.1. **ESI-HRMS** (*m/z*): $[M + Na]^+$ calcd for $C_{28}H_{35}BO_4$, 469.2526; found, 469.2522.

(*E*)-(3-(3-methylbut-2-en-1-yl)-4-((3-phenylpropanoyl)oxy)styryl)boronic acid (**7a**): The solution of **7** (20 mg, 0.05 mmol) in 1:1 MeOH/H_2O was stirred at 80°C overnight. The reaction was allowed to cool and washed with saturated aqueous NH_4Cl, brine, extracted with DCM, dried (Na_2SO_4), filtered and concentrated. Purification by column chromatography (Hexane:EtOAc = 12:1, 9:1, 4:1, 2:1, 1:1) provided the title compound as a white solid (5 mg, 0.01 mmol, 20%). **R_f:** 0.1 (Hexane:EtOAc, 4:1) **^{1}H NMR (400 MHz; $CDCl_3$):** δ 1.68 (3H, s, CH_3), 1.73 (3H, s, CH_3), 2.94 (2H, t, *J* = 7.2 Hz, CH_2), 3.06 (2H, t, *J* = 7.5 Hz, CH_2), 3.11 (2H, d, *J* = 7.4 Hz, CH_2), 5.16 (1H, t, *J* = 7.2 Hz, CH), 6.31 (1H, d, *J* = 18.0 Hz, CH), 6.90 (1H, d, *J* = 8.2 Hz, ArCH), 7.20 – 7.34 (7H, m, ArCH and CH), 7.39 (1H, dd, J_1 = 2.1 Hz, J_2 = 8.3 Hz, ArCH). **^{13}C NMR (100 MHz; $CDCl_3$):** δ 16.5, 24.4, 28.2, 30.4, 35.2, 121.4, 122.2, 124.9, 126.0, 128.0, 128.1, 128.3, 132.6, 133.6, 135.8, 140.2, 147.1, 149.2, 171.5.

(*E*)-3-(4-((3-(2-fluorophenyl)propanoyl)oxy)-3-(3-methylbut-2-en-1-yl)phenyl)acrylic acid (**8b**): Compound **6b** (250 mg, 0.6 mmol) was hydrolyzed following the general procedure B. Solvent was evaporated *in vacuo* to provide the title compound as a white solid (78 mg, 0.2 mmol, 35%). **R_f:** 0.16 (Hexane:EtOAc, 4:1) **^{1}H NMR (400 MHz, MeOD):** δ 1.67 (3H, s, CH_3), 1.72 (3H, s, CH_3), 2.93 (2H, t, *J* = 7.3 Hz, CH_2), 3.13 (2H, t, *J* = 7.1 Hz, CH_2), 3.12 (2H, d, *J* = 7.1 Hz, CH_2), 5.14 (1H, t, *J* = 7.1 Hz, CH), 6.41 (1H, d, *J* = 15.9 Hz, CH), 6.98 (1H, d, *J* = 8.2 Hz, ArCH), 7.05 – 7.13 (2H, m, ArCH), 7.23 – 7.28 (1H, m, ArCH), 7.33 (1H, t, *J* = 7.6 Hz,

ArCH), 7.41 – 7.45 (2H, m, ArCH), 7.62 (1H, d, J = 15.9 Hz, CH). **^{13}C NMR (100 MHz, MeOD):** δ 16.5, 23.9, 24.4, 28.2, 33.6, 114.7, 114.9, 117.9, 121.1, 122.7, 124.0, 126.3, 128.1, 129.5, 130.5, 132.2, 133.0, 134.2, 144.0, 150.4, 168.8, 171.0. **ESI-HRMS** (*m/z*): [M - H]$^-$ calcd for $C_{23}H_{23}O_4F$, 381.1508; found, 381.1515.

(*E*)-3-(4-((3-(3-fluorophenyl)propanoyl)oxy)-3-(3-methylbut-2-en-1-yl)phenyl)acrylic acid (**8c**): Compound **6c** (260 mg, 0.6 mmol) was hydrolyzed following the general procedure B. Solvent was evaporated *in vacuo* to provide the title compound as a white solid (103 mg, 0.3 mmol, 45%). **R_f:** 0.18 (Hexane:EtOAc, 4:1) **^{1}H NMR (400 MHz, MeOD):** δ 1.67 (3H, s, CH_3), 1.73 (3H, s, CH_3), 2.98 (2H, t, J = 7.0 Hz, CH_2), 3.07 (2H, t, J = 7.7 Hz, CH_2), 3.12 (2H, d, J=7.1 Hz, CH_2), 5.15 (1H, t, J = 7.2 Hz, CH), 6.42 (1H, d, J = 15.9 Hz, CH), 6.93 – 6.99 (2H, m, ArCH), 7.06 (1H, d, J = 8.4 Hz, ArCH), 7.12 (1H, d, J = 7.6 Hz, ArCH), 7.32 (1H, q, J_1 = 6.1 Hz, J_2 = 7.9 Hz, ArCH), 7.43 (1H, s, ArCH), 7.46 (1H, dd, J_1 = 2.1 Hz, J_2 = 8.3 Hz, ArCH), 7.63 (1H, d, J = 15.9 Hz, CH). **^{13}C NMR (100 MHz, MeOD):** δ 16.5, 24.4, 28.1, 29.9, 30.0, 34.7, 112.8, 114.9, 117.9, 121.0, 122.6, 123.9, 126.3, 129.5, 129.8, 132.3, 133.0, 134.2, 143.0, 144.0, 150.4, 161.7, 168.8, 171.1. **ESI-HRMS** (*m/z*): [M - H]$^-$ calcd for $C_{23}H_{23}O_4F$, 381.1508; found, 381.1493.

(*E*)-3-(4-((3-(4-fluorophenyl)propanoyl)oxy)-3-(3-methylbut-2-en-1-yl)phenyl)acrylic acid (**8d**): Compound **6d** (160 mg, 0.36 mmol) was hydrolyzed following the general procedure B. Solvent was evaporated *in vacuo* to provide the title compound as a white solid (72 mg, 0.2 mmol, 52%). **R_f:** 0.16 (Hexane:EtOAc, 4:1) **^{1}H NMR (400 MHz, MeOD):** δ 1.65 (3H, s, CH_3), 1.72 (3H, s, CH_3), 2.92 (2H, t, J = 7.2 Hz, CH_2), 3.08 (2H, t, J = 7.0 Hz, CH_2), 3.17 (2H, d, J=7.4Hz, CH_2), 5.13 (1H, t, J = 7.0 Hz, CH), 6.40 (1H, d, J = 15.9 Hz, CH), 7.02 (2H, t, J = 8.6 Hz, ArCH), 7.29 (2H, t, J = 8.1 Hz, ArCH), 7.40-7.44 (2H, m, ArCH), 7.62 (1H, d, J = 15.9 Hz, CH) **^{13}C NMR (100 MHz, MeOD):** δ 16.5, 24.4, 28.1, 29.5, 35.1, 114.6, 117.9, 121.0, 122.6, 129.7, 132.3, 133.0, 134.2, 136.1, 144.0, 150.4, 160.4, 162.8, 168.8, 171.1. **ESI-HRMS** (*m/z*): [M - H]$^-$ calcd for $C_{23}H_{23}O_4F$, 381.1508; found, 381.1490.

(*E*)-3-(4-((3-(2-methoxyphenyl)propanoyl)oxy)-3-(3-methylbut-2-en-1-yl)phenyl)acrylic acid (8e): Compound **6e** (150 mg, 0.3 mmol) was hydrolyzed following the general procedure B. Solvent was evaporated in vacuo to provide the title compound as a white solid (73 mg, 0.2 mmol, 56%). **R_f:** 0.1 (Hexane:EtOAc, 4:1) **^{1}H NMR (400 MHz, MeOD):** δ 1.71 (3H, s, CH_3), 1.78 (3H, s, CH_3), 2.93 (2H, t, J = 7.1 Hz, CH_2), 3.10 (2H, t, J = 7.5 Hz, CH_2), 3.20 (2H, d, J = 7.2 Hz, CH_2), 3.88 (3H, s, CH_3), 5.23 (1H, t, J = 7.2 Hz, CH), 6.41 (1H, d, J = 15.9 Hz, CH), 6.92 (2H, q, J = 6.4 Hz ArCH), 7.03 (1H, d, J = 8.9 Hz, ArCH), 7.23 – 7.28 (2H, m, ArCH), 7.42 (2H, s, ArCH), 7.678 (1H, d, J = 15.9 Hz, CH). **^{13}C NMR (100 MHz, MeOD):** δ 17.8, 25.7, 26.2, 28.5, 34.1, 55.2, 110.2, 117.0, 120.5, 120.9, 122.9, 126.9, 127.9, 128.2, 130.1, 130.2, 131.8, 133.9, 134.3, 146.4, 150.8, 157.5, 171.5, 172.3. **ESI-HRMS** (*m/z*): $[M - H]^-$ calcd for $C_{24}H_{26}O_5$, 393.1707; found, 393.1714.

(*E*)-3-(4-((3-(3-methoxyphenyl)propanoyl)oxy)-3-(3-methylbut-2-en-1-yl)phenyl)acrylic acid (8f): Compound **6f** (220 mg, 0.5 mmol) was hydrolyzed following the general procedure B. Solvent was evaporated in vacuo to provide the title compound as a white solid (60 mg, 0.15 mmol, 32%). **R_f:** 0.09 (Hexane:EtOAc, 4:1) **^{1}H NMR (400 MHz, MeOD):** δ 1.65 (3H, s, CH_3), 1.72 (3H, s, CH_3), 2.91 (2H, t, J = 7.1 Hz, CH_2), 3.00 (2H, t, J = 7.2 Hz, CH_2), 3.09 (2H, d, J = 7.1 Hz, CH_2), 3.76 (3H, s, CH_3), 5.14 (1H, t, J = 7.2 Hz, CH), 6.40 (1H, d, J = 15.9 Hz, CH), 6.76 – 6.78 (1H, m, ArCH), 6.84 (2H, s, ArCH), 6.95 (1H, d, J = 8.2 Hz, ArCH), 7.21 (1H, t, J = 8.2 Hz, ArCH), 7.39 – 7.43 (2H, m, ArCH), 7.62 (1H, d, J = 15.9 Hz, CH). **^{13}C NMR (100 MHz, MeOD):** δ 16.6, 24.5, 28.1, 30.4, 35.1, 54.1, 111.4, 113.8, 117.9, 120.3, 121.1, 122.7, 126.3, 129.1, 129.5, 132.3, 133.0, 134.2, 141.7, 144.0, 150.5, 159.9, 168.8, 171.3. **ESI-HRMS** (*m/z*): $[M - H]^-$ calcd for $C_{24}H_{26}O_5$, 393.1707; found, 393.1717.

(*E*)-3-(4-((3-(4-methoxyphenyl)propanoyl)oxy)-3-(3-methylbut-2-en-1-yl)phenyl)acrylic acid (8g): Compound **6g** (200 mg, 0.4 mmol) was hydrolyzed following the general procedure B. Solvent was evaporated *in vacuo* to provide the title compound as a white solid (73 mg, 0.2 mmol, 42%). **R_f:** 0.07 (Hexane:EtOAc, 4:1) **^{1}H NMR (400 MHz, MeOD):** δ 1.66 (3H, s, CH_3), 1.74 (3H, s, CH_3), 2.90 (2H, t, J = 7.1 Hz, CH_2), 2.98 (2H, t,

J = 7.0 Hz, CH_2), 3.07 (2H, d, J = 7.2 Hz, CH_2), 3.77 (3H, s, CH_3), 5.14 (1H, t, J = 7.2 Hz, CH), 6.41 (1H, d, J = 15.9 Hz, CH), 6.86 (2H, d, J = 8.7 Hz, ArCH), 6.96 (1H, d, J = 8.2 Hz, ArCH), 7.20 (2H, d, J = 8.7 Hz, ArCH), 7.41 (1H, s, ArCH), 7.45 (1H, dd, J_1 = 2.1 Hz, J_2 = 8.3 Hz, ArCH), 7.62 (1H, d, J = 15.9 Hz, CH). **^{13}C NMR (100 MHz, MeOD):** δ 16.5, 24.4, 28.0, 29.6, 35.4, 54.2, 133.5, 117.9, 121.0, 122.7, 126.2, 129.0, 129.4, 132.0, 132.3, 133.0, 134.2, 144.0, 150.5, 158.3, 168.8, 171.4. **ESI-HRMS** (*m/z*): $[M - H]^-$ calcd for $C_{24}H_{26}O_5$, 393.1707; found, 393.1696.

(*E*)-3-(4-acetoxy-3-(3-methylbut-2-en-1-yl)phenyl)acrylic acid (8h)[44]: Compound **6h** (100 mg, 0.3 mmol) was hydrolyzed following the general procedure B. The solvent was evaporated *in vacuo* and purified by column chromatography (Hexane:EtOAc = 9:1, 4:1, 2:1, 1:1) to provide the title compound as a white solid (86 mg, 0.3 mmol, 99%). **R_f:** 0.1 (Hexane:EtOAc, 4:1). **^{1}H NMR (400 MHz, $CDCl_3$):** δ 1.73 (3H, s, CH_3), 1.78 (3H, s, CH_3), 2.34 (3H, s, CO_2CH_3), 3.27 (2H, d, J = 7.7 Hz, CH_2), 5.24 (1H, t, J = 7.1 Hz, CH), 6.41 (1H, d, J = 15.9 Hz, CH), 7.09 (1H, d, J = 8.4 Hz, ArCH), 7.43 (2H, s, ArCH), 7.75 (1H, d, J = 15.8 Hz, CH). **^{13}C NMR (100 MHz, $CDCl_3$):** δ 17.8, 20.8, 25.7, 28.6, 116.8, 120.8, 122.9, 126.9, 130.2, 132.0, 134.3, 146.1, 150.7, 169.0, 170.1, 206.9. **M/Z ESI:** 273.0 $[M - H]^-$ (100%).

(2*E*)-3-[3-(3-methylbut-2-en-1-yl)-4-[(4-phenylbutanoyl)oxy]phenyl]prop-2-enoic acid (8i): Compound **6i** (230 mg, 0.5 mmol) was hydrolyzed following the general procedure B. The solvent was evaporated *in vacuo* and purified by column chromatography (Hexane:EtOAc = 9:1, 4:1, 2:1, 1:1) to provide the title compound as a white solid (12.2 mg, 0.03 mmol, 6%). **R_f:** 0.10 (Hexane:EtOAc, 4:1). **^{1}H NMR (400 MHz; $CDCl_3$):** δ 1.68 (3H, s, CH_3), 1.76 (3H, s, CH_3), 2.12 (2H, q, J = 7.5 Hz, CH_2), 2.62 (2H, t, J = 7.5 Hz, CH_2), 2.78 (2H, t, J = 7.5 Hz, CH_2), 3.25 (2H, d, J =7.1 Hz, CH_2), 5.23 (1H, t, J = 7.2 Hz, CH), 6.40 (1H, d, J = 15.0, CH), 7.06 (1H, d, J = 8.5 Hz, ArCH), 7.23 - 7.26 (3H, m, ArCH), 7.31 - 7.35 (2H, m, ArCH), 7.42 - 7.44 (2H, m, ArCH), 7.76 (1H, d, J = 15.95 Hz, ArCH). **^{13}C NMR (100 MHz; $CDCl_3$):** δ 17.8, 25.7, 26.2, 26.4, 28.6, 33.4,

35.1, 117.0, 120.8, 122.9, 126.1, 126.9, 128.5, 130.2, 131.9, 134.1, 134.3, 141.0, 146.3, 150.7, 171.6, 171.9. **ESI-HRMS** (*m/z*): $[M - H]^-$ calcd for $C_{24}H_{26}O_4$, 377.1758; found, 377.1761.

(2*E*)-3-{4-[(2-cyclohexylacetyl)oxy]--(3-methylbut-2-en-1-yl)phenyl}prop-2-enoic acid (**8j**): Compound **6j** (370 mg, 0.85 mmol) was hydrolyzed following the general procedure B. Purification by column chromatography (Hexane:EtOAc = 4:1, 1:1) followed by solvent evaporation *in vacuo* provided the title compound as a white solid (130 mg, 0.3 mmol, 40%). **R_f:** 0.14 (Hexane:EtOAc, 4:1). **^{1}H NMR (400 MHz; $CDCl_3$):** δ 1.05 - 1.39 (7H, m, cyc-H), 1.72 (3H, s, CH_3), 1.79 (3H, s, CH_3), 1.84-1.96 (3H, m, cyc-H), 2.47 (2H, d, J = 7 Hz, CH), 3.24 (2H, d, J = 7.1 Hz, CH_2), 5.23 (1H, t, J = 7.1 Hz, CH), 6.39 (1H, d J = 15.9, CH), 7.04 (1H, d, J = 8.8 Hz, ArCH), 7.39-7.36 (2H, m, ArCH), 7.75 (1H, d, J = 15.9, CH). **^{13}C NMR (100 MHz; $CDCl_3$):** δ 17.9, 25.7, 26.0, 28.5, 33.0, 34.9, 41.9, 117.0, 120.8, 122.9, 126.8, 128.3, 128.5, 128.9, 130.1, 131.8, 134.0, 134.3, 146.4, 150.8, 171.1, 172.3. **ESI-HRMS** (*m/z*): $[M - H]^-$ calcd for $C_{22}H_{28}O_4$, 355.1915; found, 355.1921.

(2*E*)-3-[3-(3-methylbut-2-en-1-yl)-4-{[2-(naphthalen-1-yl)acetyl]oxy}phenyl]prop-2-enoic acid (**8k**): Compound **6k** (66.1 mg, 0.15 mmol) was hydrolyzed following the general procedure B. The solvent was evaporated *in vacuo* to provide the title compound as a white solid (34 mg, 0.1 mmol, 60%). **R_f:** 0.20 (Hexane:EtOAc, 4:1). **^{1}H NMR (400 MHz; $CDCl_3$):** δ 1.57 (3H, s, CH_3), 1.70 (3H, s, CH_3), 3.00 (2H, d, J = 7.3 Hz, CH_2), 4.36 (2H, s, CH_2), 5.03 (1H, t, J = 7.2 Hz, CH), 6.37 (1H, d, J = 15.9 Hz, CH), 7.03 (1H, d, J = 8.2 Hz, ArCH), 7.34 - 7.38 (2H, m, ArCH), 7.48 - 7.62 (4H, m, ArCH) 7.72 (1H, d, J = 15.9 Hz, CH), 7.87 (1H, d, J = 8.1 Hz, ArCH), 7.89 (1H, dd, J_1 = 8.7 Hz, J_2 = 21.7 Hz, ArCH), 8.14 (1H, d, J = 8.5 Hz, ArCH). **^{13}C NMR (100 MHz; $CDCl_3$):** δ 17.7, 25.6, 28.2, 29.7, 39.3, 117.0, 120.5, 122.7, 123.6, 125.5, 125.9, 126.6, 126.8, 128.3, 128.4, 128.8, 129.7, 130.0, 131.9, 132.0, 133.8, 133.9, 134.3, 146.3, 150.6, 169.6. **ESI-HRMS** (*m/z*): $[M + Na]^+$ calcd for $C_{26}H_{24}O_4$, 423.1567; found, 423.1558.

(*E*)-3-(4-(benzoyloxy)-3-(3-methylbut-2-en-1-yl)phenyl)acrylic acid (**8l**): Compound **6l** (72 mg, 0.2 mmol) was hydrolyzed following the general procedure B. The solvent was evaporated *in vacuo* to provide the title compound as a white solid (32 mg, 0.09 mmol, 50%). **^{1}H NMR (400 MHz; MeOD):** δ 1.61 (3H, s, CH_3), 1.72 (3H, s, CH_3), 3.35 (2H, d, J = 7.0 Hz, CH_2), 5.26 (1H, t, J = 7.5 Hz, CH), 6.45 (1H, d, J = 16.0 Hz, CH), 7.23 (1H, d, J = 8.2 Hz, ArCH), 7.49 – 7.57 (4H, m, ArCH), 7.68 (1H, t, J = 7.0 Hz, ArCH), 7.81 (1H, d, J = 15.9 Hz, CH), 8.23 (2H, d, J = 7.3 Hz, ArCH). **^{13}C NMR (100 MHz; MeOD):** δ 17.8, 25.6, 28.8, 117.0, 120.8, 123.0, 127.0, 128.6, 130.2, 130.3, 132.0, 133.7, 134.0, 134.6, 146.3, 151.0, 164.7, 171.1, 171.5. **ESI-HRMS** (*m/z*): $[M - H]^-$ calcd for $C_{21}H_{20}O_4$, 335.1289; found, 335.1300.

(2*E*)-3-[3-(3-methylbut-2-en-1-yl)-4-(pyridine-4-carbonyloxy)phenyl]prop-2-enoic acid (**8m**): Compound **6m** (350 mg, 0.9 mmol) was hydrolyzed following the general procedure B. Solvent was evaporated *in vacuo* to provide the title compound as a yellow solid (150 mg, 0.4 mmol, 50 %). **R_f:** 0.2 (Hexane:EtOAc, 4:1). **^{1}H NMR (400 MHz; MeOD):** δ 1.55 (3H, s, CH_3), 1.62 (3H, s, CH_3), 3.36 (2H, d, J = 7.0 Hz, CH_2), 5.19 (1H, t, J = 7.0 Hz, CH), 6.50 (1H, d, J = 16.0 Hz, CH), 7.26 (1H, d, J = 8.0 Hz, ArCH), 7.57 (1H, s ArCH), 7.59 (1H, d, J = 2.1 Hz, ArCH), 7.69 (1H, d, J = 15.9 Hz, CH), 8.12 (2H, d, J = 6.1 Hz, ArCH), 8.86 (2H, d, J = 5.1 Hz, ArCH). **^{13}C NMR (100 MHz; MeOD):** δ 16.5, 24.3, 28.9, 60.1, 118.4, 121.2, 122.8, 123.3, 126.6, 129.9, 133.0, 134.2, 143.7, 150.1, 150.3, 163.1, 168.8. **ESI-HRMS** (*m/z*): $[M + H]^+$ calcd for $C_{20}H_{19}NO_4$, 338.1387; found, 338.1389.

(*E*)-3-(4-(hexanoyloxy)-3-(3-methylbut-2-en-1-yl)phenyl)acrylic acid (**8n**): Following the general procedure B the title compound was obtained as a white soild (50 mg, 0.15 mmol, 37%). **^{1}H NMR (400 MHz; MeOD):** δ 1.36 – 1.43 (7H, m, CH_3 and CH_2), 1.50 – 1.62 (2H, m, CH_2), 1.69 (3H, s, CH_3), 1.76 (3H, s, CH_3), 2.57 (2H, t, J = 7.4 Hz, CH_2), 3.18 (2H, d, J = 7.0 Hz, CH_2), 5.19 (1H, t, J = 7.2 Hz, CH), 6.45 (1H, d, J = 15.7 Hz, CH), 7.01 (1H, d, J = 8.3 Hz, ArCH), 7.52 – 7.54 (2H, m, ArCH), 7.46 (1H, d, J = 15.9 Hz, CH). **^{13}C NMR**

(100 MHz; MeOD): δ 12.8, 16.5, 22.0, 24.2, 24.4, 28.3, 31.0, 33.5, 121.2, 122.6, 126.1, 129.3, 132.8, 132.9, 134.1, 142.3, 150.2, 172.2. **ESI-HRMS** (*m/z*): $[M + Na]^+$ calcd for $C_{20}H_{26}O_4$, 353.1723; found, 353.1718.

(2*E*)-3-[3-(3-methylbut-2-en-1-yl)-4-(3-phenylpropanamido)phenyl]prop-2-enoic acid (14a)[47]: Compound **13a** (20 mg, 0.04 mmol) was hydrolyzed following the general procedure B. Solvent evaporated *in vacuo* to provide the title compound as a white solid (9.3 mg, 0.02 mmol, 50%) **R_f:** 0.01 (Hexane:EtOAc, 4:1). **^{1}H NMR (400 MHz; MeOD):** δ 1.70 (3H, s, CH_3), 1.77 (3H, s, CH_3), 2.72 (2H, t, *J* = 7.0 Hz, CH_2), 3.03 (2H, t, *J* = 7.3 Hz, CH_2), 3.21 (2H, d, *J* = 6.9 Hz, CH_2), 5.19 (1H, t, *J* = 7.0 Hz, CH), 6.42 (1H, d, *J* = 15.8 Hz, CH), 7.14 - 7.30 (5H, m, ArCH), 7.34 - 7.46 (3H, m, ArCH), 7.61 (1H, d, *J* = 16.5 Hz, CH). **^{13}C NMR (100 MHz; MeOD):** δ 16.6, 24.4, 29.4, 31.3, 37.8, 117.7, 121.3, 125.6, 125.9, 126.1, 127.8, 128.1, 128.1, 128.8, 132.3, 133.2, 136.5, 137.0, 140.6, 144.2, 169.0, 172.6. **HRMS-ESI:** (*m/z*) calculated for $C_{23}H_{25}NO_3$, 386.1727; found, 386.1729.

(2*E*)-3-[4-acetamido-3-(3-methylbut-2-en-1-yl)phenyl]prop-2-enoic acid (**14b**): Compound **13b** (51.0 mg, 0.5 mmol) was hydrolyzed following the general procedure B. Solvent evaporated *in vacuo* to provide the title compound as a white solid (20.3 mg, 0.07 mmol, 50%). **R_f:** 0.1 (Hexane:EtOAc, 4:1). **^{1}H NMR (400 MHz; MeOD):** δ 1.75 (3H, s, CH_3), 1.78 (3H, s, CH_3), 2.16 (3H, s, CH_3), 3.37 (2H, d, *J* = 6.9 Hz, CH_2), 5.25 (1H, t, *J* = 6.4 Hz, CH), 6.43 (1H, d, *J* = 16.0 Hz, CH), 7.43 - 7.58 (3H, m, ArCH), 7.63 (1H, d, *J* = 15.7 Hz, CH). **^{13}C NMR (100 MHz; MeOD):** δ 21.7, 24.4, 29.3, 29.6, 31.6, 117.7, 121,3, 125.7, 126.1, 132.3, 133.2, 136.4, 137.2, 144.2, 170.7. **ESI-HRMS** (*m/z*): $[M - H]^-$ calcd for $C_{16}H_{19}NO_3$, 272.1292; found, 272.1292.

(2*E*)-3-[3-(3-methylbut-2-en-1-yl)-4-(4-phenylbutanamido)phenyl]prop-2-enoic acid (**14c**): Compound **13c** (17 mg, 0.04 mmol) was hydrolyzed following the general procedure B. Solvent evaporated *in vacuo* to provide the title compound as a white solid (7.3 mg, 0.02 mmol, 50%). **R_f:** 0.01 (Hexane:EtOAc, 4:1). **^{1}H NMR (400 MHz; $CDCl_3$):** δ 1.74 (3H, s, CH_3), 1.75 (3H, s, CH_3), 2.07 (2H, d, *J* = 7.5 Hz, CH_2), 2.33 (2H, d, *J* = 7.0 Hz, CH_2), 2.73 (2H, d, *J* = 7.1 Hz, CH_2), 3.33 (2H, d, *J* = 6.5 Hz, CH_2), 5.19 (1H, t, *J* = 6.3 Hz, CH),

6.39 (1H, d, *J* = 16.9 Hz, CH), 7.20 – 7.46 (7H, m, ArCH), 7.73 (1H, d, *J* = 16.3 Hz, CH), 8.17 (1H, d, *J* = 8.6 Hz, ArCH). **^{13}C NMR (100 MHz; MeOD):** δ 13.0, 16.6, 19.4, 24.4, 27.3, 29.8, 34.9, 35.4, 60.1, 119.3, 121.5, 125.6, 126.1, 127.8, 128.1, 128.8, 132.6, 133.2, 136.5, 141.5, 143.0, 173.3. **ESI-HRMS** (*m/z*): [M - H]$^-$ calcd for $C_{24}H_{27}NO_3$, 376.1918; found, 376.1924.

(2*E*)-3-[4-(2-cyclohexylacetamido)-3-(3-methylbut-2-en-1-yl)phenyl]prop-2-enoic acid (**14d**): Compound **13d** (20 mg, 0.05 mmol) was hydrolyzed following the general procedure B. Solvent evaporated *in vacuo* to provide the title compound as a white solid (13.2 mg, 0.03 mmol, 93%). **R_f:** 0.1 (Hexane:EtOAc, 4:1)**. ^{1}H NMR (400 MHz; MeOD):** δ 1.03 - 1.38 (7H, m, CH_2), 1.73 (3H, s, CH_3), 1.78 (3H, s, CH_3), 1.78 – 1.90 (4H, m, CH_2), 2.29 (2H, d, *J* = 6.9 Hz, CH_2), 3.37 (2H, d, *J* = 6.9 Hz, CH_2), 5.27 (1H, t, *J* = 7.7 Hz, CH), 6.43 (1H, d, *J* = 15.9 Hz, CH), 7.43 – 7.49 (3H, m, ArCH), 7.63 (1H, d, *J* = 15.9 Hz, CH). **^{13}C NMR (100 MHz; MeOD):** δ 16.6, 24.4, 25.8, 25.9, 29.3, 29.6, 32.8, 35.5, 44.0, 117.9, 121.4, 125.7, 126.2, 129.0, 132.3, 133.3, 136.5, 137.1, 144.1, 173.0. **ESI-HRMS** (*m/z*): [M - H]$^-$ calcd for $C_{22}H_{29}NO_3$, 354.2075; found, 354.2089.

(2*E*)-3-[3-(3-methylbut-2-en-1-yl)-4-[2-(naphthalen-1-yl)acetamido]phenyl]prop-2-enoic acid (**14e**): Compound **13e** (50 mg, 0.1 mmol) was hydrolyzed following the general procedure B. Solvent evaporated *in vacuo* to provide the title compound as a white solid (20.7 mg, 0.05 mmol, 52%). **R_f:** 0.01 (Hexane:EtOAc, 4:1)**. ^{1}H NMR (400 MHz; MeOD):** δ 1.80 (6H, s, CH_3), 3.36 (2H, s, CH_2), 3.45 (2H, d, *J* = 5.8 Hz, CH_2), 5.23 (1H, t, *J* = 7.7 Hz, CH), 6.43 (1H, d, *J* = 16.4 Hz, CH), 7.43 – 7.64 (7H, m, ArCH and CH), 7.88 – 7.95 (3H, m, ArCH), 8.37 (1H, d, *J* = 7.9 Hz, ArCH). **^{13}C NMR (100 MHz; MeOD):** δ 24.5, 30.5, 72.7, 120.7, 122.7, 124.0, 124.8, 125.4, 125.7, 125.8, 126.3, 128.3, 128.6, 129.2, 131.3, 131.3, 133.5, 134.2, 134.8, 136.0, 137.1, 144.0, 172.4**. *m/z* (ESI):** 397.9 [M - H]$^-$ (20 %)

(*E*)-3-(4-bromo-3-hydroxyphenyl)acrylic acid (**17a**): To a solution of **17** (330 mg, 1.3 mmol) in water (8 mL) and THF (2 mL) was added NaOH (100 mg, 2.5 mmol) and the reaction refluxed overnight. The solution

was allowed to cool and was acidified with AcOH, washed with water and extracted in DCM, dried (Na_2SO_4), filtered and concentrated. Purifcation by column chromatography (Hexane:EtOAc = 9:1, 4:1, 2:1, 1:1, 0:1) provided the title compound as a white solid (150 mg, 0.6 mmol, 45%). **R_f:** 0.1 (Hexane:EtOAc, 4:1). **^{1}H NMR (400 MHz; MeOD):** δ 6.39 (1H, d, *J* = 15.8 Hz, CH), 6.78 (1H, dd, J_1 = 2.9 Hz, J_2 = 8.7 Hz, ArCH), 7.15 (1H, d, *J* = 2.9 Hz, ArCH), 7.44 (1H, d, *J* = 8.7 Hz, ArCH), 7.97 (1 H, d, *J* = 15.9 Hz, CH). **^{13}C NMR (100MHz; MeOD):** δ 113.6, 113.7, 118.9, 120.5, 133.6, 134.6, 142.9, 157.7, 168.3.

(*E*)-3-(4-(3-methylbut-2-en-1-yl)-3-((3-phenylpropanoyl)oxy)phenyl)acrylic acid (19a)[47]: To a solution of **(18)** (430 mg, 1.1 mmol) in dry DMF (8 mL) was added $CsCO_3$ (555 mg, 1.7 mmol) and Pd(dppf)Cl_2 (50 mg, 0.06 mmol). Prenyl boronic acid pinacol ester (330 µL, 1.5 mmol) was added and the flask was heated at 90^0C overnight. The reaction was allowed to cool and was filtered through a celite® pad with EtOAc, the solvent was evaporated and the residue re-dissolved in DCM. The residual DMF was removed by washing with copious amounts of water in DCM, dried (Na_2SO_4), filtered and concentrated. Purification by column chromatography (Hexane:EtOAC = 9:1, 4:1, 2:1, 1:1, 0:1) provided the title compound as a yellow oil (120 mg, 0.3 mmol, 27%). **R_f:** 0.10 (Hexane:EtOAc, 4:1). **^{1}H NMR (400 MHz; MeOD):** δ 1.72 (3H, s, CH_3), 1.77 (3H, s, CH_3), 2.90 (2H, t, *J* = 7.2 Hz, CH_2), 3.04 (2H, t, *J* = 7.2 Hz, CH_2), 3.43 (2H, d, *J* = 6.7 Hz, CH_2), 5.15 (1H, t, *J* = 5.9 Hz, CH), 6.29 (2H, d, *J* = 15.7 Hz, CH), 6.94 (1H, d, *J* = 7.2 Hz, ArCH), 7.16 – 7.33 (7H, m, ArCH), 7.93 (1H, d, *J* = 15.8 Hz, CH). **^{13}C NMR (100 MHz; MeOD):** δ 16.6, 24.4, 30.5, 31.3, 35.3, 119.0, 119.9, 122.3, 122.9, 126.0, 128.14, 128.18, 130.4, 132.3, 134.0, 138.6, 140.2, 141.5, 149.3, 168.5, 171.7. **ESI-HRMS** (*m/z*): calcd for $C_{23}H_{24}O_4$, 363.1602; found, 363.1609.

(*E*)-3-(4-allyl-3-((3-phenylpropanoyl)oxy)phenyl)acrylic acid (19b): To a solution of **(18)** (110 mg, 0.3 mmol) in dry DMF (4 mL) was added $CsCO_3$ (75 mg, 0.4 mmol) and Pd(dppf)Cl_2 (13 mg, 0.01 mmol). Allyl boronic acid pinacol ester (70 µL, 0.4 mmol) was added and the flask was heated at 90^0C overnight. The reaction was allowed to cool and was filtered through a celite® pad with EtOAc, the solvent was evaporated and the

residue re-dissolved in DCM. The residual DMF was removed by washing with copious amounts of water in DCM, dried (Na_2SO_4), filtered and concentrated. Purification by column chromatography (Hexane:EtOAC = 9:1, 4:1, 2:1, 1:1, 0:1) provided the title compound as a yellow oil (60 mg, 0.2 mmol, 60%). **R_f:** 0.10 (Hexane:EtOAc, 4:1). **^{1}H NMR (400 MHz; MeOD):** δ 2.93 (2H, t, *J* = 7.5 Hz, CH_2), 3.11 (2H, t, *J* = 7.5 Hz, CH_2), 3.53 (2H, d, *J* = 6.1 Hz, CH_2), 5.01 (1H, dd, J_1 = 1.5 Hz, J_2 = 17.0 Hz, CH_2), 5.12 (1H, dd, J_1 = 1.5 Hz, J_2 = 10.1 Hz, CH_2), 5.90 – 6.00 (1H, m, CH), 6.33 (2H, d, *J* = 15.7 Hz, CH), 7.02 (1H, dd, J_1 = 2.4 Hz, J_2 = 8.3 Hz, ArCH), 7.20 – 7.38 (7H, m, ArCH), 8.03 (1H, d, *J* = 15.8 Hz, CH). **^{13}C NMR (100 MHz; MeOD):** δ 30.9, 35.9, 36.9, 116.7, 119.4, 119.5, 123.6, 126.5, 128.4, 128.6, 131.3, 134.1, 136.1, 137.0, 139.9, 143.4, 149.3 171.3, 171.5. **ESI-HRMS** (*m/z*): $[M - H]^-$ calcd for $C_{21}H_{20}O_4$, 335.1289; found, 335.1292.

(*E*)-N-(2-bromo-5-(2-(4,4,5,5-tetramethyl-1,3,2-dioxaborolan-2-yl)vinyl)phenyl)-3-phenylpropanamide (**24**): To a solution of **21b** (64 mg, 0.1 mmol) in dry DCM (5 mL) was added DMAP (2 mg, 0.01 mmol), a solution of 3-phenyl propanoyl chloride (50 mg, 0.3 mmol) in DCM (2 mL) and NEt_3 (0.1 mL, 0.5 mmol). The reaction was heated to 70^0C and stirred overnight. The reaction was allowed to cool and was washed with saturated aqueous $NaHCO_3$, water and extracted in DCM, dried (Na_2SO_4), filtered and concentrated. Purification by column chromatography (Hexane:EtOAc = 12:1, 9:1, 4:1, 2:1) provided the title compound as a yellow oil (40 mg, 0.08 mmol, 87%). **R_f:** 0.3 (Hexane:EtOAc, 4:1). **^{1}H NMR (400 MHz; $CDCl_3$):** δ 1.33 (12H, s, CH_3), 2.67 (2H, t, *J* = 7.4 Hz, CH_2), 3.05 (2H, t, *J* = 7.6 Hz, CH_2), 6.10 (1H, d, *J* = 18.2 Hz, CH), 7.22 – 7.34 (6H, m, ArCH), 7.47 (1H, d, *J* = 8.6 Hz, ArCH), 7.59 (1H, d, *J* = 2.2 Hz, ArCH), 7.65 (1H, d, *J* = 18.0 Hz, CH). **^{13}C NMR (100 MHz; $CDCl_3$):** δ 24.8, 31.4, 39.4, 83.5, 118.2, 118.7, 121.6, 126.4, 128.3, 128.6, 133.3, 137.2, 137.8, 140.4, 147.0, 170.3. **ESI-HRMS** (*m/z*): $[M + Na]^+$ calcd for $C_{23}H_{27}NO_3BBr$, 478.1164; found, 478.1164.

(*E*)-3-(4-(3-methylbut-2-en-1-yl)-3-(3-phenylpropanamido)phenyl)acrylic acid (**26a**)[46]: Compound **25a** (80 mg, 0.2 mmol) was hydrolyzed following the general procedure B. Purification by column chromatography (Hexane:EtOAc = 9:1, 4:1, 2:1, 1:1) followed by solvent evaporation *in vacuo* provided the title

compound as a white soild (19 mg, 0.05 mmol, 27%). **R_f:** 0.1 (Hexane:EtOAc, 4:1). **^{1}H NMR (400 MHz, MeOD):** δ 1.72 (3H, s, CH_3), 1.79 (3H, s, CH_3), 2.66 (2H, t, *J* = 7.4 Hz, CH_2), 3.01 (2H, t, *J* = 7.4 Hz, CH_2), 3.43 (2H, d, *J* = 6.6 Hz, CH_2), 5.16 (1H, t, *J* = 5.9 Hz, CH), 6.33 (1H, d, *J* = 15.7 Hz, CH), 7.16 – 7.30 (6H, m, ArCH), 7.46 (1H, d, *J* = 8.0 Hz, ArCH), 7.80 (1H, s, ArCH), 7.96 (1H, d, *J* = 15.7 Hz, CH). **^{13}C NMR (100 MHz, MeOD):** δ 16.6, 24.4, 31.3, 31.3, 38.4, 117.5, 119.2, 121.7, 122.6, 125.8, 128.1, 129.9, 132.0, 133.2, 136.9, 137.0, 140.7, 142.3, 168.8, 172.2. **ESI-HRMS** (*m/z*): $[M - H]^-$ calcd for $C_{23}H_{25}NO_3$, 362.1762; found, 362.1761.

(*E*)-3-(3-(3-(2-fluorophenyl)propanamido)-4-(3-methylbut-2-en-1-yl)phenyl)acrylic acid (**26b**): Compound **25b** (200 mg, 0.4 mmol) was hydrolyzed following the general procedure B. Purification by column chromatography (Hexane:EtOAc = 9:1, 4:1, 2:1, 1:1) followed by solvent evaporation *in vacuo* provided the title compound as a white soild (130 mg, 0.34 mmol, 85%). **R_f:** 0.1 (Hexane:EtOAc, 4:1). **^{1}H NMR (400 MHz; MeOD):** δ 1.72 (3H, s, CH_3), 1.78 (3H, s, CH_3), 2.68 (2H, t, *J* = 7.4 Hz, CH_2), 3.05 (2H, t, *J* = 7.6 Hz, CH_2), 3.41 (2H, d, *J* = 6.9 Hz, CH_2), 5.14 (1H, t, *J* = 7.0 Hz, CH), 6.32 (1H, d, *J* = 15.7 Hz, CH), 7.03 – 7.11 (2H, m, ArCH), 7.16 (1H, d, *J* = 8.3 Hz, ArCH), 7.20 – 7.25 (1H, m, ArCH), 7.30 (1H, t, *J* = 7.6 Hz, ArCH), 7.45 (1H, dd, J_1 = 1.8 Hz, J_2 = 8.2 Hz, ArCH), 7.80 (1H, d, *J* = 2.1, ArCH), 7.96 (1H, d, *J* = 15.8 Hz, CH). **^{13}C NMR (100 MHz; MeOD):** δ 16.6, 24.4, 24.6, 31.3, 36.7, 114.6, 114.8, 117.6, 119.2, 121.8, 122.6, 123.9, 127.9, 129.9, 130.5, 132.0, 133.2, 137.0, 142.3, 159.8, 1652.3, 168.9, 171.9. **ESI-HRMS** (*m/z*): $[M - H]^-$ calcd for $C_{23}H_{24}NO_3F$, 380.1667; found, 380.1676.

(*E*)-3-(3-(3-(3-fluorophenyl)propanamido)-4-(3-methylbut-2-en-1-yl)phenyl)acrylic acid (**26c**): Compound **25c** (150 mg, 0.4 mmol) was hydrolyzed following the general procedure B. Purification by column chromatography (Hexane:EtOAc = 9:1, 4:1, 2:1, 1:1) followed by solvent evaporation *in vacuo* provided the title compound as a white soild (120 mg, 0.32 mmol, 80%). **R_f:** 0.1 (Hexane:EtOAc, 4:1). **^{1}H NMR (400 MHz; MeOD):** δ 1.72 (3H, s, CH_3), 1.78 (3H, s, CH_3), 2.68 (2H, t, *J* = 7.3 Hz, CH_2), 3.02 (2H, t, *J* = 7.4 Hz, CH_2), 3.41 (2H, d, *J* = 6.9 Hz, CH_2), 5.15 (1H, t, *J* = 7.0 Hz, CH), 6.33 (1H, d, *J* = 15.7 Hz, CH), 6.92 (1H, t, *J* = 8.2 Hz,

ArCH), 7.02 (1H, d, J = 9.8 Hz, ArCH), 7.08 (1H, d, J = 7.6 Hz, ArCH), 7.17 (1H, d, J = 8.3 Hz, ArCH), 7.29 (1H, q, J = 7.9 Hz, ArCH), 7.46 (1H, dd, J_1 = 2.1 Hz, J_2 = 8.2 Hz, ArCH), 7.79 (1H, d, J = 2.1, ArCH), 7.95 (1H, d, J = 15.7 Hz, CH). **^{13}C NMR (100 MHz; MeOD):** δ 16.6, 24.4, 30.9, 31.3, 37.9, 112.4, 112.6, 114.6, 114.8, 117.5, 121.7, 122.6, 123.9, 129.7, 129.8, 129.9, 132.0, 133.3, 136.8, 137.0, 161.7, 164.1, 171.9. **ESI-HRMS** (*m/z*): [M - H]$^-$ calcd for $C_{23}H_{24}NO_3F$, 380.1667; found, 380.1678.

(*E*)-3-(3-(3-(4-fluorophenyl)propanamido)-4-(3-methylbut-2-en-1-yl)phenyl)acrylic acid (**26d**): Compound **25d** (66 mg, 0.15 mmol) was hydrolyzed following the general procedure B. Purification by column chromatography (Hexane:EtOAc = 9:1, 4:1) followed by solvent evaporation *in vacuo* provided the title compound as a white soild (50 mg, 0.13 mmol, 87%). **R_f:** 0.1 (Hexane:EtOAc, 4:1). **^{1}H NMR (400 MHz; MeOD):** δ 1.73 (3H, s, CH_3), 1.79 (3H, s, CH_3), 2.66 (2H, t, J = 7.4 Hz, CH_2), 3.00 (2H, t, J = 7.4 Hz, CH_2), 3.4 (2H, d, J = 7.4 Hz, CH_2), 5.16 (1H, t, J = 7.8 Hz, CH), 6.33 (1H, d, J = 17.5 Hz, CH), 7.00 (2H, t, J = 8.6 Hz, ArCH), 7.18 (1H, d, J = 8.3 Hz, ArCH), 7.27 (2H, dd, J_1 = 3.2 Hz, J_2 = 5.5 Hz, ArCH), 7.46 (1H, dd, J_1 = 2.1 Hz, J_2 = 8.2 Hz, ArCH), 7.81 (1H, d, J = 2.0, ArCH), 7.96 (1H, d, J = 17.3 Hz, CH). **^{13}C NMR (100 MHz; MeOD):** δ 24.4, 29.2, 30.4, 31.3, 38.4, 114.5, 114.7, 117.5, 121.6, 122.6, 129.6, 129.7, 129.9, 132.2, 133.3, 136.6, 136.9, 136.9, 142.1, 162.7, 172.0. **ESI-HRMS** (*m/z*): [M - H]$^-$ calcd for $C_{23}H_{24}NO_3F$, 380.1667; found, 380.1664.

(*E*)-3-(3-(3-(2-methoxyphenyl)propanamido)-4-(3-methylbut-2-en-1-yl)phenyl)acrylic acid (**26e**): Compound **25e** (290 mg, 0.6 mmol) was hydrolyzed following the general procedure B. Purification by column chromatography (Hexane:EtOAc = 9:1, 4:1) followed by solvent evaporation *in vacuo* provided the title compound as a white soild (110 mg, 0.3 mmol, 50%). **R_f:** 0.2 (Hexane:EtOAc, 4:1). **^{1}H NMR (400 MHz; MeOD):** δ 1.73 (3H, s, CH_3), 1.79 (3H, s, CH_3), 2.64 (2H, t, J = 7.5 Hz, CH_2), 3.00 (2H, t, J = 7.6 Hz, CH_2), 3.43 (2H, d, J = 6.9 Hz, CH_2), 3.84 (3H, s, CH_3), 5.15 (1H, t, J = 7.0 Hz, CH), 6.33 (1H, d, J = 15.8 Hz, CH), 6.86 (1H, t, J = 7.5 Hz, ArCH), 6.93 (1H, d, J = 7.9 Hz, ArCH), 7.16 – 7.21 (3H, m, ArCH), 7.46 (1H, dd, J_1 = 2.2 Hz, J_2 = 8.3 Hz, ArCH), 7.81 (1H, d, J = 2.1 Hz, ArCH), 7.97 (1H, d, J = 15.7 Hz, CH). **^{13}C NMR (100 MHz;**

MeOD): δ 16.6, 24.4, 26.3, 31.3, 36.8, 54.2, 109.9, 117.7, 119.1, 120.0, 121.8, 122.6, 127.3, 128.6, 129.5, 129.9, 132.0, 133.1, 136.9, 137.0, 142.4, 157.4, 168.7, 172.7. **ESI-HRMS** (*m/z*): [M - H]$^-$ calcd for $C_{24}H_{27}NO_4$, 392.1867; found, 392.1863.

(*E*)-3-(3-(3-(3-methoxyphenyl)propanamido)-4-(3-methylbut-2-en-1-yl)phenyl)acrylic acid (**26f**): Compound **25f** (240 mg, 0.5 mmol) was hydrolyzed following the general procedure B. Purification by column chromatography (Hexane:EtOAc = 9:1, 4:1, 2:1, 1:1) followed by solvent evaporation *in vacuo* provided the title compound as a white soild (62 mg, 0.16 mmol, 31%). **R_f:** 0.2 (Hexane:EtOAc, 4:1). **^{1}H NMR (400 MHz; MeOD):** δ 1.73 (3H, s, CH_3), 1.79 (3H, s, CH_3), 2.67 (2H, t, J = 7.4 Hz, CH_2), 2.99 (2H, t, J = 7.6 Hz, CH_2), 3.43 (2H, d, J = 6.7 Hz, CH_2), 3.76 (3H, s, CH_3), 5.16 (1H, t, J = 7.0 Hz, CH), 6.33 (1H, d, J = 15.7 Hz, CH), 6.76 (1H, dd, J_1 = 2.5 Hz, J_2 = 7.9 Hz, ArCH), 6.83 – 6.85 (2H, m, ArCH), 7.16 – 7.22 (2H, m, ArCH), 7.46 (1H, dd, J_1 = 2.2 Hz, J_2 = 8.2 Hz, ArCH), 7.80 (1H, d, J = 2.1 Hz, ArCH), 7.97 (1H, d, J = 15.8 Hz, CH). **^{13}C NMR (100 MHz; MeOD):** δ 16.6, 24.4, 31.3, 31.4, 38.3, 5.1, 111.3, 113.6, 117.6, 129.3, 120.3, 121.8, 122.6, 129.0, 129.9, 132.0, 133.2, 136.9, 137.0, 142.2, 142.3, 159.8, 168.8, 172.3. **ESI-HRMS** (*m/z*): [M - H]$^-$ calcd for $C_{24}H_{27}NO_4$, 392.1867; found, 392.1869.

(*E*)-3-(3-(3-(4-methoxyphenyl)propanamido)-4-(3-methylbut-2-en-1-yl)phenyl)acrylic acid (**26g**): Compound **25g** (50 mg, 0.1 mmol) was hydrolyzed following the general procedure B. Purification by column chromatography (Hexane:EtOAc = 9:1, 4:1, 2:1, 1:1) followed by solvent evaporation *in vacuo* provided the title compound as a white soild (25 mg, 0.06 mmol, 53%). **R_f:** 0.25 (Hexane:EtOAc, 4:1). **^{1}H NMR (400 MHz; MeOD):** δ 1.73 (3H, s, CH_3), 1.79 (3H, s, CH_3), 2.64 (2H, t, J = 7.4 Hz, CH_2), 2.95 (2H, t, J = 7.6 Hz, CH_2), 3.44 (2H, d, J = 7.2 Hz, CH_2), 3.76 (3H, s, CH_3), 5.15 (1H, t, J = 8.4 Hz, CH), 6.33 (1H, d, J = 15.7 Hz, CH), 6.85 (2H, d, J = 8.6 Hz, ArCH), 7.18 (3H, d, J = 8.4 Hz, ArCH), 7.46 (1H, d, J_1 = 2.3 Hz, J_2 = 8.2 Hz, ArCH), 7.79 (1H, d, J = 2.1 Hz, ArCH), 7.96 (1H, d, J = 15.8 Hz, CH). **^{13}C NMR (100 MHz; MeOD):** δ 16.5, 24.4, 30.5, 31.3, 38.7, 54.2, 113.4, 117.6, 119.4, 121.7, 122.6, 128.9, 129.9, 132.0, 132.6, 133.2, 136.9, 136.9, 142.2, 157.8,

158.2, 172.4. **ESI-HRMS** (*m/z*): $[M - H]^-$ calcd for $C_{23}H_{24}NO_3F$, 380.1667; found, 380.1664. **ESI-HRMS** (*m/z*): $[M + H]^+$ calcd for $C_{24}H_{27}NO_4$, 394.2013; found, 394.2003.

(*E*)-3-(3-cinnamamido-4-(3-methylbut-2-en-1-yl)phenyl)acrylic acid (**26h**): Compound **25h** (80 mg, 0.2 mmol) was hydrolyzed following the general procedure B. Purification by column chromatography (Hexane:EtOAc = 9:1, 4:1, 2:1, 1:1) followed by solvent evaporation *in vacuo* provided the title compound as a white soild (20 mg, 0.05 mmol, 30%). **R_f:** 0.1 (Hexane:EtOAc, 4:1). **^{1}H NMR (400 MHz, MeOD):** δ 1.74 (3H, s, CH_3), 1.80 (3H, s, CH_3), 3.47 (2H, d, J = 7.0 Hz, CH_2), 5.19 (1H, t, J = 7.1 Hz, CH), 6.39 (1H, d, J = 15.8 Hz, CH), 6.81 (1H, d, J = 15.6 Hz, CH), 7.23 (1H, d, J = 8.3 Hz, ArCH), 7.39 – 7.46 (3H, m, ArCH), 7.61 – 7.64 (3H, m, ArCH), 7.69 (1H, d, J = 15.6 Hz, CH), 8.0 (1H, d, J = 15.7 Hz, CH), 8.0 (1H, d, J = 2.1 Hz, ArCH). **^{13}C NMR (100MHz, MeOD):** δ 16.6, 24.5, 31.4, 99.9, 117.4, 119.5, 120.7, 121.6, 122.6, 127.5, 128.6, 129.6, 130.0, 132.1, 133.4, 134.8, 137.1, 137.1, 141.5, 142.2, 165.2. **ESI-HRMS** (*m/z*): $[M + Na]^+$ calcd for $C_{23}H_{23}NO_3$, 384.1570; found, 384.1564.

(*E*)-3-(4-(3-methylbut-2-en-1-yl)-3-(3-(3-(tosyloxy)phenyl)propanamido)phenyl)acrylic acid (**26i**): Compound **25i** (290 mg, 0.5 mmol) was hydrolyzed following the general procedure B. Solvent was evaporated *in vacuo to* provide the title compound as a white soild (110 mg, 0.2 mmol, 41%). **R_f:** 0.2 (EtOAC). **^{1}H NMR (400 MHz; MeOD):** δ 1.70 (3H, s, CH_3), 1.76 (3H, s, CH_3), 2.39 (3H, s, CH_3), 2.61 (2H, t, J = 7.5 Hz, CH_2), 2.94 (2H, t, J = 7.5 Hz, CH_2), 3.40 (2H, d, J = 6.9 Hz, CH_2), 5.13 (1H, t, J = 7.0 Hz, CH), 6.32 (1H, d, J = 15.7 Hz, CH), 6.75 (1H, d, J = 7.3 Hz, ArCH), 6.95 (1H, s, ArCH), 7.14 – 7.22 (3H, m, ArCH), 7.30 (2H, d, J = 8.0 Hz, ArCH), 7.47 (1H, dd, J_1 = 8.2 Hz, J_2 = 2.1 Hz, ArCH), 7.61 (2H, d, J = 8.3 Hz, ArCH), 7.81 (1H, d, J = 2.1 Hz, ArCH), 7.95 (1H, d, J = 15.8 Hz, CH). **^{13}C NMR (100 MHz; MeOD):** δ 16.6, 20.2, 24.5, 30.7, 31.3, 37.7, 117.6, 119.4, 119.6, 121.7, 121.9, 122.6, 127.0, 128.2, 129.2, 129.5, 129.9, 132.0, 132.1, 133.2, 136.9, 137.0, 142.2, 143.0, 145.6, 149.7, 168.8, 171.6. **ESI-HRMS** (*m/z*): $[M + H]^+$ calcd for $C_{30}H_{31}NO_6S$, 534.1945; found, 534.1947.

(*E*)-3-(4-(3-methylbut-2-en-1-yl)-3-(3-(4-(tosyloxy)phenyl)propanamido)phenyl)acrylic acid (**26j**): Compound **25j** (400 mg, 0.7 mmol) was hydrolyzed following the general procedure B. Solvent was evaporated *in vacuo to* provide the title compound as a white soild (104 mg, 0.2 mmol, 28%). **R_f:** 0.4 (DCM:MeOH, 20:1). **^{1}H NMR (400 MHz; MeOD):** δ 1.72 (3H, s, CH_3), 1.79 (3H, s, CH_3), 2.39 (3H, s, CH_3), 2.65 (2H, t, *J* = 7.5 Hz, CH_2), 2.99 (2H, t, *J* = 7.5 Hz, CH_2), 3.45 (2H, d, *J* = 6.8 Hz, CH_2), 5.16 (1H, t, *J* = 7.0 Hz, CH), 6.34 (1H, d, *J* = 15.7 Hz, CH), 6.88 (2H, d, *J* = 8.5 Hz, ArCH), 7.18 – 7.31 (5H, m, ArCH), 7.44 (1H, d, *J* = 8.3 Hz, ArCH), 7.59 (2H, d, *J* = 8.2 Hz, ArCH), 7.82 (1H, d, *J* = 1.8 Hz, ArCH), 7.97 (1H, d, *J* = 15.8 Hz, CH). **^{13}C NMR (100 MHz; MeOD):** δ 16.5, 20.1, 24.4, 30.5, 31.3 38.0, 117.4, 121.6, 122.0, 122.6, 128.2, 129.3, 129.4, 129.9, 132.0, 132.1, 133.3, 136.9, 137.0, 140.0, 142.0, 145.6, 148.1. **ESI-HRMS** (*m/z*): $[M + Na]^+$ calcd for $C_{30}H_{31}NO_6S$, 556.1764; found, 556.1761.

(*E*)-3-(3-(3-(3-hydroxyphenyl)propanamido)-4-(3-methylbut-2-en-1-yl)phenyl)acrylic acid (**26k**): Compound **26i** (15 mg, 0.02 mmol) was dissolved in MeOH (2 mL) and refluxed with 1M NaOH (2 mL) overnight. Purification by column chromatography (Hexane:EtOAc = 9:1, 4:1) provided the title compound as a white soild (8 mg, 0.02 mmol, 90%). **R_f:** 0.2 (DCM:MeOH, 20:1). **^{1}H NMR (400 MHz; MeOD):** δ 1.73 (3H, s, CH_3), 1.79 (3H, s, CH_3), 2.65 (2H, t, *J* = 7.5 Hz, CH_2), 2.94 (2H, t, *J* = 7.5 Hz, CH_2), 3.44 (2H, d, *J* = 7.0 Hz, CH_2), 5.17 (1H, t, *J* = 7.0 Hz, CH), 6.35 (1H, d, *J* = 15.6 Hz, CH), 6.63 (1H, d, J_1 = 2.1 Hz, J_2 = 8.2 Hz, ArCH), 6.71 – 6.74 (2H, m, ArCH), 7.10 (1H, t, *J* = 7.4 Hz, ArCH), 7.17 (1H, d, *J* = 8.3 Hz, ArCH), 7.47 (1H, d, J_1 = 2.1 Hz, J_2 = 8.4 Hz, ArCH), 7.81 (1H, d, *J* = 2.4 Hz, ArCH), 7.95 (1H, d, *J* = 15.7 Hz, CH). **^{13}C NMR (100 MHz; MeOD):** δ 16.5, 24.4, 31.3, 31.3, 99.9, 122.7, 114.8, 117.6, 119.1, 121.7, 122.6, 129.0, 129.8, 132.0, 133.3, 136.9, 142.2, 157.1, 172.3. **ESI-HRMS** (*m/z*): $[M + Na]^+$ calcd for $C_{23}H_{25}NO_4$, 402.1676; found, 402.1666.

(*E*)-3-(3-(3-(4-hydroxyphenyl)propanamido)-4-(3-methylbut-2-en-1-yl)phenyl)acrylic acid (**26l**): Compound **26j** (80 mg, 0.15 mmol) was dissolved in MeOH (4 mL) and refluxed with 1M NaOH (2 mL)

overnight. Purification by column chromatography (Hexane:EtOAc = 9:1, 4:1) provided the title compound as a white soild (50 mg, 0.12 mmol, 84%). **R_f:** 0.1 (Hexane:EtOAc, 4:1). **^{1}H NMR (400 MHz; MeOD):** δ 1.73 (3H, s, CH_3), 1.79 (3H, s, CH_3), 2.62 (2H, t, *J* = 7.5 Hz, CH_2), 2.92 (2H, t, *J* = 7.5 Hz, CH_2), 3.44 (2H, d, *J* = 7.4 Hz, CH_2), 5.16 (1H, t, *J* = 7.0 Hz, CH), 6.33 (1H, d, *J* = 15.7 Hz, CH), 6.71 (2H, d, *J* = 8.5 Hz, ArCH), 7.08 (2H, d, *J* = 8.5 Hz, ArCH), 7.17 (1H, d, *J* = 8.3 Hz, ArCH), 7.46 (1H, d, J_1 = 2.1 Hz, J_2 = 8.2 Hz, ArCH), 7.81 (1H, d, *J* = 2.1 Hz, ArCH), 7.97 (1H, d, *J* = 15.8 Hz, CH). **^{13}C NMR (100 MHz; MeOD):** δ 16.5, 24.4, 30.6, 31.3, 38.8, 114.8, 117.6, 121.7, 122.6, 128.9, 129.8, 131.4, 132.2, 133.2, 136.9, 142.2, 155.3, 168.9, 172.5. **ESI-HRMS** (*m/z*): $[M - H]^-$ calcd for $C_{23}H_{25}NO_4$, 378.1711; found, 378.1700.

(*E*)-3-(3'-(hydroxymethyl)-2-(3-phenylpropanamido)-[1,1'-biphenyl]-4-yl)acrylic acid (28): Compound **27** (70 mg, 0.15 mmol) was hydrolyzed following the general procedure B. Solvent was evaporated *in vacuo to* provide the title compound as a white soild (27 mg, 0.06 mmol, 45%). **R_f:** 0.3 (DCM:MeOH, 10:1).**^{1}H NMR (400MHz , MeOD):** δ 2.72 (2H, t, *J* = 7.6 Hz, CH_2), 3.04 (2H, t, *J* = 7.6 Hz, CH_2), 4.68 (2H, s, CH_2), 6.41 (1H, d, *J* = 15.8 Hz, CH), 7.18 - 7.23 (2H, m, ArCH), 7.28 - 7.32 (6H, m, ArCH), 7.39 - 7.45 (2H, m, ArCH), 7.62 - 7.66 (2H, m, ArCH and CH), 7.99 (1H, d, *J* = 2.0 Hz, ArCH). **^{13}C NMR (100 MHz , MeOD):** δ 31.3, 38.5, 63.6, 117.3, 119.5, 121.3, 125.6, 125.8, 127.9, 128.0, 128.1, 128.5, 130.5, 132.6, 138.1, 138.6, 139.7, 140.7, 141.6, 143.2, 172.4. **ESI-HRMS** (*m/z*): $[M + Na]^+$ calcd for $C_{25}H_{23}NO_4$, 424.1519; found, 424.1510.

(*E*)-3-(5-((E)-3-methylbut-1-en-1-yl)-2-(3-phenylpropanamido)phenyl)acrylic acid (33a): Compound **32a** (30 mg, 0.07 mmol) was hydrolyzed following the general procedure B. Purification by column chromatography (Hexane:EtOAc = 10:1, 4:1, 2:1, 1:1) followed by solvent evaporation *in vacuo* provided the title compound as a white soild (18 mg, 0.05 mmol, 71%). **R_f:** 0.4 (DCM:MeOH, 10:1). **^{1}H NMR (400 MHz , MeOD):** δ 1.75 (3H, s, CH_3), 1.74 (3H, s, CH_3), 2.74 (2H, t, *J* = 7.6 Hz, CH_2), 3.04 (2H, t, *J* = 7.4 Hz, CH_2), 3.37 (2H, d, *J* = 8.7 Hz, CH_2), 5.33 (1H, t, *J* = 8.8 Hz, CH), 6.42 (1H, d, *J* = 15.7 Hz, CH), 7.15 – 7.23 (3H, m, ArCH), 7.29 – 7.33 (4H, m, ArCH), 7.50 (1H, s, ArCH), 7.70 (1H, d, *J* = 15.9 Hz, CH). **^{13}C NMR (100 MHz, MeOD):**

δ 24.4, 31.5, 33.2, 37.7, 122.5, 125.8, 126.8, 128.0, 128.1, 129.9, 130.1, 132.6, 132.8, 133.6, 133.7, 139.1, 140.4, 140.6, 173.2. **ESI-HRMS** (*m/z*): $[M + Na]^+$ calcd for $C_{23}H_{25}NO_3$, 386.1727; found, 386.1724.

(*E*)-3-(3'-(hydroxymethyl)-4-(3-phenylpropanamido)-[1,1'-biphenyl]-3-yl)acrylic acid (**33b**): Compound **32b** (20 mg, 0.05 mmol) was hydrolyzed following the general procedure B. Solvent was evaporated *in vacuo* to provide the title compound as a white soild (13 mg, 0.03 mmol, 73%). **R_f:** 0.5 (Hexane:EtOAc, 1:1). **^{1}H NMR (400 MHz , MeOD):** δ 2.79 (2H, t, *J* = 7.3 Hz, CH_2), 3.07 (2H, t, *J* = 7.8 Hz, CH_2), 4.70 (2H, s, CH_2), 6.57 (1H, d, *J* = 15.8 Hz, CH), 7.21 (1H, q, *J* = 4.4 Hz, ArCH), 7.31 – 7.47 (7H, m, ArCH), 7.57 (1H, d, *J* = 7.6 Hz, ArCH), 7.65 – 7.67 (2H, m, ArCH), 7.79 (1H, d, *J* = 15.8 Hz, CH), 7.94 (1H, s, ArCH). **^{13}C NMR (100 MHz, MeOD):** δ 31.4, 37.7, 63.7, 124.7, 125.0, 125.4, 125.8, 125.8, 126.9, 128.0, 128.1, 128.4, 128.6, 130.2, 135.1, 139.2, 139.4, 139.9, 140.6, 142.1 173.2. **ESI-HRMS** (*m/z*): $[M + Na]^+$ calcd for $C_{25}H_{23}NO_4$, 424.1519; found, 424.1523.

(*E*)-3-(3-(3-methylbut-2-en-1-yl)-5-(3-phenylpropanamido)phenyl)acrylic acid (**39a**): Compound **38a** (100 mg, 0.2 mmol) was hydrolyzed following the general procedure B. Solvent was evaporated *in vacuo* to provide the title compound as a white soild (55 mg, 0.15 mmol, 75%). **R_f:** 0.2 (DCM:MeOH, 20:1). **^{1}H NMR (400 MHz; MeOD):** δ 1.75 (3H, s, CH_3), 1.78 (3H, s, CH_3), 2.68 (2H, t, *J* = 7.6 Hz, CH_2), 3.01 (2H, d, *J* = 7.6 Hz, CH_2), 3.35 (2H, d, *J* = 7.4 Hz, CH_2), 5.33 (1H, t, *J* = 7.3 Hz, CH), 6.44 (1H, d, *J* = 15.9 Hz, CH), 7.13 (1H, s, ArCH), 7.17 – 7.21 (1H, m, ArCH), 7.29 – 7.32 (2H, m, ArCH), 7.38 (1H, s, ArCH), 7.55 – 7.70 (3H, m, ArCH). **^{13}C NMR (100 MHz; MeOD):** 27.2, 31.3, 33.5, 38.4, 110.3, 116.4, 118.6, 121.5, 122.3, 123.5, 125.8, 128.0, 128.0, 132.7, 139.0, 140.7, 143.2, 144.4, 172.3. **ESI-HRMS** (*m/z*): $[M + Na]^+$ calcd for $C_{23}H_{25}NO_3$, 386.1727; found, 386.1739.

(*E*)-3-(3'-(hydroxymethyl)-5-(3-phenylpropanamido)-[1,1'-biphenyl]-3-yl)acrylic acid (**39b**): Compound **38b** (100 mg, 0.2 mmol) was hydrolyzed following the general procedure B. Solvent was evaporated

in vacuo to provide the title compound as a white soild (50 mg, 0.1 mmol, 60%). **R_f:** 0.2 (DCM:MeOH, 20:1). **^{1}H NMR (400 MHz; MeOD):** δ 2.72 (2H, t, *J* = 7.3 Hz, CH_2), 3.02 (2H, t, *J* = 7.7 Hz, CH_2), 6.54 (1H, d, *J* = 15.8 Hz, CH), 7.17 – 7.22 (1H, m, ArCH), 7.28 – 7.29 (4H, m, ArCH), 7.37 – 7.39 (1H, m, ArCH), 7.44 (1H, t, *J* = 7.5 Hz, ArCH), 7.53 – 7.56 (2H, m, ArCH), 7.64 (1H, s, ArCH), 7.70 (1H, d, *J* = 16.0 Hz CH) 7.78 (1H, s, ArCH), 7.85 (1H, s, ArCH). **^{13}C NMR (100 MHz; MeOD):** 31.3, 38.5, 63.7, 117.5, 120.1, 122.2, 125.2, 125.5, 125.8, 126.0, 128.0, 128.1, 128.6, 135.5, 139.5, 140.0, 140.7, 142.1, 142.4, 144.5, 172.5. **ESI-HRMS** (*m/z*): $[M + H]^+$ calcd for $C_{25}H_{23}NO_4$, 402.1700; found, 402.1701.

(*E*)-3-(3-(3-methylbut-2-en-1-yl)-5-(phenethylcarbamoyl)phenyl)acrylic acid (**49a**): Compound (**45a**) (50 mg, 0.12 mmol) was hydrolyzed following the general procedure B. Solvent was evaporated *in vacuo* to provide the title compound as a white solid (21.7 mg, 0.06 mmol, 50%). **R_f:** 0.27 (DCM:MeOH, 20:1). **^{1}H NMR (400 MHz; MeOD):** δ 1.77 (3H, s, CH_3), 1.78 (3H, s, CH_3), 2.94 (2H, t, *J* = 7.3 Hz, CH_2), 3.43 (2H, d, *J* = 7.4 Hz, CH_2), 3.59 – 3.64 (2H, m, CH_2), 5.35 (1H, t, *J* = 7.4 Hz), 6.53 (1H, d, *J* = 16.0 Hz, CH), 7.20 – 7.32 (5H, m, ArCH), 7.54 (1H, s, ArCH), 7.63 (1H, s, ArCH), 7.68 (1H, d, *J* = 16.0 Hz, CH), 7.80 (1H, s, ArCH). **^{13}C NMR (100 MHz; MeOD):** δ 16.5, 24.5, 33.4, 35.0, 41.2, 119.1, 122.0, 123.7, 125.9, 128.1, 128.5, 128.6, 130.6, 133.0, 134.8, 135.2, 139.1, 143.1, 143.9, 168.3, 168.6. **ESI-HRMS** (*m/z*): $[M + Na]^+$ calcd for $C_{23}H_{25}NO_3$, 386.1727; found, 386.1736.

(*E*)-3-(3-((4-fluorophenethyl)carbamoyl)-5-(3-methylbut-2-en-1-yl)phenyl)acrylic acid (**49b**): Following the general procedure B the title compound was obtained as a white solid (20 mg, 0.05 mmol, 41%). **R_f:** 0.22 (DCM:MeOH, 20:1). **^{1}H NMR (400 MHz; MeOD):** δ 1.77 (3H, s, CH_3), 1.79 (3H, s, CH_3), 2.92 (2H, t, *J* = 7.3 Hz, CH_2), 3.44 (2H, d, *J* = 7.2 Hz, CH_2), 3.58 – 3.62 (2H, m, CH_2), 5.35 (1H, t, *J* = 7.2 Hz, CH), 6.54 (1H, d, *J* = 16.0 Hz, CH), 7.03 (2H, t, *J* = 8.9 Hz, ArCH). 7.28 (2H, q, J_1 = 5.4 Hz, J_2 = 3.1 Hz, ArCH), 7.56 (1H, s, ArCH), 7.63 (1H, s, ArCH), 7.68 (1H, d, *J* = 15.9 Hz, CH), 7.81 (1H, s, ArCH). **^{13}C NMR (100 MHz; MeOD):**

δ 16.5, 24.5, 33.4, 34.2, 41.2, 110.7, 114.5, 114.7, 122.0, 123.7, 128.5, 130.1, 130.1, 130.6, 133.1, 134.8, 135.1, 143.2, 147.0, 160.4, 168.3. **ESI-HRMS** (*m/z*): $[M + H]^+$ calcd for $C_{23}H_{24}NO_3F$, 382.1813; found, 382.1804.

(*E*)-3-(3-((4-methoxyphenethyl)carbamoyl)-5-(3-methylbut-2-en-1-yl)phenyl)acrylic acid (**49c**): Following the general procedure B the title compound was obtained as a white solid (26 mg, 0.06 mmol, 30%). **R_f:** 0.25 (DCM:MeOH, 20:1). **^{1}H NMR (400 MHz; MeOD):** δ 1.77 (3H, s, CH_3), 1.79 (3H, s, CH_3), 2.87 (2H, t, J = 7.4 Hz, CH_2), 3.44 (2H, d, J = 7.2 Hz, CH_2), 3.57 (2H, q, J_1 = 7.3 Hz, J_2 = 6.3 Hz, CH_2), 3.77 (3H, s, CH_3), 5.35 (1H, t, J = 7.3 Hz, CH), 6.54 (1H, d, J = 15.9 Hz, CH), 6.87 (2H, d, J = 8.6 Hz, ArCH), 7.18 (2H, d, J = 8.6 Hz, ArCH), 7.55 (1H, s, ArCH), 7.63 (1H, s, ArCH), 7.67 (1H, d, J = 16.0 Hz, CH), 7.80 (1H, s, ArCH), 8.61 (1H, t, J = 5.5 Hz, -NH). **^{13}C NMR (100 MHz; MeOD):** δ 16.5, 24.5, 33.4, 34.2, 41.4, 54.2, 110.7, 113.4, 122.0, 123.6, 128.5, 129.4, 130.6, 131.0, 133.0, 134.8, 135.2, 135.3, 143.1, 149.9, 158.3, 168.3.

(*E*)-3-(3-((4-methoxybenzyl)carbamoyl)-5-(3-methylbut-2-en-1-yl)phenyl)acrylic acid (**49d**): Following the general procedure B the title compound was obtained as a white solid (12 mg, 0.03 mmol, 45%). **R_f:** 0.25 (DCM:MeOH, 20:1). **^{1}H NMR (400 MHz; MeOD):** δ 1.76 (3H, s, CH_3), 1.78 (3H, s, CH_3), 3.44 (2H, d, J = 7.3 Hz, CH_2), 3.78 (3H, s, CH_3), 4.52 (2H, d, J = 4.1 Hz, CH_2), 5.35 (1H, t, J = 7.3 Hz, CH), 6.55 (1H, d, J = 16.0 Hz, CH), 6.90 (2H, d, J = 8.7 Hz, ArCH), 7.29 (2H, d, J = 8.7 Hz, ArCH), 7.55 (1H, s, ArCH), 7.68 (1H, d, J = 16.0 Hz, CH), 7.71 (1H, s, ArCH), 7.89 (1H, s, ArCH), 9.00 (1H, t, J = 5.6 Hz, -NH). **^{13}C NMR (100 MHz; MeOD):** δ 16.5, 24.4, 33.4, 42.6, 54.2, 110.7, 113.5, 119.4, 122.0, 123.8, 128.5, 130.6, 130.7, 133.0, 134.9, 135.1, 143.2, 143.7, 159.0, 168.0. **ESI-HRMS** (*m/z*): $[M + Na]^+$ calcd for $C_{23}H_{25}NO_4$, 402.1676; found, 402.1669.

(*E*)-3-(3-(3-methylbut-2-en-1-yl)-5-((4-(trifluoromethoxy)benzyl)carbamoyl)phenyl)acrylic acid (**49e**): Following the general procedure B the title compound was obtained as a white solid (39 mg, 0.09 mmol, 75%). **R_f:** 0.25 (DCM:MeOH, 20:1). **^{1}H NMR (400 MHz; MeOD):** δ 1.77 (3H, s, CH_3), 1.78 (3H, s, CH_3), 3.45 (2H, d, J = 7.2 Hz, CH_2), 4.61 (2H, s, CH_2), 5.36 (1H, t, J = 7.3 Hz, CH), 6.56 (1H, d, J = 15.9 Hz, CH), 7.26

(2H, d, *J* = 7.9 Hz, ArCH), 7.47 (2H, d, *J* = 8.7 Hz, ArCH), 7.58 (1H, s, ArCH), 7.69 (1H, d, *J* = 16.0 Hz, CH), 7.73 (1H, s, ArCH), 7.92 (1H, s, ArCH). **NMR (100 MHz; MeOD):** δ 16.5, 24.4, 33.4, 42.4, 119.3, 119.3, 120.7, 122.0, 123.8, 128.7, 128.8, 130.7, 133.1, 134.8, 134.9, 138.1, 143.3, 143.8, 148.1, 168.2. **ESI-HRMS** (*m/z*): [M + Na]$^+$ calcd for $C_{23}H_{22}NO_4F_3$, 456.1393; found, 456.1403.

(*E*)-3-(3-(3-methylbut-2-en-1-yl)-5-((3-(trifluoromethoxy)benzyl)carbamoyl)phenyl)acrylic acid (**49f**): Following the general procedure B the title compound was obtained as a white solid (18 mg, 0.04 mmol, 33%). **R_f:** 0.21 (DCM:MeOH, 20:1). **^{1}H NMR (400 MHz; MeOD):** δ 1.77 (3H, s, CH_3), 1.78 (3H, s, CH_3), 2.87 (2H, t, *J* = 7.4 Hz, CH_2), 3.45 (2H, d, *J* = 7.5 Hz, CH_2), 4.63 (2H, d, J_1 = 4.0 Hz, CH_2), 5.36 (1H, t, *J* = 7.3 Hz, CH), 6.56 (1H, d, *J* = 16.0 Hz, CH), 7.18 (2H, d, *J* = 8.1 Hz, ArCH), 7.29 (1H, s, ArCH), 7.37 – 7.47 (2H, m, ArCH), 7.58 (1H, s, ArCH), 7.73 (1H, s, ArCH), 7.70 (1H, d, *J* = 16.0 Hz, CH), 7.92 (1H, s, ArCH). **NMR (100 MHz; MeOD):** δ 16.5, 24.4, 33.4, 42.6, 119.2, 119.6, 122.0, 123.8, 125.8, 128.6, 129.8, 130.8, 133.1, 134.8, 134.9, 141.6, 143.3, 143.9, 149.3, 150.1, 168.2, 168.6. **ESI-HRMS** (*m/z*): [M + Na]$^+$ calcd for $C_{23}H_{22}NO_4F_3$, 456.1393; found, 456.1387.

(*E*)-3-(3-((4-methylbenzyl)carbamoyl)-5-(3-methylbut-2-en-1-yl)phenyl)acrylic acid (**49g**): Following the general procedure B the title compound was obtained as a white solid (18 mg, 0.05 mmol, 30%). **R_f:** 0.20 (DCM:MeOH, 20:1). **^{1}H NMR (400 MHz; MeOD):** δ 1.76 (3H, s, CH_3), 1.77 (3H, s, CH_3), 2.31 (3H, s, CH_3), 3.43 (2H, d, *J* = 7.3 Hz, CH_2), 4.54 (2H, d, *J* = 5.4 Hz, CH_2), 5.35 (1H, t, *J* = 7.3 Hz, CH), 6.54 (1H, d, *J* = 16.0 Hz, CH), 7.15 (2H, d, *J* = 7.8 Hz, ArCH), 7.24 (2H, d, *J* = 8.0 Hz, ArCH), 7.55 (1H, s, ArCH), 7.68 (1H, d, *J* = 16.0 Hz, CH), 7.71 (1H, s, ArCH), 7.90 (1H, s, ArCH), 9.03 (1H, t, *J* = 5.7 Hz, -NH). **NMR (100 MHz; MeOD):** δ 16.5, 19.7, 24.5, 33.4, 42.9, 119.1, 122.0, 123.8, 127.1, 128.7, 128.7, 130.6, 133.0, 134.8, 135.0, 135.6, 136.5, 143.2, 143.9, 168.0, 168.7. **ESI-HRMS** (*m/z*): [M + H]$^+$ calcd for $C_{23}H_{25}NO_3$, 364.1907; found, 364.1899.

(*E*)-3-(3-((4-(dimethylamino)benzyl)carbamoyl)-5-(3-methylbut-2-en-1-yl)phenyl)acrylic acid (**49h**): Following the general procedure B the title compound was obtained as a white solid (15 mg, 0.04 mmol, 42%). **R_f:** 0.27 (DCM:MeOH, 20:1). **^{1}H NMR (400 MHz; MeOD):** δ 1.77 (3H, s, CH_3), 1.78 (3H, s, CH_3), 2.91 (6H, s, $N(CH_3)_2$), 3.44 (2H, d, J = 7.2 Hz, CH_2), 4.48 (2H, d, J = 5.6 Hz, CH_2), 5.36 (1H, t, J = 7.3 Hz, CH), 6.55 (1H, d, J = 16.0 Hz, CH), 6.78 (2H, d, J = 8.7 Hz, ArCH), 7.23 (2H, d, J = 8.7 Hz, ArCH), 7.55 (1H, s, ArCH), 7.67 (1H, d, J = 16.0 Hz, CH), 7.71 (1H, s, ArCH), 7.89 (1H, s, ArCH), 8.92 (1H, t, J = 5.9 Hz, -NH). **NMR (100 MHz; MeOD):** δ 16.5, 24.4, 33.4, 39.7, 42.8, 112.9, 119.4, 122.1, 123.7, 126.9, 128.2, 128.7, 130.5, 133.0, 134.9, 135.2, 143.1, 143.7, 150.2, 168.0, 168.9 **ESI-HRMS** (*m/z*): $[M + H]^+$ calcd for $C_{24}H_{28}N_2O_3$, 393.2173; found, 393.2169.

(*E*)-3-(3-allyl-5-(phenethylcarbamoyl)phenyl)acrylic acid (**50**): Following the general procedure B the title compound was synthesized using **46** as a white solid (11 mg, 0.03 mmol, 27%). **R_f:** 0.26 (DCM:MeOH, 20:1). **^{1}H NMR (400 MHz; MeOD):** δ 2.94 (2H, t, J = 7.1 Hz, CH_2), 3.48 (2H, d, J = 6.7 Hz, CH_2), 3.60 (2H, t, J = 7.8 Hz, CH_2), 5.11 – 5.17 (2H, m, CH_2), 5.96 – 6.06 (1H, m, CH), 6.55 (1H, d, J = 16.0 Hz, CH), 7.20 – 7.32 (5H, m, ArCH), 7.59 (1H, s, ArCH), 7.66 (1H, s, ArCH), 7.70 (1H, s, ArCH), 7.82 (1H, d, J = 16.0 Hz, CH). **^{13}C NMR (100 MHz; $CDCl_3$,):** δ 35.0, 39.3, 41.2, 115.5, 124.0, 125.9, 127.6, 128.1, 128.5, 128.8, 129.4, 130.8, 134.9, 135.3, 136.5, 139.1, 141.5, 143.6, 168.1. **ESI-HRMS** (*m/z*): $[M + H]^+$ calcd for $C_{21}H_{21}NO_3$, 336.1594; found, 336.1595.

(*E*)-3-(3'-(hydroxymethyl)-5-(phenethylcarbamoyl)-[1,1'-biphenyl]-3-yl)acrylic acid (**51**): Following the general procedure B the title compound was synthesized using **47** as a white solid (14 mg, 0.03 mmol, 35%). **R_f:** 0.19 (DCM:MeOH, 20:1). **^{1}H NMR (400 MHz; $CDCl_3$):** δ 2.97 (2H, t, J = 7.1 Hz, CH_2), 3.65 (2H, t, J = 7.5 Hz, CH_2), 4.72 (2H, s, CH_2), 6.66 (1H, d, J = 16.0 Hz, CH), 7.22 – 7.50 (7H, m, ArCH), 7.62 (1H, d, J = 7.5 Hz, ArCH), 7.71 (1H, s, ArCH), 7.75 (1H, d, J = 15.9 Hz, CH), 7.99 (2H, d, J = 4.8 Hz, ArCH), 8.06 (1H, s, ArCH). **^{13}C NMR (100 MHz; $CDCl_3$):** δ 35.0, 41.3, 63.6, 124.7, 124.8, 125.2, 125.6, 126.0, 126.3, 126.9, 128.1, 128.5,

128.7, 129.1, 129.6, 135.6, 135.7, 139.1, 139.5, 142.1, 142.2, 168.0. **ESI-HRMS** (*m/z*): $[M + Na]^+$ calcd for $C_{25}H_{23}NO_4$, 424.1519; found, 424.1513.

(*E*)-3-(3-(3-methylbut-2-en-1-yl)-5-(phenethoxycarbonyl)phenyl)acrylic acid (**52**): Following the general procedure B the title compound was synthesized using **48** as a white solid (30 mg, 0.08 mmol, 51%). **^{1}H NMR (400 MHz; $CDCl_3$):** δ 1.76 (3H, s, CH_3), 1.80 (3H, s, CH_3), 3.12 (2H, t, J = 7.0 Hz, CH_2), 3.42 (2H, d, J = 7.2 Hz, CH_2), 4.57 (2H, t, J = 6.9 Hz, CH_2), 5.32 (1H, t, J = 7.3 Hz, CH), 6.51 (1H, d, J = 15.9 Hz, CH), 7.29 – 7.38 (5H, m, ArCH), 7.53 (1H, s, ArCH), 7.80 (1H, d, J = 15.9 Hz, CH), 7.87 (1H, s, ArCH), 8.02 (1H, s, ArCH). **^{13}C NMR (100 MHz; $CDCl_3$):** δ 17.9, 25.7, 33.9, 35.2, 65.7, 118.1, 121.8, 126.7, 128.5, 128.9, 129.0, 131.1, 131.5, 132.5, 133.9, 134.3, 137.7, 143.1, 146.0, 166.0, 171.3. **ESI-HRMS** (*m/z*): $[M + Na]^+$ calcd for $C_{23}H_{24}O_4$, 387.1567; found, 387.1573.

(*E*)-3-(3-(benzyloxy)-5-(phenethylcarbamoyl)phenyl)acrylic acid (**59a**): Following the general procedure B the title compound was obtained as a white solid (8 mg, 0.02 mmol, 33%). **R_f:** 0.3 (DCM:MeOH, 20:1). **^{1}H NMR (400 MHz; MeOD):** δ 2.94 (2H, t, J = 7.0 Hz, CH_2), 3.61 (2H, t, J = 6.0 Hz, CH_2), 5.18 (2H, s, CH_2), 6.55 (1H, d, J = 15.9 Hz, CH), 7.20 – 7.49 (12H, m, ArCH), 7.58 (1H, s, ArCH), 7.65 (1H, d, J = 15.9 Hz, CH). **^{13}C NMR (100 MHz; MeOD):** δ 35.0, 41.3, 69.9, 115.0, 116.8, 118.8, 125.9, 127.3, 127.6, 128.1, 128.1, 128.5, 136.2, 136.4, 136.7, 139.1, 143.4, 159.3, 167.8. **ESI-HRMS** (*m/z*): $[M + Na]^+$ calcd for $C_{25}H_{23}NO_4$, 424.1519; found, 424.1520.

(*E*)-3-(3-((3-methoxybenzyl)oxy)-5-(phenethylcarbamoyl)phenyl)acrylic acid (**59b**): Following the general procedure B the title compound was obtained as a white solid (10 mg, 0.02 mmol, 38%). **R_f:** 0.2 (DCM:MeOH, 20:1). **^{1}H NMR (400 MHz; $CDCl_3$):** δ 2.93 (2H, t, J = 7.0 Hz, CH_2), 3.61 (2H, t, J = 6.0 Hz, CH_2), 3.81 (3H, s, CH_3), 5.15 (2H, s, CH_2), 6.55 (1H, d, J = 15.9 Hz, CH), 6.89 (1H, dd, J_1 = 2.1 Hz, J_2 = 8.0 Hz, ArCH), 7.03 – 7.05 (2H, m, ArCH), 7.19 – 7.33 (6H, m, ArCH), 7.37 (1H, s, ArCH), 7.44 (1H, s, ArCH), 7.58 (1H, s,

ArCH), 7.61 (1H, d, J = 16.0 Hz, CH). **^{13}C NMR (100 MHz; $CDCl_3$):** δ 35.0, 41.3, 54.2, 69.7, 112.6, 113.1, 114.9, 116.7, 118.7, 119.3, 125.9, 128.1, 128.5, 129.2, 136.3, 136.4, 138.2, 139.1, 142.7, 159.2, 159.9, 167.8. **ESI-HRMS** (*m/z*): $[M + Na]^+$ calcd for $C_{26}H_{25}NO_5$, 454.1625; found, 454.1630.

Enzyme Inhibition Assay: (*S*)-(+)-1,2,3,4-tetrahydro-1-naphthol (*S*-tetralol) was purchased from Sigma-Aldrich (St. Louis, MO). Nicotinamide adenine dinucleotide (NAD^+) and nicotinamide adenine dinucleotide phosphate ($NADP^+$) were purchased from Roche Diagnostics (Indianapolis, IN). Homogeneous recombinant enzymes AKR1C3 and AKR1C2 were prepared and purified as previously described.[70] The specific activities of AKR1C3 and AKR1C2 for the oxidation of *S*-tetralol are 2.0 and 1.5 μmol min^{-1} mg^{-1}, respectively.

Assay of enzyme activity: The dehydrogenase activities of AKR1C3 and AKR1C2 were determined by measuring the UV absorption of NADH formation at 340 nm using Beckman DU640 spectrophotometer. A typical assay solution contained 100 mM potassium phosphate pH 7.0, 2.3 mM NAD^+, 3.0 mM (*S*)-(+)-1,2,3,4-tetrahydro-1-naphthol (*S*-tetralol), 4% acetonitrile (v/v). The mixtures were incubated at 37 °C for 3 min followed by adding a serial dilution of AKR1C3 or AKR1C2 solution to a final volume of 1 mL to initiate the reaction. After continuously monitoring for 5 min, the increase in UV absorption using different concentrations of enzyme were recorded to calculate the initial velocity and determine enzyme specific activity.

IC_{50} value determination: The inhibitory potency for each compound was represented by IC_{50} value and measured as described before.[24, 34, 71] The IC_{50} value of baccharin and baccharin analogues was determined by measuring their inhibition of the $NADP^+$ dependent oxidation of *S*-tetralol catalyzed by AKR1C3 or AKR1C2. The concentration of *S*-tetralol used in this assay for AKR1C3 and AKR1C2 was 165 μM and 15 μM respectively, which was equal to the K_m value for each enzyme isoform in order to make a direct comparison of IC_{50} values. The IC_{50} value of each compound was acquired from a single experiment with each inhibitor concentration run in quadruplicate and directly calculated by fitting the inhibition data to an equation [y = (range) / [1 + (I/IC_{50})S] + background] using Grafit 5.0 software. In this equation, "range" is the fitted uninhibited value minus the

"background", and "S" is a slope factor. "I" is the concentration of inhibitor. The equation assumes that y falls with increasing "I".

Adjuvant assay: HL-60 (ATCC® CCL-240™), KG1a (ATCC® CCL-246.1™) and THP-1 (ATCC® TIB-202™) cells were procured from ATCC. Isocove's Modified Dulbecco's Media (IMDM) supplemented with 20% fetal bovine serum (FBS) and penicillin/streptomycin (1%) was used to culture HL-60 and KG1a cells whereas THP-1 cells were cultured using Roswell Park Memorial Institute (RPMI)-1640 medium, supplemented with 20% fetal bovine serum (FBS), 0.05 mM 2-mercaptoethanol and penicillin/streptomycin (1%). Cells were maintained at a density of 0.1–1 x 10^6 cells/mL under 5% CO_2 at 37 ^oC. To screen the test compounds, cells were seeded at a density of 0.1 x 10^6 cells/mL in 96-well plates containing 100 μL cell suspension per well. Stock solutions of the test compounds, etoposide, daunorubicin and cytarabine (AraC) were prepared in DMSO. Cells were treated at the indicated concentrations of test compounds with or without the chemotherapeutic agents, limiting the final DMSO concentration to less than 1%. After incubation at 37 ^OC, 5% CO_2 for 24, 48, 72 or 96 h, 20 μL of MTS reagent (CellTiter 96® AQueous One Solution Reagent) was added to each well and incubated at the above mentioned conditions for 2-3 h. Plates were read at OD 490 nm on a plate reader and the viability of cells were plotted as percentage of controls.

Quantification of the degree of synergism: To quantify the degree of synergism, the results of the co-treatment and pre-treatment experiments were analyzed by CompuSyn software (Paramus, NJ) based on the median effect principle or 'Chou-Talalay' method.[72] The method is based on the median-effect equation that encompasses the Michaelis-Menten, Hill, Henderson-Hasselbach, and Scatchard equations to provide combination and dose reduction indices.[66] The combination index (CI) and dose reduction index (DRI) values were calculated at a constant ratio of chemotherapeutic to AKR1C3 inhibitor at 50% cytotoxic effect (F_a = 0.5). CompuSyn software was used to generate the CI and DRI values. CI<1, synergism; CI>1.1, antagonism; CI=1.1, additive.[66]

Western blotting: HL-60 and KG1a cells were treated with compound (**4**) over a period of 48 and 72 h at indicated concentrations after which they were harvested and pelleted. The whole cell lysates were prepared in radioimmunoprecipitation assay RIPA buffer containing protease and phosphatase inhibitors (1 mM PMSF, 38 μg/mL aprotinin, 2.5 mM Na_3VO_4). Samples were incubated on ice for 30 min after which they were sonicated, centrifuged (16000 x g) and supernatant collected. Protein concentration in each sample was estimated following bicinchoninic acid BCA assay protocol by comparing with the BSA standards (Pierce™ BCA protein kit). Protein samples (40 μg) containing loading dye (7 μL) were loaded onto 12% SDS polyacrylamide gel and electrophoresed (80 V, 2 hr). Transferred onto a PVDF membrane overnight (25 V, 4 °C). The membrane was blocked with 5 % non-fat milk (1 h) and probed with human anti-AKR1C3 mouse monoclonal antibody (1:500, R&D Systems, MAB7678) and corresponding horseradish peroxidase (HRP) conjugated anti-mouse secondary antibody followed by immunodetection using VersaDoc™ (MP 5000). Membrane was stripped and re-probed for β-actin (1:5000, Sigma-Aldrich, A5441). Quantity One® software was used to analyze the band intensities and fold change in AKR1C3 enzyme expression was determined based on β-actin controls.

ASSOCIATED CONTENT

Supporting Information

The supporting information is available free of charge on the ACS publications website at DOI:

Cell viability curves of AKR1C3 inhibitors **1**, **26a**, **49a** and **49g**, daunorubicin and AraC single treatment in HL-60, KG1a and THP-1 cells. AKR1C3 expression in leukemic cells. Cell viability curves of leukemic cells upon co-treatment of AKR1C3 inhibitor and daunorubcin and AKR1C3 inhibitor and AraC. Cell viability curves of COG T-ALL cells treated with inhibitor **49a**, daunorubicin and AraC. Cell viability curves of BMMNC cells treated with combination AKR1C3 inhibitor **49a** and either AraC or daunorubicin. Synthetic details and characterization data for all intermediates and ^{1}H and ^{13}C NMR spectra of final compounds.

Molecular formula strings (CSV)

PDB file for docking model of **49a** with AKR1C3 (Figure 3B).

AUTHOR INFORMATION

Corresponding Author

*Phone: +01-806-414-9245. E-mail: paul.trippier@ttuhsc.edu

ORCID

Trevor M. Penning: 0000-0002-3937-1066

Paul C. Trippier: 0000-0002-4947-5782

Notes

The authors declare the following competing financial interest(s):

A patent application has been filed describing the compounds in this paper. *Highly selective AKR1C3 inhibitors and methods of use thereof*. PCT Int. Appl. (2018) WO 2018148721 A1.

ACKNOWLEDGMENTS

Research reported in this publication was supported in part by the National Cancer Institute of the National Institutes of Health under Award Number R01 CA226436 (P.C.T) and by a research grant from Leukemia Texas (P.C.T). The content is solely the responsibility of the authors and does not necessarily represent the official views of the National Institutes of Health.

ABBREVIATIONS

AKR1C3, aldo–keto reductase 1C3; ALL, acute lymphoblastic leukemia; AR, androgen receptor; AraC, cytarabine; ATRA, all-trans retinoic acid; APL, acute promyelocytic leukemia; COG, children's oncology group; CRPC, castration-resistant prostate cancer; CI, combination index; DHT, dihydrotestosterone; DPPA, di-phenyl phosphoryl azide; DRI, dose reduction index; FAB, French–American–British; FP, prostaglandin $F_{2\alpha}$ receptor; LLE, ligand-lipophilicity efficiency; 4-MDDT, 4-methyl(de-dimethylamine)-tetracycline; MPA,

medroxyprogesterone acetate; OX, oxyanion site; PG, prostaglandin; PGFS, prostaglandin F synthase; PML, promyelocytic leukemia; RARα, retinoic acid receptor alpha; SP, sub pocket;

REFERENCES

1. Siegel, R. L.; Miller, K. D.; Jemal, A. Cancer statistics, 2018. *CA Cancer J. Clin.* **2018,** 68, 7-30.
2. Shipley, J. L.; Butera, J. N. Acute myelogenous leukemia. *Exp. Hematol.* **2009,** 37, 649-658.
3. Renneville, A.; Roumier, C.; Biggio, V.; Nibourel, O.; Boissel, N.; Fenaux, P.; Preudhomme, C. Cooperating gene mutations in acute myeloid leukemia: a review of the literature. *Leukemia* **2008,** 22, 915-931.
4. Grimwade, D.; Enver, T. Acute promyelocytic leukemia: where does it stem from? *Leukemia* **2004,** 18, 375-384.
5. Brown, G.; Hughes, P. Retinoid differentiation therapy for common types of acute myeloid leukemia. *Leuk. Res. Treat.* **2012,** 2012, 939021.
6. Huang, M.; Ye, Y.-c.; Chen, S.; Chai, J.-R.; Lu, J.-X.; Zhoa, L.; Gu, L.; Wang, Z.-Y. Use of all-trans retinoic acid in the treatment of acute promyelocytic leukemia. *Blood* **1988,** 72, 567-572.
7. Deschler, B.; de Witte, T.; Mertelsmann, R.; Lubbert, M. Treatment decision-making for older patients with high-risk myelodysplastic syndrome or acute myeloid leukemia: problems and approaches. *Haematologica* **2006,** 91, 1513-1522.
8. Kuendgen, A.; Germing, U. Emerging treatment strategies for acute myeloid leukemia (AML) in the elderly. *Cancer Treat. Rev.* **2009,** 35, 97-120.
9. Terwilliger, T.; Abdul-Hay, M. Acute lymphoblastic leukemia: a comprehensive review and 2017 update. *Blood Cancer J.* **2017,** 7, e577.
10. Van Vlierberghe, P.; Ferrando, A. The molecular basis of T cell acute lymphoblastic leukemia. *J. Clin. Invest.* **2012,** 122, 3398-3406.
11. Marks, D. I.; Rowntree, C. Management of adults with T-cell lymphoblastic leukemia. *Blood* **2017,** 129, 1134-1142.
12. Desmond, J. C.; Mountford, J. C.; Drayson, M. T.; Walker, E. A.; Hewison, M.; Ride, J. P.; Luong, Q. T.; Hayden, R. E.; Vanin, E. F.; Bunce, C. M. The aldo-keto reductase AKR1C3 is a novel suppressor of cell differentiation that provides a plausible target for the non-cyclooxygenase-dependent antineoplastic actions of nonsteroidal anti-inflammatory drugs. *Cancer Res.* **2003,** 63, 505-512.
13. Manesh, D. M.; El-Hoss, J.; Evans, K.; Richmond, J.; Toscan, C. E.; Bracken, L. S.; Hedrick, A.; Sutton, R.; Marshall, G. M.; Wilson, W. R. AKR1C3 is a biomarker of sensitivity to PR-104 in preclinical models of T-cell acute lymphoblastic leukemia. *Blood* **2015,** 126, 1193-1202.
14. Sales, K. J.; Milne, S. A.; Williams, A. R.; Anderson, R. A.; Jabbour, H. N. Expression, localization, and signaling of prostaglandin F2α receptor in human endometrial adenocarcinoma: regulation of proliferation by activation of the epidermal growth factor receptor and mitogen-activated protein kinase signaling pathways. *J. Clin. Endocrinol. Metab.* **2004,** 89, 986-993.
15. Straus, D. S.; Glass, C. K. Cyclopentenone prostaglandins: new insights on biological activities and cellular targets. *Med. Res. Rev.* **2001,** 21, 185-210.
16. Khanim, F. L.; Hayden, R. E.; Birtwistle, J.; Lodi, A.; Tiziani, S.; Davies, N. J.; Ride, J. P.; Viant, M. R.; Gunther, U. L.; Mountford, J. C. Combined bezafibrate and medroxyprogesterone acetate: potential novel therapy for acute myeloid leukaemia. *PLoS One* **2009,** 4, e8147.
17. Ji, Q.; Chang, L.; Stanczyk, F. Z.; Ookhtens, M.; Sherrod, A.; Stolz, A. Impaired dihydrotestosterone catabolism in human prostate cancer: critical role of AKR1C2 as a pre-receptor regulator of androgen receptor signaling. *Cancer Res.* **2007,** 67, 1361-1369.
18. Penning, T. M.; Bauman, D. R.; Jin, Y.; Rizner, T. L. Identification of the molecular switch that regulates access of 5α-DHT to the androgen receptor. *Mol. Cell. Endocrinol.* **2007,** 265, 77-82.

19. Hofman, J.; Malcekova, B.; Skarka, A.; Novotna, E.; Wsol, V. Anthracycline resistance mediated by reductive metabolism in cancer cells: The role of aldo-keto reductase 1C3. *Toxicol. Appl. Pharmacol.* **2014,** 278, 238-248.
20. Heibein, A. D.; Guo, B.; Sprowl, J. A.; MacLean, D. A.; Parissenti, A. M. Role of aldo-keto reductases and other doxorubicin pharmacokinetic genes in doxorubicin resistance, DNA binding, and subcellular localization. *BMC Cancer* **2012,** 12, 381.
21. Byrns, M. C.; Penning, T. M. Type 5 17β-hydroxysteroid dehydrogenase/prostaglandin F synthase (AKR1C3): role in breast cancer and inhibition by non-steroidal anti-inflammatory drug analogs. *Chem. Biol. Interact.* **2009,** 178, 221-227.
22. Matsunaga, T.; Hojo, A.; Yamane, Y.; Endo, S.; El-Kabbani, O.; Hara, A. Pathophysiological roles of aldo–keto reductases (AKR1C1 and AKR1C3) in development of cisplatin resistance in human colon cancers. *Chem. Biol. Interact.* **2013,** 202, 234-242.
23. Adeniji, A. O.; Chen, M.; Penning, T. M. AKR1C3 as a target in castrate resistant prostate cancer. *J. Steroid Biochem. Mol. Biol.* **2013,** 137, 136-149.
24. Liedtke, A. J.; Adeniji, A. O.; Chen, M.; Byrns, M. C.; Jin, Y.; Christianson, D. W.; Marnett, L. J.; Penning, T. M. Development of potent and selective indomethacin analogues for the inhibition of AKR1C3 (type 5 17β-hydroxysteroid dehydrogenase/prostaglandin F synthase) in castrate-resistant prostate cancer. *J. Med. Chem.* **2013,** 56, 2429-2446.
25. Rižner, T. L.; Šmuc, T.; Rupreht, R.; Šinkovec, J.; Penning, T. M. AKR1C1 and AKR1C3 may determine progesterone and estrogen ratios in endometrial cancer. *Mol. Cell. Endocrinol.* **2006,** 248, 126-135.
26. Byrns, M. C.; Jin, Y.; Penning, T. M. Inhibitors of type 5 17β-hydroxysteroid dehydrogenase (AKR1C3): overview and structural insights. *J. Steroid Biochem. Mol. Biol.* **2011,** 125, 95-104.
27. Lan, Q.; Mumford, J. L.; Shen, M.; DeMarini, D. M.; Bonner, M. R.; He, X.; Yeager, M.; Welch, R.; Chanock, S.; Tian, L. Oxidative damage-related genes AKR1C3 and OGG1 modulate risks for lung cancer due to exposure to PAH-rich coal combustion emissions. *Carcinogenesis* **2004,** 25, 2177-2181.
28. Škarydová, L.; Živná, L.; Xiong, G.; Maser, E.; Wsól, V. AKR1C3 as a potential target for the inhibitory effect of dietary flavonoids. *Chem. Biol. Interact.* **2009,** 178, 138-144.
29. Davies, N. J.; Hayden, R. E.; Simpson, P. J.; Birtwistle, J.; Mayer, K.; Ride, J. P.; Bunce, C. M. AKR1C isoforms represent a novel cellular target for jasmonates alongside their mitochondrial-mediated effects. *Cancer Res.* **2009,** 69, 4769-4775.
30. Adeniji, A.; Uddin, M. J.; Zang, T.; Tamae, D.; Wangtrakuldee, P.; Marnett, L. J.; Penning, T. M. Discovery of (R)-2-(6-methoxynaphthalen-2-yl) butanoic acid as a potent and selective aldo-keto reductase 1C3 inhibitor. *J. Med. Chem.* **2016,** 59, 7431-7444.
31. Bydal, P.; Luu-The, V.; Labrie, F.; Poirier, D. Steroidal lactones as inhibitors of 17β-hydroxysteroid dehydrogenase type 5: chemical synthesis, enzyme inhibitory activity, and assessment of estrogenic and androgenic activities. *Eur. J. Med. Chem.* **2009,** 44, 632-644.
32. Bauman, D. R.; Rudnick, S. I.; Szewczuk, L. M.; Jin, Y.; Gopishetty, S.; Penning, T. M. Development of nonsteroidal anti-inflammatory drug analogs and steroid carboxylates selective for human aldo-keto reductase isoforms: potential antineoplastic agents that work independently of cyclooxygenase isozymes. *Mol. Pharmacol.* **2005,** 67, 60-68.
33. Byrns, M. C.; Steckelbroeck, S.; Penning, T. M. An indomethacin analogue, N-(4-chlorobenzoyl)-melatonin, is a selective inhibitor of aldo-keto reductase 1C3 (type 2 3α-HSD, type 5 17β-HSD, and prostaglandin F synthase), a potential target for the treatment of hormone dependent and hormone independent malignancies. *Biochem. Pharmacol.* **2008,** 75, 484-493.
34. Adeniji, A. O.; Twenter, B. M.; Byrns, M. C.; Jin, Y.; Chen, M.; Winkler, J. D.; Penning, T. M. Development of potent and selective inhibitors of aldo–keto reductase 1C3 (type 5 17β-hydroxysteroid dehydrogenase) based on N-phenyl-aminobenzoates and their structure–activity relationships. *J. Med. Chem.* **2012,** 55, 2311-2323.
35. Chen, M.; Adeniji, A. O.; Twenter, B. M.; Winkler, J. D.; Christianson, D. W.; Penning, T. M. Crystal structures of AKR1C3 containing an N-(aryl) amino-benzoate inhibitor and a bifunctional AKR1C3 inhibitor

and androgen receptor antagonist. Therapeutic leads for castrate resistant prostate cancer. *Bioorg. Med. Chem. Lett.* **2012,** 22, 3492-3497.
36. Yin, Y. D.; Fu, M.; Brooke, D. G.; Heinrich, D. M.; Denny, W. A.; Jamieson, S. M. The activity of SN33638, an inhibitor of AKR1C3, on testosterone and 17β-estradiol production and function in castration-resistant prostate cancer and ER-positive breast cancer. *Front. Oncol.* **2014,** 4, 159.
37. Loriot, Y.; Fizazi, K.; Jones, R. J.; Van den Brande, J.; Molife, R. L.; Omlin, A.; James, N. D.; Baskin-Bey, E.; Heeringa, M.; Baron, B.; Holtkamp, G. M.; Ouatas, T.; De Bono, J. S. Safety, tolerability and anti-tumour activity of the androgen biosynthesis inhibitor ASP9521 in patients with metastatic castration-resistant prostate cancer: multi-centre phase I/II study. *Invest. New Drugs* **2014,** 32, 995-1004.
38. Kikuchi, A.; Furutani, T.; Azami, H.; Watanabe, K.; Niimi, T.; Kamiyama, Y.; Kuromitsu, S.; Baskin-Bey, E.; Heeringa, M.; Ouatas, T. In vitro and in vivo characterisation of ASP9521: a novel, selective, orally bioavailable inhibitor of 17β-hydroxysteroid dehydrogenase type 5 (17βHSD5; AKR1C3). *Invest. New Drugs* **2014,** 32, 860-870.
39. Yepuru, M.; Wu, Z.; Kulkarni, A.; Yin, F.; Barrett, C. M.; Kim, J.; Steiner, M. S.; Miller, D. D.; Dalton, J. T.; Narayanan, R. Steroidogenic Enzyme AKR1C3 Is a Novel Androgen Receptor-Selective Coactivator that Promotes Prostate Cancer Growth. *Clin. Cancer. Res.* **2013,** 19, 5613-5625.
40. Pippione, A. C.; Carnovale, I. M.; Bonanni, D.; Sini, M.; Goyal, P.; Marini, E.; Pors, K.; Adinolfi, S.; Zonari, D.; Festuccia, C. Potent and selective aldo-keto reductase 1C3 (AKR1C3) inhibitors based on the benzoisoxazole moiety: application of a bioisosteric scaffold hopping approach to flufenamic acid. *Eur. J. Med. Chem.* **2018,** 150, 930-945.
41. Mills, K.; Gilkes, A.; Sweeney, M.; Choudhry, M.; Woodgate, L.; Bunce, C.; Brown, G.; Burnett, A. Identification of a retinoic acid responsive aldoketoreductase expressed in HL60 leukaemic cells. *FEBS Lett.* **1998,** 440, 158-162.
42. Khanim, F.; Davies, N.; Velica, P.; Hayden, R.; Ride, J.; Pararasa, C.; Chong, M.; Gunther, U.; Veerapen, N.; Winn, P. Selective AKR1C3 inhibitors do not recapitulate the anti-leukaemic activities of the pan-AKR1C inhibitor medroxyprogesterone acetate. *Br. J. Cancer* **2014,** 110, 1506.
43. Endo, S.; Matsunaga, T.; Kanamori, A.; Otsuji, Y.; Nagai, H.; Sundaram, K.; El-Kabbani, O.; Toyooka, N.; Ohta, S.; Hara, A. Selective inhibition of human type-5 17β-hydroxysteroid dehydrogenase (AKR1C3) by baccharin, a component of Brazilian propolis. *J. Nat. Prod.* **2012,** 75, 716-721.
44. Zang, T.; Verma, K.; Chen, M.; Jin, Y.; Trippier, P. C.; Penning, T. M. Screening baccharin analogs as selective inhibitors against type 5 17β-hydroxysteroid dehydrogenase (AKR1C3). *Chem. Biol. Interact.* **2015,** 234, 339-348.
45. Endo, S.; Hu, D.; Matsunaga, T.; Otsuji, Y.; El-Kabbani, O.; Kandeel, M.; Ikari, A.; Hara, A.; Kitade, Y.; Toyooka, N. Synthesis of non-prenyl analogues of baccharin as selective and potent inhibitors for aldo-keto reductase 1C3. *Bioorg. Med. Chem.* **2014,** 22, 5220-5233.
46. Verma, K.; Gupta, N.; Zang, T.; Wangtrakuldee, P.; Srivastava, S. K.; Penning, T. M.; Trippier, P. C. AKR1C3 Inhibitor KV-37 Exhibits Antineoplastic Effects and Potentiates Enzalutamide in Combination Therapy in Prostate Adenocarcinoma Cells. *Mol. Cancer Ther.* **2018,** 17, 1833-1845.
47. Verma, K.; Zang, T.; Gupta, N.; Penning, T. M.; Trippier, P. C. Selective AKR1C3 inhibitors potentiate chemotherapeutic activity in multiple acute myeloid leukemia (AML) cell lines. *ACS Med. Chem. Lett.* **2016,** 7, 774-779.
48. Tani, H.; Hasumi, K.; Tatefuji, T.; Hashimoto, K.; Koshino, H.; Takahashi, S. Inhibitory activity of Brazilian green propolis components and their derivatives on the release of cys-leukotrienes. *Bioorg. Med. Chem.* **2010,** 18, 151-157.
49. Bates, R. W.; Gabel, C. J.; Ji, J.; Rama-Devi, T. Synthesis of phenolic natural products using palladium catalyzed coupling reactions. *Tetrahedron* **1995,** 51, 8199-8212.
50. Heck, R. F. Mechanism of arylation and carbomethoxylation of olefins with organopalladium compounds. *J. Am. Chem. Soc.* **1969,** 91, 6707-6714.
51. Heck, R. F. Palladium-catalyzed vinylation of organic halides. *Org. React.* **2004,** 27, 345-390.

52. Jackson, R. W. A mild and selective method for the cleavage of tert-butyl esters. *Tetrahedron Lett.* **2001,** 42, 5163-5165.
53. Trippier, P. C.; McGuigan, C.; Balzarini, J. Phenylboronic-acid-based carbohydrate binders as antiviral therapeutics: monophenylboronic acids. *Antiviral Chem. Chemother.* **2010,** 20, 249-257.
54. Trippier, P. C.; Balzarini, J.; McGuigan, C. Phenylboronic-acid-based carbohydrate binders as antiviral therapeutics: bisphenylboronic acids. *Antiviral Chem. Chemother.* **2011,** 21, 129-142.
55. Morin, J.-F.; Shirai, Y.; Tour, J. M. En route to a motorized nanocar. *Org. Lett* **2006,** 8, 1713-1716.
56. Fitton, P.; Rick, E. A. The addition of aryl halides to tetrakis (triphenylphosphine) palladium (0). *J. Organomet. Chem.* **1971,** 28, 287-291.
57. Miyaura, N.; Yamada, K.; Suzuki, A. A new stereospecific cross-coupling by the palladium-catalyzed reaction of 1-alkenylboranes with 1-alkenyl or 1-alkynyl halides. *Tetrahedron Lett.* **1979,** 20, 3437-3440.
58. Gerbino, D. C.; Mandolesi, S. D.; Schmalz, H. G.; Podesta, J. C. Introduction of Allyl and Prenyl Side‐Chains into Aromatic Systems by Suzuki Cross‐Coupling Reactions. *Eur. J. Org. Chem.* **2009,** 2009, 3964-3972.
59. Shetty, R. S.; Lee, Y.; Liu, B.; Husain, A.; Joseph, R. W.; Lu, Y.; Nelson, D.; Mihelcic, J.; Chao, W.; Moffett, K. K. Synthesis and Pharmacological Evaluation of N-(3-(1 H-Indol-4-yl)-5-(2-methoxyisonicotinoyl) phenyl) methanesulfonamide (LP-261), a Potent Antimitotic Agent. *J. Med. Chem.* **2010,** 54, 179-200.
60. Groll, M.; Berkers, C. R.; Ploegh, H. L.; Ovaa, H. Crystal structure of the boronic acid-based proteasome inhibitor bortezomib in complex with the yeast 20S proteasome. *Structure* **2006,** 14, 451-456.
61. Trippier, P. C.; McGuigan, C. Boronic acids in medicinal chemistry: anticancer, antibacterial and antiviral applications. *MedChemComm* **2010,** 1, 183-198.
62. Brožič, P.; Golob, B.; Gomboc, N.; Rižner, T. L.; Gobec, S. Cinnamic acids as new inhibitors of 17β-hydroxysteroid dehydrogenase type 5 (AKR1C3). *Mol. Cell. Endocrinol.* **2006,** 248, 233-235.
63. Gert, J.; Harry, C.; von Lilienfeld, T.; Bart, J.; van Marwijk, K.; Leo, F.; German, A. High-dose daunorubicin in older patients with acute myeloid leukemia. *N. Engl. J. Med.* **2009,** 361, 1235-1248.
64. Mandelli, F.; Vignetti, M.; Suciu, S.; Stasi, R.; Petti, M.-C.; Meloni, G.; Muus, P.; Marmont, F.; Marie, J.-P.; Labar, B. Daunorubicin versus mitoxantrone versus idarubicin as induction and consolidation chemotherapy for adults with acute myeloid leukemia: the EORTC and GIMEMA Groups Study AML-10. *J. Clin. Oncol.* **2009,** 27, 5397.
65. Matsunaga, T.; Yamaguchi, A.; Morikawa, Y.; Kezuka, C.; Takazawa, H.; Endo, S.; El-Kabbani, O.; Tajima, K.; Ikari, A.; Hara, A. Induction of aldo-keto reductases (AKR1C1 and AKR1C3) abolishes the efficacy of daunorubicin chemotherapy for leukemic U937 cells. *Anti-Cancer Drugs* **2014,** 25, 868-877.
66. Chou, T.-C. Drug combination studies and their synergy quantification using the Chou-Talalay method. *Cancer Res.* **2010,** 70, 440-446.
67. Laurent, G.; Jaffrézou, J.-P. Signaling pathways activated by daunorubicin. *Blood* **2001,** 98, 913-924.
68. Bailly, J.; Skladanowski, A.; Bettaieb, A.; Mansat, V.; Larsen, A.; Laurent, G. Natural resistance of acute myeloid leukemia cell lines to mitoxantrone is associated with lack of apoptosis. *Leukemia* **1997,** 11, 1523.
69. Novotná, E.; Büküm, N.; Hofman, J.; Flaxová, M.; Kouklíková, E.; Louvarová, D.; Wsól, V. Roscovitine and purvalanol A effectively reverse anthracycline resistance mediated by the activity of aldo-keto reductase 1C3 (AKR1C3): A promising therapeutic target for cancer treatment. *Biochem. Pharmacol.* **2018,** 156, 22.
70. Penning, T. M.; Burczynski, M. E.; Jez, J. M.; Hung, C.-F.; Lin, H.-K.; Ma, H.; Moore, M.; Palackal, N.; Ratnam, K. Human 3alpha-hydroxysteroid dehydrogenase isoforms (AKR1C1-AKR1C4) of the aldo-keto reductase superfamily: functional plasticity and tissue distribution reveals roles in the inactivation and formation of male and female sex hormones. *Biochem. J.* **2000,** 351, 67.
71. Adeniji, A. O.; Twenter, B. M.; Byrns, M. C.; Jin, Y.; Winkler, J. D.; Penning, T. M. Discovery of substituted 3-(phenylamino) benzoic acids as potent and selective inhibitors of type 5 17β-hydroxysteroid dehydrogenase (AKR1C3). *Bioorg. Med. Chem. Lett.* **2011,** 21, 1464-1468.

72. Chou, T. C. Theoretical basis, experimental design, and computerized simulation of synergism and antagonism in drug combination studies. *Pharmacol. Rev.* **2006,** 58, 621-81.

TOC Graphic

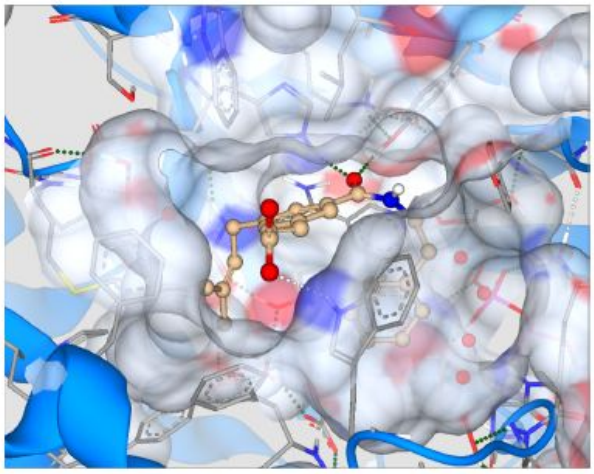

49a

AKR1C3 IC_{50} = 70 nM

>2800-fold selectivity for C3 over C1,C2,C4

- Counters daunorubicin resistance in AML cells
- Counters daunorubicin resistance in primary T-ALL cells
- Potentiates Cytarabine in AML cells
- Potentiates Cytarabine in T-ALL cells
- Widens therapeutic window
- No toxicity to bone marrow